International Ocean Discovery Program Expedition 386 Scientific Prospectus

Japan Trench Paleoseismology

Michael Strasser
Co-Chief Scientist
Department of Geology
Universität Innsbruck
Austria

Ken Ikehara
Co-Chief Scientist
AIST
Geological Survey of Japan
Research Institute of Geology and Geoinformation
Japan

Carol Cotterill
ESO Expedition Project Manager
British Geological Survey
The Lyell Centre
United Kingdom

IODP
INTERNATIONAL OCEAN DISCOVERY PROGRAM

Publisher's notes

This publication was prepared by the European Consortium for Ocean Research Drilling (ECORD) Science Operator (ESO) and Texas A&M University (TAMU) as an account of work performed under the International Ocean Discovery Program (IODP). Funding for IODP is provided by the following international partners:

National Science Foundation (NSF), United States
Ministry of Education, Culture, Sports, Science and Technology (MEXT), Japan
European Consortium for Ocean Research Drilling (ECORD)
Ministry of Science and Technology (MOST), People's Republic of China
Korea Institute of Geoscience and Mineral Resources (KIGAM)
Australia-New Zealand IODP Consortium (ANZIC)
Ministry of Earth Sciences (MoES), India
Coordination for Improvement of Higher Education Personnel (CAPES), Brazil

Portions of this work may have been published in whole or in part in other IODP documents or publications.

This IODP *Scientific Prospectus* is based on precruise ECORD Science Operator discussions and scientific input from the designated Co-Chief Scientists on behalf of the drilling proponents. During the course of the cruise, actual site operations may indicate to the Co-Chief Scientists and the Staff Scientist/Expedition Project Manager that it would be scientifically or operationally advantageous to amend the plan detailed in this prospectus. It should be understood that any proposed changes to the science deliverables outlined in the plan presented here are contingent upon the approval of the IODP ESO Director.

Disclaimer

Any opinions, findings, and conclusions or recommendations expressed in this publication are those of the author(s) and do not necessarily reflect the views of the participating agencies or TAMU.

Copyright

Citation

Strasser, M., Ikehara, K., and Cotterill, C., 2019. *Expedition 386 Scientific Prospectus: Japan Trench Paleoseismology*. International Ocean Discovery Program. https://doi.org/10.14379/iodp.sp.386.2019

ISSN

World Wide Web: 2332-1385

October 2019

Abstract

Short historical and even shorter instrumental records limit our perspective of earthquake maximum magnitude and recurrence and thus are inadequate to fully characterize Earth's complex and multiscale seismic behavior and its consequences. Examining prehistoric events preserved in the geological record is essential to reconstruct the long-term history of earthquakes and to deliver observational data that help to reduce epistemic uncertainties in seismic hazard assessment for long return periods. "Submarine paleoseismology" is a promising approach to investigate deposits from the deep sea, where earthquakes leave traces preserved in the stratigraphic succession. However, at present we lack the comprehensive data sets and long-term records that allow for conclusive distinctions between quality and completeness of the paleoseismic archives.

Motivated by the mission to fill the gap in long-term records of giant (Mw 9 class) earthquakes, International Ocean Discovery Program (IODP) Expedition 386, Japan Trench Paleoseismology, aims at testing and developing submarine paleoseismology in the Japan Trench. We will implement a multicoring approach by Mission Specific Platform shallow subsurface (40 m) giant piston coring to recover the continuous upper Pleistocene to Holocene stratigraphic successions of trench-fill basins along an axis-parallel transect of the 7–8 km deep trench. The cores from 18 proposed primary (and/or 13 alternate) sites will be used for multimethod applications to characterize event deposits for which the detailed stratigraphic expressions and spatiotemporal distribution will be analyzed for proxy evidence of earthquakes.

Sediment remobilization related to the 2011 Mw 9.0 Tohoku-Oki earthquake and the respective deposits are preserved in trench basins formed by flexural bending of the subducting Pacific plate. These basins are ideal study areas for testing event deposits for earthquake triggering because they are poorly connected for sediment transport from the shelf and experience high sedimentation rates and low benthos activity (and thus high preservation potential) in the hadal environment. Results from conventional coring covering the last ~1,500 y reveal good agreement between the sedimentary record and historical documents. Subbottom profile images are consistent with basin-fill successions of episodic muddy turbidite deposition and thus define clear targets for paleoseismologic investigations on longer timescales accessible only by IODP coring.

We will apply, further refine, and implement new methods for establishing event stratigraphy in the deep sea and for recognizing giant versus smaller earthquakes versus other driving mechanisms. Our results can potentially produce a fascinating record that unravels an earthquake history that is 10–100 times longer than currently available information. This would contribute to a tremendous advance in the understanding of the recurrence pattern of giant earthquakes and earthquake-induced geohazards globally and provide new constraints on sediment and carbon flux of event-triggered sediment mobilization to a deep-sea trench and its influence on the hadal environment.

Schedule for Expedition 386

Expedition 386 is based on International Ocean Discovery Program (IODP) drilling Proposal 866-Full. Following ranking by the IODP Science Advisory Structure, the expedition was scheduled by the European Consortium for Ocean Research Drilling (ECORD) Facility Board as a Mission Specific Platform (MSP) expedition to be implemented by the ECORD Science Operator (ESO) in collaboration with the Institute for Marine-Earth Exploration and Engineering (MarE3)/Japan Agency for Marine-Earth Science and Technology (JAMSTEC). The offshore phase of the expedition is scheduled for April–June 2020 on board the R/V *Kaimei* with a total of 50 days available for the piston coring and measurements described in this report and on the ESO Expedition 386 webpage. The onshore science party (OSP) is provisionally scheduled to start mid-October 2020 utilizing the facilities on board the D/V *Chikyu*. It is anticipated to run for a maximum of 4 weeks (dependent on core recovery).

The following links should be used in conjunction with this *Scientific Prospectus*:

- The Expedition 386 webpage will be periodically updated with expedition-specific information on the platform, facilities, coring strategy, measurements plan, and schedule. The full proposal and addenda can be accessed via this page (**http://www.ecord.org/expedition386**).
- General details about the laboratory facilities provided by JAMSTEC can be found on the *Chikyu* wiki page (**http://cdex-science.jamstec.go.jp/chikyu-wiki/index.php/Chikyu_onboard_laboratory**).
- Supporting site survey data for Expedition 386 are archived in the IODP Site Survey Data Bank (SSDB; **http://ssdb.iodp.org/SSDBquery/SSDBquery.php**; select P866 for the proposal number). Please note that not all of the site survey data associated with this expedition is currently publicly available.

Introduction

The 2004 Mw 9.2 Sumatra and the 2011 Mw 9.0 Tohoku-Oki earthquakes and tsunamis were catastrophic geologic events with major societal consequences. Both ruptured portions of subduction plate boundaries that had been deemed incapable of these "giant" earthquakes and had unexpectedly shallow and large coseismic slip, which contributed to the large tsunamis (Ide et al., 2011; Fujii and Satake, 2007). More than 90% of the stress accumulated by global plate tectonics is released along active margins by subduction earthquakes. On a global average, one Mw 8 class earthquake occurs per year, and most subduction boundaries have produced such "great" earthquakes. In contrast, only four giant (Mw 9 class) earthquakes are well documented by instrumental data. Despite considerable research since the 1960 Mw 9.5 Chile and 1964 Mw 9.2 Alaska events, our understanding of giant earthquakes is still limited. From the restricted historic records, we can tentatively generalize the following about giant earthquakes:

- They are multisegment ruptures of patches of the megathrust that may not have previously ruptured in Mw 8 events (Sieh et al., 2008).
- They rupture over large distances and into the shallowest part of the subduction boundary (Lay, 2015).
- They produce long-period, high-amplitude, long-duration seismic waves that can lead to resonance with offshore sediment layers (Nakamura et al., 2015).
- They generate tsunamis that propagate into the far field (Fujii et al., 2011).

The long recurrence time causes these catastrophic geologic events to be poorly sampled in the instrumental and historic records. Thus, answers to critical questions such as "What are the effects of giant earthquakes?" and "How often to expect them?" rely on limited examples. Examining prehistoric events preserved in the geological record is essential to reconstruct the history of giant earthquakes on timescales long enough to study relevant subduction zone processes. Furthermore, such paleoseismic data interpretation remains the only path to deliver data that help reduce epistemic uncertainties in seismic hazard assessment for long return periods.

Expedition 386, Japan Trench Paleoseismology, is motivated by the mission to fill the gap in long-term records of giant earthquakes and aims to test and develop submarine paleoseismology in the deep-sea environment of the Japan Trench.

Subduction earthquakes affect offshore environments including deep-sea trenches formed by the downward bending of the oceanic lithosphere along convergent plate boundary systems. Most trenches are deeper than 6000 m and compose (or are located in) the hadal zone, one of the least explored aquatic environments on Earth (Jamieson et al., 2010). Sediment supply to terminal trench basins has been linked to large-scale sediment remobilization and translocation processes initiated by earthquake shaking (Oguri et al., 2013; Ikehara et al., 2016; Migeon et al., 2017; Kioka et al., 2019). Shaking of the seafloor can trigger landslides or surficial sediment resuspension that evolve downslope into turbidity currents or mud density flows, respectively (Talling, 2014; Goldfinger et al., 2017; Molenaar et al., 2019). Widespread shaking causes nearly synchronous sediment instability over hundreds of kilometers, producing widely distributed event deposits (Cattaneo et al., 2012; McHugh et al., 2016; Kioka et al., 2019). Widespread remobilization over such large distances are not expected with other triggers. Exceptional supertyphoons might have comparable spatial footprints, but initiation of sediment remobilization would be limited to relatively shallow waters.

Submarine paleoseismology relies on the premise that the marine environment preserves long and continuous records that allow for identification of earthquake-triggered deposits (and to distinguish them from nonseismically triggered deposits). In subaquatic environments, the sedimentary archive provides high sensitivity and continuity, so event deposits are better preserved and dateable than their terrestrial counterparts. Because of eustatic sea level fluctuations, for example, coastal records (e.g., tsunami deposits) only cover the last 8 ky of the Holocene highstand.

Several submarine paleoseismic studies along subduction zones (Cascadia, Calabria, Chile, Sumatra, Hikurangi, and the Japan Trench; see compilations by Strasser et al. [2015], De Batist et al. [2017], and references therein) have been successful in obtaining sedimentary event records that can be positively correlated to instrumentally recorded and historical earthquakes and/or reveal evidence for prehistoric events. These studies, which are mostly based on conventional 10 m long cores, demonstrate the potential to advance our understanding of earthquake recurrence beyond timescales of the last few thousand years.

IODP is uniquely positioned to provide such paleoseismologic data by coring sedimentary sequences comprising continuous depositional conditions and records of earthquakes occurrence over longer time periods. The 2015 IODP workshop in Zürich discussed and identified strategies on how and where we could best make use of giant piston coring efforts in IODP to make some major advancements in submarine paleoseismology (Strasser et al., 2015; McHugh et al., 2015). Workshop discussion revealed the endorsement of the Japan Trench as a primary target for understanding the causes, consequence, and recurrence of giant earthquakes (see **Background** for a description of why). Thus, the central theme of Expedition 386 is to test and develop submarine paleoseismology en route to understanding earthquakes and tsunamis in the Japan Trench and eventually other margins with similar settings.

Background

At subduction margins, earthquake sources include faults in the upper and lower plates and the interpolated megathrust that can rupture over a wide range of depths that possibly reach the trench. Differences in seafloor motion from these distinct sources result in distinct driving forces for sediment remobilization (Ye et al., 2013; Nakamura et al., 2015). Accordingly, recent observations have demonstrated a wide range of earthquake-related sedimentary signatures linked to exceptionally large subduction earthquakes and their aftershock sequences:

- Slumps in the trench linked to the 2011 Tohoku-Oki earthquake (Fujiwara et al., 2011; Strasser et al., 2013);
- Turbidites released simultaneously in different canyon heads traveling downcanyon to merge below confluences during the 1700 AD Mw 9.0 Cascadia earthquake (Goldfinger et al., 2012, 2017);
- Homogeneous sediment extending for large distances across the abyssal plain of the Mediterranean linked to the 365 AD Crete earthquake (Polonia et al., 2013, 2016);
- Dense plumes of sediment remaining in suspension above the seafloor for months after the 2004 Mw 9.2 Sumatra and 2011 Mw 9.0 Tohoku-Oki earthquakes (Seeber et al., 2007; Oguri et al., 2013); and
- Significant sediment volume and carbon transport to the deep sea by canyon flushing and remobilization of young organic carbon (OC)–rich surficial sediments over wide areas, triggered by the 2016 Mw 7.8 Kaikōura (New Zealand; Mountjoy et al., 2018) and 2011 Mw 9.0 Tohoku-Oki (Kioka et al., 2019) earthquakes, respectively.

For a given margin where physiography, sediment properties, sediment-routing systems, and downslope transport can be reliably assessed, this complexity in both structure and sedimentary deposits provides opportunities and suggests that distinct classes of earthquakes may leave characteristic sedimentary signatures.

Multimethod characterization for detailed structural, physical, chemical, and microbiological characterization has revealed distinct signatures and patterns for event deposit sedimentary sequences that result from (1) the remobilized material and its original provenance (as a proxy for sediment source and/or routing processes), (2) grain size distribution and structural orientation reflecting transport and depositional dynamics, and (3) consolidation and microbial organic matter (OM) degradation reflecting postdepositional processes (McHugh et al., 2011; Polonia, et al., 2016; Goldfinger et al., 2017). Positive stratigraphic correlation of such multiproxy signatures between widely separated sites favors a common causative mechanism, especially if the respective sites are isolated from each other (Goldfinger et al., 2012; Talling, 2014; Ikehara et al., 2018). The above referenced studies and more, many of which investigated event deposits positively correlated to historic earthquakes, have proposed characteristic patterns or signals to be potentially distinctive for earthquake origin, subsequent tsunamis, and

their aftershock series (Goldfinger et al., 2012; Oguri et al., 2013; Ikehara et al., 2016, 2018, Polonia et al., 2016, 2017; Kioka et al., 2019). The currently available data sets are mostly limited by conventional 10 m long coring. They often only comprise few event deposits that can be linked to earthquakes for a given margin. Therefore, the conceptual depositional models are not validated against a longer temporal record. Furthermore, deposition and preservation of event layers and their stratigraphic signal varies by location and may change through time (Sumner et al., 2013; Bernhardt, et al., 2015; Ikehara et al., 2018). Long temporal (i.e., reaching back in time to sample several low-recurrence events) and spatially extensive (to sample different types of events over long distances at locations with different preservation potential) records are needed to test the robustness of the proposed models and relations.

Gràcia et al. (2010), Pouderoux et al. (2012), and St-Onge et al. (2012) tracked inferred earthquake-related event deposits recovered by the CALYPSO coring system further back in time. These few pioneer studies demonstrated the potential for paleoseismologic application. However, they were performed on a limited number of cores taken where paleoceanography was one of the primary objectives, and site location may not have been optimal for paleoseismology. Site localization and assessing site variability is a key issue in subaquatic paleoseismology (Goldfinger et al., 2017; Ikehara et al., 2018; Kioka et al., submitted). Detailed characterization of the depositional history of a site can reveal the causes of apparent gaps in the paleoseismic record and identify sites ideal for preserving earthquake-related deposits.

Because likely no single technique can provide the full paleoseismic history at an individual site and because feedback between earthquake type, seafloor motion, and its eventual manifestation in the stratigraphic record are complicated, our strategy includes (1) a multicoring approach to sample, characterize, and date a wide range of event deposits over a wide area along the entire Japan Trench and (2) accompanying studies that will combine field observation with physical experiments and numerical models. The latter will explore mechanisms that link coseismic seafloor motions, shaking and deformation, sediment remobilization, and transport dynamics with their signatures in the sedimentary record while providing the knowledge base to translate sedimentary observations into constraints on prehistoric seismicity. This multidisciplinary approach is expected to deliver answers to research questions including the following:

- Can we distinguish different earthquake events and types from the sedimentary records?
- Is there an earthquake magnitude threshold for a given signal/pattern in the sedimentary record?
- Does record sensitivity change along strike and/or through time?
- Can we link the sedimentary signal to the earthquake rupture characteristics?
- Can we assess seismic activity of different along-strike segments?

Building on what we have learned from the 2011 Mw 9.0 Tohoku-Oki earthquake, an established correlation of event deposits to historical earthquakes, and the Japan Trench characteristics that are suitable for submarine paleoseismology (see below), there is high potential that our objectives can be achieved. At a minimum, we will identify the giant Mw 9 class tsunamigenic earthquakes that stand in contrast to the frequently occurring Mw 7.5–8 earthquakes that have relatively modest consequences. This is expected to provide a long-term record of Mw 9 class earthquakes, significantly expanding currently available paleoseismic records of such upper end-member events at other subduction margins (e.g., Chile at 5.5 ka [Kempf et al., 2017; Moernaut et al., 2018], Cascadia at 7.6 ka [Goldfinger et al., 2017], Sumatra at 6.5 ka [Patton et al., 2015], and Hikurangi at 16 ka [Pouderoux et al., 2014]). Based on these so far available records, the occurrence of earthquake supercycles has been hypothesized (Sieh et al., 2008; Goldfinger et al., 2013; Ratzov et al., 2015; Usami et al., 2018). Earthquake supercycles have also been proposed based on seismomechanical models (Herrendörfer et al., 2015; Shibazaki, et al., 2011). Some seismologists (e.g., Geller, 2011; Mulargia et al., 2017) question the seismic cycle hypothesis. Instead, they propose Poissonian behavior for earthquake recurrence (i.e., large earthquakes can occur any time with a low but on average constant probability).

Studying prehistoric events preserved in the geological record is the best way to reconstruct the history of megathrust earthquakes on timescales long enough to provide statistically rigorous tests to answer the research question: Do giant earthquakes recur quasiperiodically, clustered, or randomly through time?

Japan Trench

Recent literature and community input during the IODP paleoseismology workshop in 2015 have described characteristics that predispose margins to being suitable for submarine paleoseismology and formulated guidelines to be considered for designing scientific experiments (Sumner et al., 2013; Goldfinger et al., 2014; Strasser et al., 2015; McHugh et al., 2015). The Japan Trench (Figure **F1**) is a well-suited area according to these criteria.

The 2011 Tohoku-Oki earthquake is the first event of its kind worldwide for which the entire activity was recorded by offshore geophysical, seismological, and geodetic instruments. Additionally, direct observation for sediment resuspension and redeposition was documented across the entire margin by seafloor monitoring systems and/or rapid-response research missions. Shirasaki et al. (2012) and Pope et al. (2017) reported submarine cable breaks along the southern and central Japan Trench due to turbidity currents generated by the 2011 Tohoku-Oki earthquake. Sediment remobilization related to the earthquake and tsunami is also attested by measured turbidity in the bottom waters (Noguchi et al., 2012; Oguri et al., 2013) and ocean-bottom instrument data (Arai et al., 2013). Submarine landslides were documented by differential bathymetry (Fujiwara et al., 2011; Strasser et al., 2013). However, the most significant volumetric contribution of earthquake-triggered sediment remobilization occurs through surficial sediment remobilization of just the uppermost few centimeters of young, unconsolidated, and OC-rich seafloor sediments over a very wide area (McHugh et al., 2016; Kioka et al., 2019) as documented by the occurrence of centimeter-thick gaps in the slope stratigraphic succession correlating to large earthquakes (Molenaar et al., 2019). Overall, cores document various distinct earthquake-related event deposits throughout an extensive region from the coastal sea to the Japan Trench floor (Figure **F1**; see references in caption). Correlation of the event deposit to the 2011 earthquake has been proved positive by short-lived radionuclide (Oguri et al., 2013; McHugh et al., 2016; Ikehara et al., 2016; Kioka et al., 2019) and transient disequilibrium pore water profiles (Strasser et al., 2013). Although there is local variability in deposition and preservation of the event layers (Yoshikawa et al., 2016; Ikehara et al., 2018), the general pattern obtained from >70 cores revealed a good along-strike correlation of documented event deposit occurrence within the

reconstructed rupture area (McHugh et al., 2016, Ikehara et al., 2018; Kioka et al., 2019). Extensive research is still ongoing to further calibrate the sedimentary record of the 2011 Tohoku-Oki earthquake and assess what earthquake parameters can reliably be deduced from the geological record, making the Japan Trench among the best study areas for calibration of submarine paleoseismology.

High sedimentation rates of diatomaceous hemipelagic mud reflect the influence of high oceanic productivity as a consequence of the interplay between the cold Oyashio Current and warm Tsugaru and Kuroshio Currents (Saino et al., 1998). Bioturbation of 2011 event deposits as documented from surface cores is strong to moderate on the upper and lower slopes, respectively (Ikehara et al., 2018). There, comparably low sedimentation rates (6–50 cm/ky on the upper slope [von Huene et al., 1980] and ~23 cm/ky on the midslope terrace [Shipboard Scientific Party, 1980]) and thinner deposition observed for the 2011 event layer suggest a lower preservation potential of the earthquake-related bed in the stratigraphic record but also provide evidence of past earthquake-related event deposits (Usami et al., 2018). In contrast, very high sedimentation rates occur in the Japan Trench (1–3 m/ky; Ikehara et al., 2018), which prevents the destruction of thick, fine-grained event deposits by currents and benthos activity, resulting in a high preservation potential of the earthquake-related bed.

Indeed, cores obtained during the last 8 y from trench-fill basins preserve evidence for at least two older major sediment remobilization events. These deposits comprise thick, multipulse, fine-grained turbidite sequences that correlate throughout cores taken from separated trench-fill basins and extend along strike for ~120 km (Ikehara et al., 2016, 2018; Kioka et al., submitted) (Figures **F1**, **F2**). Interbedded volcanic ash provides well-constrained tephra chronological age control (Ikehara et al., 2017), suggesting that the prominent event deposits correlate to the 869 AD Jogan and 1454 AD Kyotoku earthquakes (Ikehara et al., 2016). Sawai et al. (2015) and Namegaya and Satake (2014) also suggested major megathrust earthquakes as the source of the 1454 AD and 869 AD tsunamis based on onshore tsunami records and historical documents. Age chronology of Japan Trench event deposits and their correlation to historical earthquakes is corroborated by pioneer studies applying innovative dating methods for deep-sea sediments (i.e., below the carbonate compensation depth, where traditional ^{14}C dating and stable isotope stratigraphy on carbonate biominerals are confounded). Bao et al. (2018) showed a successful application of OM radiocarbon analyses for constraining the chronology of event deposits related to historic earthquakes (Figure **F3**); Kanamatsu et al. (2017) found that the sediment recovered in the Japan Trench contains excellent paleomagnetic secular variation.

These studies show that large-scale resedimentation events recorded as widespread fine-grained turbidite sequences occur less frequently despite the generally high seismicity with Mw 7–8 earthquakes occurring regularly every few tens to hundreds of years. This finding supports the hypothesis that the Japan Trench event deposit record is representative for exceptionally large events with low recurrence. The occurrence of three giant earthquakes in the last 1500 y is consistent with return times of 260–880 y for Mw 9 earthquakes off Tohoku as calculated from seismic moment frequency relation (Uchida and Matsuzawa, 2011). Smaller earthquakes may have the potential to locally resuspend unconsolidated seafloor sediments, as reported by Oguri et al. (2016) for an Mw 7.3 aftershock of the 2011 Tohoku-Oki earthquake. The global cable break database by Pope et al. (2017) revealed that for the time period covered by cable monitoring in the Japan Trench, no earthquakes below Mw 7.0 and only 5 earthquakes out of 25 earthquakes Mw 7 or above actually triggered cable breaking sediment flows. These data support the concept that slope stability is greater in areas with high seismic activity where sediments are consolidated and strengthened during low-magnitude events (Sawyer and DeVore, 2015; ten Brink et al., 2016; Molenaar et al., 2019). During regional moderate-sized earthquakes (Mw 7–8 range) and potentially even triggered by remotely generated earthquake waves (Johnson et al., 2017), sediment resuspension and remobilization in regions with high sedimentation rates may redistribute sediment to the trench floor. These processes do not form distinct thick and regionally extensive event deposits but may instead contribute to and maintain the high "background" (with respect to the great events) sedimentation rate in the trench (Ikehara et al., 2016, 2018).

Examination of the acoustic facies from high-resolution subbottom (HRS) profiles of the trench fill reveals variably thick, acoustically transparent bodies interbedded in the otherwise parallel reflection pattern of the trench-fill basins (Ikehara et al., 2018; Kioka et al., submitted). Seismic-core correlation reveals groundtruthing of the uppermost acoustically transparent bodies to reflect thick, massive, fine-grained event deposits linked to historic earthquakes (Kioka et al., submitted) (Figure **F4**). HRS profiles from the small isolated trench basins along the entire Japan Trench axis image acoustic reflection patterns are consistent with basin-fill successions interbedded by episodic deposition of fine-grained turbidites (Kioka et al., submitted) (Figure **F5**), thus defining clear target successions for deeper coring to sample older events not reached by conventional coring.

According to the available data and research results, large earthquakes and related tsunamis are the most probable origin of major sediment remobilization events recorded in Japan Trench stratigraphic sequences. However, alternative mechanisms have to be considered and will be a primary objective for this expedition (see **Scientific objectives**). With the exception of the Ogawara and Nakaminato Submarine Canyons in the north and south, respectively (Figure **F1**), the Japan Trench margin contains no submarine canyon systems directly connecting the shore or shelf to the deepwater trench floor. Instead, several isolated basins that form in concert with tectonic subsidence on the upper slope (Arai et al., 2014) (Figure **F1**) serve as natural sediment traps receiving sediment from the shelf. The Ogawara and Nakaminato Submarine Canyons have not been reported as significant sediment routing systems. Thus, the physiographic setting of the entire Japan Trench convergent margin limits the formation and mobility of meteorologically induced turbidity currents such as by storm surges, hyperpycnal flows from rivers (floods), and large storm waves to reach the central part of the deep-sea trench (Ikehara et al., 2018; Kioka et al., submitted).

At this stage, we cannot exclude the possibility that sediment delivery mobilized in shallow waters and routed through the Ogawara and Nakaminato Submarine Canyons, potentially enhanced during Upper Pleistocene sea level lowstands, may reach the trench. This possibility is suggested by results from sediment routing systems analysis by Kioka et al. (submitted). The influence of sediment remobilization of these two submarine canyons on the event stratigraphic record will be investigated during Expedition 386.

Scientific objectives

Primary objectives:

1. Identify the sedimentological, physical, chemical, and biogeochemical proxies of event deposits in the sedimentary archive that allow for confident recognition and dating of past Mw 9 class earthquakes versus smaller earthquakes versus other driving mechanisms.
2. Explore the spatial and temporal distribution of such event deposits to investigate along-strike and time-dependent variability of sediment sources, transport and deposition processes, and stratigraphic preservation.
3. Develop a long-term earthquake record for giant earthquakes.

Objectives 1 and 2 are related to the mission of testing and developing submarine paleoseismology to produce robust long-term records as input for addressing Objective 3 in the Japan Trench, as compared with global examples. To address these objectives, Expedition 386 will implement MSP shallow subsurface (40 m) giant piston coring to recover the continuous upper Pleistocene–Holocene stratigraphic successions of isolated trench-fill basins along an axis-parallel transect of the 7–8 km deep Japan Trench. The cores from 18 primary (and/or 13 alternate) sites will be used for multimethod applications to characterize event deposits for which the detailed stratigraphic expressions and spatiotemporal distribution will be analyzed for proxy evidence of extreme events.

Site characterization and site selection

Japan Trench structural characteristics

The Pacific plate is subducting beneath the Okhotsk plate along the Japan Trench at a rate of 8.0–8.6 cm/y (DeMets et al., 2010). The trench strikes north–south to NNE–SSW, originating at the triple junction of the Pacific, Philippine Sea, and Okhotsk plates at the south and intersecting the Kuril Trench to the north. The plate interface is erosional, and subduction erosion produces tectonic subsidence (von Huene and Lallemand, 1990) that forms a low-gradient (1°–2°) upper slope terrace. Although there is no clear fore-arc basin, isolated basins occur on the upper slope terrace (Arai et al., 2014) (Figure **F1**). The lower slope is steeper with an average gradient of ~5°. Active faulting along the subduction margin (Tsuru et al., 2002; Kodaira et al., 2017) forms a narrow midslope terrace at water depths of 4000–6000 m. North–south to NNW–SSE trending horst and graben structures formed by flexural bending of the subducting Pacific plate result in relatively rough trench floor morphology with small elongated, physically separated trench- and graben-fill basins. Vertical relief within the basins is typically on the order of a few hundreds of meters.

The study area of the deep Japan Trench (7600, 7500, and 8000 m water depths in the northern, central, and southernmost parts, respectively) is bounded to the north and south by subducting seamounts (the Erimo and Daiichi-Kashima Seamounts, respectively), where the trench floor is elevated to 6000 and 5500 m deep, respectively. The trench floor is also relatively shallower (~7400 m) around 39.4°N, where a petit-spot volcano field (Hirano et al., 2006) enters the subduction system. There, a large >1 km high escarpment suggests large-scale gravitational collapse and megalandslides on the lowermost landward slope. HRS profiles, however, do not show young large-scale landslide deposits, suggesting that the collapse structure is significantly older (Kioka et al., submitted).

Site survey data, site selection, and prioritization

The Japan Trench is a well-imaged margin with many seismic surveys conducted since the 1970s, including high-resolution multichannel seismic (HRMCS) data collected across the trench axis since 2011 (Kodaira et al., 2017) (Figure **F6**). In 2016, we collected ~2000 km of HRS data (Parasound system on board the R/V *Sonne*) (Figures **F4**, **F5**, **F6**) that are now being integrated with HRS Chirp data acquired during recent R/V *Shinsei-Maru* cruises (Kioka et al., submitted). The footprint of such (parametric) ship-mounted systems is a few hundred meters in diameter for >7 km deep waters, but the data from the small trench- and graben-fill basins confirm coherent, horizontally stratified sediments interbedded with acoustically transparent event deposits (Figures **F4**, **F5**) that define clear targets that (1) are bigger than the accuracy of positioning coring equipment (~100 m; see below) and (2) show well-imaged promising event stratigraphy of mostly 40 m and more (Kioka et al., submitted).

Isopach maps of trench-fill sediments (Figure **F6**) reveal variable thicknesses ranging from practically 0 to >300 m, reflecting along-strike variation in the structural style of horst-graben basins bending along faults in the downgoing slab and Mesozoic–Cenozoic sediment cover of the Pacific plate (Nakamura et al., 2013; Boston et al., 2014). Based on HRMCS data, we located sites in basins where trench-fill sediment thickness is >50 m. This confirms that the upper 50 m of sediment can be cored, even where the lower part of the trench fill is not well imaged in the HRS data. There, the acoustic basement in HRS data is interpreted to be linked to local landslides or deformation of trench-fill sediments by coseismic slip propagation to the trench (Kodaira et al., 2012; Strasser et al., 2013; Kioka et al., submitted). Although likely linked to past giant earthquakes, our site locations generally avoid such features because stratigraphic control will be difficult to assess. At proposed Sites JTPC-01A, JTPC-02A, JTPN-01A, and JTPN-02A, the well-stratified trench-fill deposits composing our coring targets overlie such trench-fill deformation structures by less than 40 m. Thus, these sites constitute opportunities to groundtruth, sample, characterize, and date the interpreted occurrence of slumps in and/or coseismic rupture propagation to the trench.

We identified 31 sites that allow sampling of event deposits that are well characterized by homogeneous acoustic facies intercalated within acoustically stratified sediments as imaged by HRS data (Figures **F4**, **F5**, **F6**). In most cases, two sites are located <2–5 km apart in an individual trench-fill basin for which site-to-site correlation is well constrained by good reflector continuity (Kioka et al., submitted). The two sites form a couple that allow for coring both an expanded and a condensed stratigraphic section, applying our "composite-stratigraphy concept" (Figure **F6**) to address Objective 1 and reaching further back in time (Objective 3). Correlation between sites across different basins is possible in many cases in the northern and southern Japan Trench (Kioka et al., submitted; Figure **F5**). However, these correlations are partly obscured by steep morphologies across subducting horst or landslide structures. To study along-strike variability (Objective 2), we located fewer coring sites in basins with better along-strike continuity, whereas a high density of site locations are chosen where basins are smaller and continuity is restricted.

Proposed coring sites

Site locations

A total of 18 primary sites and 13 alternate sites were selected that span the southern, central, and northern Japan Trench. The sites are all located in water depths ranging from 7000 to 8000 m and with total penetration depths between 30 and 40 m (Table **T1**).

Sediments are expected to be predominantly diatomaceous muds intercalated with centimeter- to meter-thick fine sand with muddy turbidites and thin tephra layers. The sites targeted include basinal areas with undisturbed expanded sequences and accompanying trench floor highs that show condensed sequences, both in deep-sea hadal trench settings.

Site survey data

A network of seismic reflection profiles is available from published material (Nakamura et al., 2013; Ikehara et al., 2018; Kioka et al., 2019, submitted) and collaborating groups (Figure **F6**; Table **T2**), including the multichannel seismic (MCS) data acquired in 2012–2015 by the R/Vs *Kairei* and *Kaiyo* and the subbottom profiler (SBP) data acquired in 2012–2018 by *Sonne* (Parasound system), *Shinsei-Maru* (Topas system), the R/V *Mirai* (Bathy2010 system), and the R/V *Yokosuka* (EdgeTech system). The ability to correlate event deposits imaged in SBP data has been demonstrated by Kioka et al. (2019, submitted). Multibeam bathymetry data are available along the entire Japan Trench axis (Kioka et al., 2019).

Operational strategy

Coring platform

The proposal calls for a coring platform that can operate in deep water and deploy a 40 m Giant Piston Corer (GPC). ESO has secured the Japanese *Kaimei* in partnership with MarE3/JAMSTEC. This dynamically positioned vessel incorporates an ocean depth Ocean Scientific International LTD (OSIL) GPC system. This system has routinely acquired 20 m length cores, and further cruises being planned between the time of writing and the offshore phase of Expedition 386 will take this capability up to 40 m lengths.

A midway port call in Sendai, Japan, will allow restocking of core liner. During this port call, any microbiology samples that have been taken will be shipped under temperature-controlled conditions to the receiving laboratory, and two temperature-controlled containers of core will be offloaded and taken to Yokosuka, Japan, for storage until the OSP.

Downhole depth control

The water depth will be logged in five ways:

- Multibeam data previously acquired,
- Multibeam acquired prior to coring,
- Distance/depth between the ship and an acoustic transponder fitted onto the head of the GPC,
- Cable length paid out in association with the depth at which the pilot corer/trigger is activated, and
- Vessel mounted echo sounder depth.

Coring methodology

The GPC is deployed from the starboard side of the vessel using a dedicated winch system, which uses an aramid fiber rope. The main corer is triggered by an "adjustable free-fall distance" weight that incorporates a short pilot corer. The system is lowered through the water column until the GPC is approximately 200 m above the seabed. It is then halted for 5 min to allow the corer to settle. The GPC is then lowered until the pilot corer reaches the seabed. This action takes a short 1.5 m pilot core and releases the GPC to free fall from a preset adjustable height above the seafloor for maximum penetration. The internal piston system is designed to reduce internal friction and prevent plugging. Acceleration and depth sensors are fitted onto the GPC head as well as ~20 m above the GPC head, which allows accurate positioning of the GPC. Core orientation is estimated using an azimuth meter attached to the GPC.

Cores will be obtained in translucent polyvinylidene chloride (PVDC) liners. The inner diameter of these liners is 11 cm, and the outer diameter is 12.5 cm. The liners come in 5 m lengths that are screwed together to the maximum length required (i.e., 20 or 40 m). Prior to insertion into the core barrel, the liners will be screwed together and marked up to indicate position and orientation inside the barrel.

Sampling regime

The expedition's sampling regime is as follows:

- Continuous sampling regime.
- Two holes will be cored at each of the primary sites (in addition to the pilot hole accompanying each GPC deployment). It is therefore planned to acquire a minimum of four holes at each site:
  - Two short (1.5 m) pilot holes,
  - One 20 m hole, and
  - One hole as deep as 40 m.
- Coring may be undertaken in a different sequence to that specified in this document to suit operations and site-specific conditions. This could include coring at multiple sites using a shorter barrel length prior to returning and recoring with longer barrel lengths at the same sites, which reduces operational time spent changing the core barrel lengths after every coring attempt.

Typically, a shorter core will be attempted first to clarify the lithology and therefore the weight and fall rate required to maximize penetration to the full 40 m target depth.

Downhole logging

Because of the nature of operations with the GPC, Expedition 386 will not have a downhole logging program.

Site priorities and contingency considerations

In this section, we briefly describe overarching priorities for sites and coring given the scientific goals of the expedition and examples of possible contingency strategies.

Primary site couples are defined preferentially in basins where the <10 m long cores already available show promising event stratigraphy in the shallow subsurface and high potential for expanding the record further back in time. Where already cored, event stratigraphic patterns can be correlated across several separated basins (Ikehara et al., 2017) and/or where HRS data suggest correlatable reflection patterns across basins (Kioka et al., submitted). High spatial coverage of proposed site couples seems less critical to achieve the scientific objectives, and not all correlatable basins must necessarily be sampled by the composite-stratigraphy concept. Following this logic, we prioritize 18 sites that need to be cored to meet all scientific objectives. The remaining 13 sites could be considered as alternate sites to one or more of the primary sites. However, coring these "second priority" sites in addition to the primary sites remains a

highly valuable operational objective to refine the spatial resolution for reconstructing the earthquake history of different along-strike segments. To this end, we also located coring sites in small graben-fill basins on the incoming downward-bending Pacific plate (proposed Sites JTPC-04A, JTPC-07A, JTPC-08A, and JTPN-03A; Figures **F5**, **F6**) to secure enough site location density in structurally complicated areas.

Because it is important to core all 18 of the primary sites, it is possible that a single hole will be acquired at each site first and the vessel will then return to acquire the second hole at each location following the midway port call. This possibility will mitigate the chance of not reaching a site at all should external factors such as breakdowns or weather hinder operations. A second possibility is that some geographical areas will be given priority over others based on information obtained during the offshore phase.

If recovery of key locations/intervals is particularly poor, we would consider coring an additional nearby hole. Throughout the offshore phase we will apply lessons learned during the expedition about the most effective coring strategy to improve efficiency or recovery, and if time allows, this could result in additional holes. Similar to any offshore operation, should any issues occur with acquiring the full 40 m length cores, modifications to the sampling plan might have to be considered by the science party.

In addition to the above, subbottom profile (Topas) and multibeam data will be acquired prior to deploying the GPC. As well as providing real-time information on the site to be cored, the data will also ensure that no new event deposits have been emplaced that render the site inadequate in any way. The Topas and multibeam data will be acquired during the hours of darkness when it is not possible to deploy the GPC or during weather downtime when hydroacoustics can be acquired but the GPC cannot be safely launched.

Core on deck

The GPC will come onto the deck where the corer will be dismantled starting from the base up. The liner will be cut, numbered, sampled for ephemeral properties, and capped on deck before being transferred to Laboratory 3 for full curation, labeling, and entry into the Expedition Drilling Information System (DIS).

Because the cores will be collected in plastic liners, the usual IODP curation procedures will be followed, and these will be documented in the ESO Expedition 386 Core Curation, Initial Sampling, and Analyses Handbook. After curation, extraction of interstitial water, and temperature equilibration, unsplit core sections and shoe materials will be passed to the European Petrophysics Consortium (EPC) staff for physical properties measurements (Multi-Sensor Core Logger [MSCL]) and to science party members for shipboard description, analysis, and sampling as described in **Offshore science activities**.

Coring will occur during the daytime shift only, and curation, measurements, and preliminary analysis of the cores will occur over a 24 h period to enable core processing to keep up with core recovery.

Science operations

A Sampling and Measurements Plan (SMP) for Expedition 386 will be prepared by ESO and the Co-Chief Scientists to meet the scientific objectives of Expedition 386.

Offshore science activities

It is the nature of MSP expeditions that there is limited laboratory space and accommodation on the platforms used compared to the larger research drilling vessels R/V *JOIDES Resolution* and D/V *Chikyu*, and as such there will be no splitting of the cores at sea during Expedition 386. Selected scientific analysis will be carried out on board by a subset of the science party and ESO personnel.

Science activities on the platform are confined to those essential for decision making at sea, core curation, measurement of ephemeral properties, and securing of samples for pore water chemistry and microbiology. Cores will typically be cut into 1 m lengths (because of the increased core diameter and associated increase in weight) for curation. Most of the scientific analyses will be carried out during the OSP on board *Chikyu* when the cores are split.

The following is a summary of the offshore scientific activities that will be undertaken on *Kaimei*:

- Basic curation and labeling of core.
- Marking positions for thermal conductivity measurements to be taken prior to the OSP.
- Measuring all cores (>15 cm in length) on the MSCL (gamma density, *P*-wave velocity, electrical resistivity, magnetic susceptibility, and natural gamma radiation).
- Describing and sampling for initial sedimentological, micropaleontological, and petrophysical characterization, including taking an image from the GPC shoe (if available). If no micropaleontologists sail, it is proposed that subsamples from the shoes and additional smear slides at 1 m intervals be made available to the micropaleontological members of the science party prior to the OSP. Age information will be critical to determining the depositional ages of sediments acquired, and as such would be crucial to have at the start of the OSP.
- Acquiring and splitting of interstitial pore water samples by Rhizons (if this is not possible, then by using a hydraulic press system in a lower resolution) using the following sampling frequency:
  - Bottom water taken from the water/sediment interface captured in the pilot core,
  - Every 20 cm in the trigger core,
  - Every 50 cm down to 5 m depth,
  - Every 100 cm down to 10 m depth, and
  - Every 2–3 m deeper than 10 m.
- Taking and proper storage of samples for headspace gas analyses at a sampling frequency of 1 double headspace sample every 2 m (every second section).
- Taking and proper storage (+4° and −80°C) of samples for microbiological postexpedition research (sampling frequency to be determined in personal sample request).
- Pore water geochemistry analysis and taking any other samples for ephemeral properties (alkalinity [pH], ammonium, and salinity) as agreed on in the SMP.
- Core storage (in reefers at a maintained temperature of +4°C).
- Determining preliminary core-seismic integration using subbottom profiles from previous site survey cruises, new data collected during this expedition, and the MSCL data acquired on board *Kaimei* to guide offshore decision making.
- Associated data management of all activities (see below).

To deliver the scientific requirements on the platform with a subset of the science party, a staffing plan has been devised. The

plan requires flexibility of approach from all participants, with priority given to safety, core recovery, curation, and procedures for the measurement of ephemeral properties.

Report preparation will take place on board as required; the reports to be compiled are as follows:

- Daily and weekly operational reports will be compiled by ESO and provided to the management and panels of ECORD and IODP, science party members, and any other relevant parties. Scientific reports are provided by the Co-Chief Scientists. Summarized daily reports will be publicly available on the ESO website for any interested parties.
- Completion of the offshore sections of the Expedition reports (primarily the Expedition 386 methods chapter, but also recording of initial results from offshore observations, measurements, and analyses) will be undertaken by offshore science party members and ESO staff.
- Press releases in line with ECORD outreach policy and information for posting on the ESO expedition website will be managed by the ESO Outreach Team.

Onshore science activities

The OSP will be held on board *Chikyu*, which will be alongside in Shimizu, Japan. The scientific work will follow the SMP to be developed in conjunction with the Co-Chief Scientists. The majority of the scientific reporting for the expedition will also be undertaken during the OSP by science party members.

Details of the facilities that will be available for the OSP can be found on the *Chikyu* wiki page (**http://cdex-science.jamstec.go.jp/chikyu-wiki/index.php/Main_Page**). The SMP will take account of MSP specifications for quality assurance/quality control procedures. The following briefly summarizes the OSP scientific activities:

- Prior to the OSP, all cores will be scanned using the X-ray computed tomography (CT) scanner, providing 0.625 mm thick slices with dimensions of 512 × 512 pixels.
- Prior to the OSP, thermal conductivity measurements will be taken on all cores (as appropriate) using a needle probe. Additional standard IODP physical properties measurements may be undertaken on whole cores at this time in the event offshore data sets are incomplete.
- Core splitting: a permanent archive half will be set aside from each site as per IODP procedure. Should there be a copy of an interval from parallel holes, they may be classified as temporary archives. Both the working and archive halves will be stored long term at the Kochi Core Center (KCC).
- Core description: ESO will provide a data entry system that is IODP standard. For data entry, ESO will employ the Expedition DIS, which is entirely compatible with others being used in IODP. Please see **Data management**.
- High-resolution digital imaging using a digital linescan camera system.
- Color reflectance spectrophotometry using a spectrophotometer.
- Core sampling (1 per section) for expedition ("shipboard") samples (to produce IODP measurements data for the Expedition reports; e.g., petrophysical properties, *P*-wave, and moisture and density [MAD] analyses).
- *P*-wave velocity measurements will be acquired on soft sediments using a pressurized elastic wave velocity measurement system. If lithified sediment occurs, measurements will be acquired on discrete samples using an MSCL Discrete *P*-Wave (MSCL-DPW) system instead.
- MAD will be measured on discrete samples using pycnometers.
- Undrained shear strength will be tested using a vane shear apparatus (model WF23500) by Wykeham Farrance.
- Unconfined compressive strength of the sediments will be tested using a Geotest Instrument Corporation ST315 penetrometer.
- Smear slide preparation (undertaken by sedimentologists and/or micropaleontologists at regular intervals as required; 1 cm^3 volume).
- Thin section preparation (as requested). Please note that only five thin sections can be made per day and that the setting times of the epoxy resin used when preparing soft-sediment thin sections (approximately 5 days) means that there may be a delay to analyzing and reporting on the final thin section slides.
- Biostratigraphy for radiolarians and diatoms as well as characterization of transported benthic foraminifers and calcareous pelagic micro- and nannofossils in event deposits.
- Inorganic geochemistry (whole-rock and pore fluid chemistry) and organic geochemistry. Major, minor, and trace element analysis will be carried out using the acidified pore water samples acquired offshore; in addition, ESO will rerun some samples analyzed offshore on board *Chikyu*:
  - OSP standard headspace gas analysis on a gas chromatograph (GC)-flame ionization detector (FID) (mainly for CH_4).
  - OSP standard chloride measurement by titration (Metrohm Titrino) and, if possible, by ion chromatograph (IC) (ICS-2100 IC system).
  - OSP standard sulfate measurement by IC (ICS-2100 IC system).
  - OSP standard silicate and cation measurement by inductively coupled plasma–atomic emission spectrometer (ICP-AES) (Horiba Jobin Yvon, model Ultima 2).
  - OSP standard trace cation measurement by ICP–mass spectrometer (MS) (Agilent ICP-MS 7500CE).
  - Rerun interstitial water samples:
    - Salinity measured with a refractometer (Atago; RX5000α RX5000i),
    - pH and alkalinity measured by titration (Metrohm Titrino), and
    - Ammonium.
- Bulk mineralogy and X-ray fluorescence (XRF) whole-rock geochemistry: we propose to process one sample every 3 m (maximum) and analyze all X-ray diffraction (XRD), XRF, and total organic carbon (TOC) on board *Chikyu*:
  - OSP standard carbon analysis (total carbon [TC]/TOC) on powdered bulk samples on a carbonate analyzer (UIC coulometer).
  - OSP standard XRF spectroscopy on powdered bulk samples by wavelength dispersive XRF spectrometry (WDXRF) elemental analysis.
  - OSP standard carbon-hydrogen-nitrogen-sulfur (CHNS) elemental analysis on powdered bulk samples with a CHNS/O analyzer (Flash 2000).
  - OSP standard mineralogy: XRD analysis on powdered bulk samples (for bulk mineralogy), likely at a lower resolution.
- Paleomagnetic measurements (using U-channels) including those for magnetostratigraphy.
- Core sampling for personal postexpedition research: a detailed sampling plan will be devised after the scientists have submitted

their revised sample requests following completion of the offshore phase (please see **Research planning: sampling and data sharing strategy**). Sample allocation will be determined by the Sample Allocation Committee (SAC; see below for further details).

In view of the existing geographical distribution of all Deep Sea Drilling Project (DSDP)/Ocean Drilling Program (ODP)/Integrated Ocean Drilling Program/IODP cores, it is understood that the IODP KCC will be the long-term location for the Expedition 386 cores.

Report preparation will take place during the OSP as required by ECORD. The reports to be compiled include the following:

- Weekly progress reports to ECORD and relevant parties. Scientific reports are provided by the Co-Chief Scientists.
- Preliminary Report compiled by the science party (submission to *JOIDES Resolution* Science Operator [JRSO] Publication Services at the end of the OSP).
- Expedition reports compiled by the science party (submission to JRSO Publication Services as soon as practically possible after the OSP).

Staffing

Scientific staffing is determined on the basis of task requirements and nominations from the IODP Program Member Offices (**http://www.iodp.org/program-member-offices**). ESO staffing is based on the need to carry out the drilling and scientific operations safely and efficiently (Tables **T3**, **T4**).

Data management

A data management plan for the expedition will be developed once the data requirements and operational logistics are finalized. The outline plan is as follows:

- The primary data capture and management system will be the Expedition DIS. This is a relational database that will capture drilling, curation, and geoscience metadata and data during the offshore and onshore phases of the expedition.
- The Expedition DIS includes tools for data input, visualization, report generation, and data export.
- The database can be accessed directly by other interpretation or decision-making applications if required.
- A file server will be used for the storage of data not captured in the database (e.g., documents and image files) and the inputs/outputs of any data processing, interpretation, and visualization applications used during the expedition.
- On completion of the offshore phase of the expedition, the Expedition DIS database and the file system will be transferred to *Chikyu* to continue data capture during the OSP.
- Between the end of the offshore phase and the start of the OSP, the expedition scientists will have access to the data via a password-protected website.
- On completion of the OSP, expedition scientists will continue to have access to all data through a password-protected website throughout the moratorium period.
- During the moratorium, all metadata and data will be transferred to PANGAEA for long-term archiving.
- The Petrophysics Staff Scientist will manage the MSCL data and other physical properties data.
- After the moratorium, cores and samples will be archived at the KCC.
- After the moratorium, all the expedition data will be made accessible to the public via the IODP MSP expedition data portal (**http://iodp.pangaea.de**).

Outreach

The ECORD Outreach Task Force (EOTF) will be working to promote the expedition and the science generated by this investigation studying the history of giant earthquakes by sampling in the hadal zone of ultradeepwater trenches—one of the least explored environments in the world. To assist with this, ECORD will be working closely with the JAMSTEC and MarE3 outreach teams to help with both in-country and international outreach activities. As guidance, the EOTF and JAMSTEC produced a communications plan that will be distributed to the science party prior to sailing. The main objectives are as follows:

- To interact positively with the media, nongovernmental organizations, governments, and the general public to demonstrate the benefits of the IODP Japan Trench Paleoseismology scientific expedition and IODP in general;
- To maximize the expedition's publicity impact among scientists and the public;
- To ensure that all outreach is conducted in a consistent way;
- To promote scientific research in respect to the scientific goals;
- To strengthen links between the IODP/ECORD community, JAMSTEC/MarE3 outreach, and the international media; and
- To successfully continue the media relationships established during the previous eight ECORD MSP and other IODP expeditions.

To facilitate the above, a number of outreach activities will be conducted throughout the expedition.

The following outreach activities will take place before the start of the Japan Trench Paleoseismology expedition:

- Develop a detailed Communications Plan in close cooperation with Co-Chief Scientists, ECORD/ESO staff, and JAMSTEC/MarE3. This plan will also include a guide to social media and expedition hashtags, frequently asked questions, and roles and responsibilities.
- Produce and distribute an expedition flyer.
- Produce a media pack on the ECORD website, including the expedition's webpage and biographies of the Co-Chief Scientists and other members of the science party.
- Organize start-up media briefings in Tokyo/Yokosuka, Japan.
- Distribute an international media release in parallel with the start-up media briefing.
- Organize ship visits for the media during mobilization in Japan, if possible and if requested.
- Network with participants' university media offices, particularly the Co-Chief Scientists' host organizations.
- Produce an official expedition logo for use on all promotional materials.

The following outreach activities will take place during the offshore phase of the Japan Trench Paleoseismology expedition:

- Maintain daily/weekly expedition logbook on ESO website (coordinated by ESO Outreach Manager);

- Publish media releases (in the case of special events/findings and, if appropriate, at the end of the expedition);
- Organize video coverage of the working processes on board the expedition vessel (B-roll footage) to be collected by ESO staff and science party members when time allows;
- Promote the expedition through national and international media and organize interviews with Co-Chief Scientists and other science party members as necessary/requested;
- Promote social media blogs compiled by science party and ESO members;
- Collate photographs and video footage that document the entire expedition; and
- Facilitate Ask Me Anything (AMA) Reddit sessions from offshore and onshore, dependent on available bandwidth and connection speeds.

The following outreach activities will take place during the OSP (Autumn/Winter 2020):

- Prepare background material to provide to the media,
- Hold a media day toward the end of the OSP and invite key journalists and TV teams,
- Publish an international media release (tentative results), and
- Document activities with photos and video footage.

The following outreach activities will take place after the expedition:

- Promotion at international conferences (booths and talks) at, for example, the European Geosciences Union (EGU) and American Geophysical Union (AGU) Fall and Ocean Sciences Meetings;
- Promotion of the science through development of education resources in collaboration with teachers, science communicators, and national organizations/visitor attractions and museums;
- General outreach to the media as scientific results of the expedition become available; and
- Continued logging of any outreach activities undertaken by any of the science party members including interviews, blogs, and abstracts submitted. The ESO outreach team will depend on science party members to alert us to anything they do in addition to ESO setting up an Agility Alert for the expedition, which will scan all printed media globally.

Research planning: sampling and data sharing strategy

All researchers requesting samples should refer to the IODP Sample, Data, and Obligations Policy and Implementation Guidelines posted at **http://www.iodp.org/program-documents**. This document outlines the policy for distributing IODP samples and data to research scientists, curators, and educators. The document also defines the obligations that sample and data recipients incur. The SAC (composed of Co-Chief Scientists, Expedition Project Manager, and IODP Curator for Europe [Bremen Core Repository (BCR) and MSPs] or offshore curatorial representative) will work with the entire science party to formulate an expedition-specific sampling plan for shipboard (expedition: offshore and OSP) and postexpedition (personal postexpedition research) sampling.

Members of the science party are expected to carry out scientific research for the expedition and publish it. Before the expedition, all members of the science party are required to submit research plans and associated sample/data requests via the IODP Sample and Data Request (SaDR) system at **http://web.iodp.tamu.edu/sdrm** before the deadline specified in their invitation letters. Based on sample requests submitted by this deadline, the SAC will prepare a tentative sampling plan that can be revised on the ship once cores are split and as dictated by recovery and expedition objectives. All postexpedition research projects should provide scientific justification for desired sample size, numbers, and frequency. The sampling plan will be subject to modification depending upon the material recovered and collaborations that may evolve between scientists during the expedition. This planning process is necessary to coordinate the research to be conducted and to ensure that the scientific objectives are achieved. Modifications to the sampling plan and access to samples and data during the expedition and the 1 y postexpedition moratorium period require the approval of the SAC.

Offshore sampling will be restricted to that necessary for acquiring ephemeral data types that are critical to the overall objectives of the expedition and to preliminary lithologic and biostratigraphic sampling to aid decision making at sea and planning for the OSP.

The permanent archive halves are officially designated by the IODP Curator for the BCR and MSPs. All sample frequencies and volumes must be justified on a scientific basis and will depend on core recovery, the full spectrum of other requests, and the expedition objectives. Some redundancy of measurements is unavoidable, but minimizing the duplication of measurements among the shipboard party and identified shore-based collaborators will be a factor in evaluating sample requests.

If critical intervals are recovered, there may be considerable demand for samples from a limited amount of cored material. A sampling plan coordinated by the SAC will be required before critical intervals are sampled.

The SAC strongly encourages and may require collaboration and/or sharing among the shipboard and shore-based scientists so that the best use is made of the recovered core. Coordination of postexpedition analytical programs is anticipated to ensure that the full range of geochemical, isotopic, and physical properties studies are undertaken on a representative sample suite. The majority of sampling will take place at the OSP on board *Chikyu* in Japan, and the SAC encourages scientists to start developing collaborations before and during the expedition.

Acknowledgments

This publication was prepared by the authors using contributions provided by the proponents of IODP Proposal P866, staff members of the European Consortium for Ocean Research Drilling (ECORD) Science Operator (ESO), Japan Agency for Marine-Earth Science and Technology (JAMSTEC), and Institute for Marine-Earth Exploration and Engineering (MarE3). The following ESO and JAMSTEC staff members contributed to the planning of Expedition 386:

Sarah Davies, European Petrophysics Consortium (EPC) Manager
Nobuhisa Eguchi, Head of Operations, MarE3
Jez Everest, Expedition Project Manager
Patrizia Geprägs, ESO Assistant Laboratory and Curation Manager
Katharina Hochmuth, Petrophysics Staff Scientist
Erwan LeBer, Petrophysics Staff Scientist
Lena Maeda, MarE3/JAMSTEC Liaison

David McInroy, ESO Science Manager
Ursula Röhl, ESO Laboratory and Curation Manager/Onshore Operations Manager
David Smith, Operations Manager
Graham Tulloch, ESO Drilling Coordinator

References

Arai, K., Inoue, T., Ikehara, K., and Sasaki, T., 2014. Episodic subsidence and active deformation of the forearc slope along the Japan Trench near the epicenter of the 2011 Tohoku Earthquake. *Earth and Planetary Science Letters,* 408:9–15. **https://doi.org/10.1016/j.epsl.2014.09.048**

Arai, K., Naruse, H., Miura, R., Kawamura, K., Hino, R., Ito, Y., Inazu, D., et al., 2013. Tsunami-generated turbidity current of the 2011 Tohoku-Oki earthquake. *Geology,* 41(11):1195–1198. **https://doi.org/10.1130/G34777.1**

Bao, R., Strasser, M., McNichol, A.P., Haghipour, N., McIntyre, C., and Wefer, G., 2018. Tectonically-triggered sediment and carbon export to the Hadal zone. *Nature Communication,* 9:121. **https://doi.org/10.1038/s41467-017-02504-1**

Bernhardt, A., Melnick, D., Hebbeln, D., Lückge, A., and Streckera, M.R., 2015. Turbidite paleoseismology along the active continental margin of Chile – Feasible or not? *Quaternary Science Reviews,* 120:71–92. **https://doi.org/10.1016/j.quascirev.2015.04.001**

Boston, B., Moore, G.F., Nakamura, Y., and Kodaira, S., 2014. Outer-rise normal fault development and influence on near-trench décollement propagation along the Japan Trench, off Tohoku. *Earth, Planets and Space,* 66(1):135. **https://doi.org/10.1186/1880-5981-66-135**

Cattaneo, A., Babonneau, N., Ratzov, G., Dan-Unterseh, G., Yelles, K., Bracène, R., Mercier de Lépinay, B., Boudiaf, A., and Déverchère, J., 2012. Searching for the seafloor signature of the 21 May 2003 Boumerdès earthquake offshore central Algeria. *Natural Hazard and Earth System Sciences,* 12(7):2159–2172. **https://doi.org/10.5194/nhess-12-2159-2012**

Chester, F.M., Rowe, C., Ujiie, K., Kirkpatrick, J., Regalla, C., Remitti, F., Moore, J.C., et al., 2013. Structure and composition of the plate-boundary slip zone for the 2011 Tohoku-Oki earthquake. *Science,* 342(6163):1208–1211. **https://doi.org/10.1126/science.1243719**

De Batist, M., Talling, P., Strasser, M., and Girardclos, S., 2017. Subaquatic paleoseismology: records of large Holocene earthquakes in marine and lacustrine sediments. *Marine Geology,* 384:1–224. **https://doi.org/10.1016/j.margeo.2017.04.010**

DeMets, C., Gordon, R.G., and Argus, D.F., 2010. Geologically current plate motions. *Geophysical Journal International,* 181(1):1–80. **https://doi.org/10.1111/j.1365-246X.2009.04491.x**

Fink, H.G., Strasser, M., Römer, M., Kölling, K., Kanamatsu, T., Dinten, D., Kioka, A., et al., 2014. Evidence for mass transport deposits at the IODP JFAST-site in the Japan Trench. *In* Krastel, S., Behrmann, J.-H., Volker, D., Stipp, M., Berndt, C., Urgeles, R., Chaytor, J., Huhn, K., Strasser, M., and Bonnevie Harbitz, C. (Eds.), *Advances in Natural and Technological Hazards Research* (Volume 37): *Submarine Mass Movements and Their Consequences:* Heidelberg, Germany (Springer, Cham), 33–43. **https://doi.org/10.1007/978-3-319-00972-8_4**

Fujii, Y., and Satake, K., 2007. Tsunami source of the 2004 Sumatra-Andaman earthquake inferred from tide gauge and satellite data. *Bulletin of the Seismological Society of America,* 97(1A):S192–S207. **https://doi.org/10.1785/0120050613**

Fujii, Y., Satake, K., Sakai, S., Shinohara, M., and Kanazawa, T., 2011. Tsunami source of the 2011 off the Pacific coast of Tohoku earthquake. *Earth Planets and Space,* 63(7):815–820. **https://doi.org/10.5047/eps.2011.06.010**

Fujiwara, T., Kodaira, S., No, T., Kaiho, Y., Takahashi, N., and Kaneda, Y., 2011. The 2011 Tohoku-Oki earthquake: displacement reaching the trench axis. *Science,* 334(6060):1240. **https://doi.org/10.1126/science.1211554**

Geller, R.J., 2011. Shake-up time for Japanese seismology. *Nature,* 472(7344):407–409. **https://doi.org/10.1038/nature10105**

Goldfinger, C., Galer, S., Beeson, J., Hamilton, T., Black, B., Romsos, C., Patton, J., Nelson, C.H., Hausmann, R., and Morey, A., 2017. The importance of site selection, sediment supply, and hydrodynamics: a case study of submarine paleoseismology on the northern Cascadia margin, Washington USA. *Marine Geology,* 384:4–46. **https://doi.org/10.1016/j.margeo.2016.06.008**

Goldfinger, C., Morey, A.E., Black, B., Beeson, J., Nelson, C.H., and Patton, J., 2013. Spatially limited mud turbidites on the Cascadia margin: segmented earthquake ruptures? *Natural Hazards and Earth System Sciences,* 13(8):2109–2146. **https://doi.org/10.5194/nhess-13-2109-2013**

Goldfinger, C., Nelson, C.H., Morey, A.E., Johnson, J.E., Patton, J.R., Karabanov, E., Gutiérrez-Pastor, J., et al., 2012. Turbidite event history: methods and implications for Holocene paleoseismicity of the Cascadia subduction zone. *USGS Professional Paper,* 1661-F. **https://pubs.usgs.gov/pp/pp1661f/**

Goldfinger, C., Patton, J.R., Van Daele, M., Moernaut, J., Nelson, C.H., de Batist, M., and Morey, A.E., 2014. Can turbidites be used to reconstruct a paleoearthquake record for the central Sumatran margin?: comment. *Geology,* 42(9):e344. **https://doi.org/10.1130/G35558C.1**

Gràcia, E., Vizcaino, A., Escutia, C., Asioli, A., Rodés, Á., Pallàs, R., Garcia-Orellana, J., Lebreiro, S., and Goldfinger, C., 2010. Holocene earthquake record offshore Portugal (SW Iberia): testing turbidite paleoseismology in a slow-convergence margin. *Quaternary Science Reviews,* 29(9–10):1156–1172. **https://doi.org/10.1016/j.quascirev.2010.01.010**

Herrendörfer, R., van Dinther, Y., Gerya, T., and Dalguer, L.A., 2015. Earthquake supercycle in subduction zones controlled by the width of the seismogenic zone. *Nature Geoscience,* 8(6):471–474. **https://doi.org/10.1038/ngeo2427**

Hirano, N., Takahashi, E., Yamamoto, J., Abe, N., Ingle, S.P., Kaneoka, I., Hirata, T., et al., 2006. Volcanism in response to plate flexure. *Science,* 313(5792):1426–1428. **https://doi.org/10.1126/science.1128235**

Ide, S., Baltray, A., and Beroza, G.C., 2011. Shallow dynamic overshoot and energetic deep rupture in the 2011 Mw 9.0 Tohoku-Oki earthquake. *Science,* 332(6036):1426–1429. **https://doi.org/10.1126/science.1207020**

Ikehara, K., Irino, T., Usami, K., Jenkins, R., Omura, A., and Ashi, J., 2014. Possible submarine tsunami deposits on the outer shelf of Sendai Bay, Japan resulting from the 2011 earthquake and tsunami off the Pacific coast of Tohoku. *Marine Geology,* 349:91. **https://doi.org/10.1016/j.margeo.2014.01.001**

Ikehara, K., Kanamatsu, T., Nagahashi, Y., Strasser, M., Fink, H., Usami, K., Irino, T., and Wefer, G., 2016. Documenting large earthquakes similar to the 2011 Tohoku-Oki earthquake from sediments deposited in the Japan Trench over the past 1500 years. *Earth and Planetary Science Letters,* 445:48–56. **https://doi.org/10.1016/j.epsl.2016.04.009**

Ikehara, K., Usami, K., Kanamatsu, T., Arai, K., Yamaguchi, A., and Fukuchi, R., 2018. Spatial variability in sediment lithology and sedimentary processes along the Japan Trench: use of deep-sea turbidite records to reconstruct past large earthquakes. *In* Scourse, E.M., Chapman, N.A., Tappin, D.R., and Wallis, S.R. (Eds.), *Tsunamis: Geology, Hazards and Risks.* Geological Society Special Publications, 456:75–89. **https://doi.org/10.1144/SP456.9**

Ikehara, K., Usami, K., Kanamatsu, T., Danhara, T., and Yamashita, T., 2017. Three important Holocene tephras off the Pacific coast of the Tohoku region, Northeast Japan: implications for correlating onshore and offshore event deposits. *Quaternary International,* 456:138–153. **https://doi.org/10.1016/j.quaint.2017.08.022**

Jamieson, A.J., Fujii, T., Mayor, D.J., Solan, M., and Priede, I.G., 2010. Hadal trenches: the ecology of the deepest places on Earth. *Trends in Ecology & Evolution,* 25(3):190–197. **https://doi.org/10.1016/j.tree.2009.09.009**

Johnson, H.P., Gomberg, J.S., Hautala, S.L., and Salmi, M.S., 2017. Sediment gravity flows triggered by remotely generated earthquake waves. *Journal of Geophysical Research: Solid Earth,* 122(6):4584–4600. **https://doi.org/10.1002/2016JB013689**

Kanamatsu, T., Usami, K., McHugh, C.M.G., and Ikehara, K., 2017. High-resolution chronology of sediment below CCD based on Holocene paleomagnetic secular variations in the Tohoku-Oki earthquake rupture zone. *Geochemistry, Geophysics, Geosystems,* 18(8):2990–3002. **https://doi.org/10.1002/2017GC006878**

Kempf, P., Moernaut, J., Van Daele, M., Vandoorne, W., Pino, M., Urrutia, R., and De Batist, M., 2017. Coastal lake sediments reveal 5500 years of tsunami history in south central Chile. *Quaternary Science Reviews,* 161:99–116. **https://doi.org/10.1016/j.quascirev.2017.02.018**

Kioka, A., et al., submitted. Event stratigraphy in a hadal oceanic trench: The Japan Trench as sedimentary archive recording recurrent giant subduction zone earthquakes and their role in organic carbon export to the deep sea. *Frontiers in Earth Science.*

Kioka, A., Schwestermann, T., Moernaut, J., Ikehara, K., Kanamatsu, T., McHugh, C.M., dos Santos Ferreira, C., et al., 2019. Megathrust earthquake drives drastic organic carbon supply to the hadal trench. *Scientific Reports,* 9:1553. **https://doi.org/10.1038/s41598-019-38834-x**

Kodaira, S., Nakamura, Y., Yamamoto, Y., Obana, K., Fujie, G., No, T., Kaiho, Y., Sato, T., and Miura, S., 2017. Depth-varying structural characters in the rupture zone of the 2011 Tohoku-Oki earthquake. *Geosphere,* 13(5):1408–1424. **https://doi.org/10.1130/GES01489.1**

Kodaira, S., No, T., Nakamura, Y., Fujiwara, T., Kaiho, Y., Miura, S., Takahashi, N., Kaneda, Y., and Taira, A., 2012. Coseismic fault rupture at the trench axis during the 2011 Tohoku-Oki earthquake. *Nature Geoscience,* 5(9): 646–650. **https://doi.org/10.1038/ngeo1547**

Lay, T., 2015. The surge of great earthquakes from 2004 to 2014. *Earth and Planetary Science Letters,* 409:133–146. **https://doi.org/10.1016/j.epsl.2014.10.047**

McHugh, C., Strasser, M., Cattaneo, A., and Ikehara, K., 2015. Submarine paleoseismology: using giant piston coring within IODP to fill the gap in long-term records of great earthquakes [paper presented at U.S. Science Support Program Workshop, Zürich, Switzerland, 16–18 July 2015]. **https://usoceandiscovery.org/wp-content/uploads/2016/02/USSSP-Submarine-Paleoseismology-Workshop-Report.pdf**

McHugh, C.M., Kanamatsu, T., Seeber, L., Bopp, R., Cormier, M.-H., and Usami, K., 2016. Remobilization of surficial slope sediment triggered by the A.D. 2011 M_w 9 Tohoku-Oki earthquake and tsunami along the Japan Trench. *Geology,* 44(5):391–394. **https://doi.org/10.1130/G37650.1**

McHugh, C.M., Seeber, L., Braudy, N., Cormier, M.-H., Davis, M.B., Diebold, J.B., Dieudonne, N., et al., 2011. Offshore sedimentary effects of the 12 January 2010 Haiti earthquake. *Geology,* 39(8):723–726. **https://doi.org/10.1130/G31815.1**

McIntyre, C.P., Wacker, L., Haghipour, N., Blattmann, T., Fahrni, S., Usman, M., Eglinton, T.I., and Synal, H.-A., 2016. Online ^{13}C and ^{14}C gas measurements by EA-IRMS–AMS at ETH Zürich. *Radiocarbon,* 59(3):893–903. **https://doi.org/10.1017/RDC.2016.68**

Migeon, S., Garibaldi, C., Ratzov, G., Schmidt, S., Collot, J.-Y., Zaragosi, S., and Texier, L., 2017. Earthquake-triggered deposits in the subduction trench of the north Ecuador/south Colombia margin and their implication for paleoseismology. *Marine Geology,* 384:47–62. **https://doi.org/10.1016/j.margeo.2016.09.008**

Miura, R., Hino, R., Kawamura, K., Kanamastu, T., and Kaiho, Y., 2014. Accidental sediments trapped in ocean bottom seismometers during the 2011 Tohoku-Oki earthquake. *Island Arc,* 23(4):365–367. **https://doi.org/10.1111/iar.12079**

Moernaut, J., Van Daele, M., Fontijn, K., Heirman, K., Kempf, P., Pino, M., Valdebenito, G., Urrutia, R., Strasser, M., and De Batist, M., 2018. Larger earthquakes recur more periodically: new insights in the megathrust earthquake cycle from lacustrine turbidite records in south-central Chile. *Earth and Planetary Science Letters,* 481:9–19. **https://doi.org/10.1016/j.epsl.2017.10.016**

Molenaar, A., Moernaut, J., Wiemer, G., Dubois, N., and Strasser, M., 2019. Earthquake impact on active margins: tracing surficial remobilization and seismic strengthening in a slope sedimentary sequence. *Geophysical Research Letters,* 46: 6015– 6023. **https://doi.org/10.1029/2019GL082350**

Mountjoy, J.J., Howarth, J.D., Orpin, A.R., Barnes, P.M., Bowden, D.A., Rowden, A.A., Schimel, A.C.G., et al., 2018. Earthquakes drive large-scale submarine canyon development and sediment supply to deep-ocean basins. *Science Advances,* 4(3):eaar3748. **https://doi.org/10.1126/sciadv.aar3748**

Mulargia, F., Stark, P.B., and Geller, R.J., 2017. Why is probabilistic seismic hazard analysis (PSHA) still used? *Physics of the Earth and Planetary Interiors,* 264:63–75. **https://doi.org/10.1016/j.pepi.2016.12.002**

Nakamura, T., Takenaka, H., Okamoto, T., Ohori, M., and Tsuboi, S., 2015. Long-period ocean-bottom motions in the source areas of large subduction earthquakes. *Scientific Reports,* 5:16648. **https://doi.org/10.1038/srep16648**

Nakamura, Y., Kodaira, S., Miura, S., Regalla, C., and Takahashi, N., 2013. High-resolution seismic imaging in the Japan Trench axis area off Miyagi, northeastern Japan. *Geophysical Research Letters,* 40(9):1713–1718. **https://doi.org/10.1002/grl.50364**

Namegaya, Y., and Satake, K., 2014. Reexamination of the A.D. 869 Jogan earthquake size from tsunami deposit distribution, simulated flow depth, and velocity. *Geophysical Research Letters,* 41(7):2297–2303. **https://doi.org/10.1002/2013GL058678**

Noguchi, T., Tanikawa, W., Hirose, T., Lin, W., Kawagucci, S., Yoshida-Takashima, Y., Honda, M.C., Takai, K., Kitazato, H., and Okamura, K., 2012. Dynamic process of turbidity generation triggered by the 2011 Tohoku-Oki earthquake. *Geochemistry, Geophysics, Geosystems,* 13(11):Q11003. **https://doi.org/10.1029/2012GC004360**

Nomaki, H., Arai, K., Suga, H., Toyofuku, T., Wakita, M., Nunoura, T., Oguri, K., Kasaya, T., and Watanabe, S., 2016. Sedimentary organic matter contents and porewater chemistry at upper bathyal depths influenced by the 2011 off the Pacific coast of Tohoku Earthquake and tsunami. *Journal of Oceanography,* 72(1):99–111. **https://doi.org/10.1007/s10872-015-0315-3**

Oguri, K., Furushima, Y., Toyofuku, T., Kasaya, T., Wakita, M., Watanabe, S., Fujikura, K., and Kitazato, H., 2016. Long-term monitoring of bottom environments of the continental slope off Otsuchi Bay, northeastern Japan. *Journal of Oceanography,* 72(1):151–166. **https://doi.org/10.1007/s10872-015-0330-4**

Oguri, K., Kawamura, K., Sakaguchi, A., Toyofuku, T., Kasaya, T., Murayama, M., Fujikura, K., Glud, R.N., and Kitazato, H., 2013. Hadal disturbance in the Japan Trench induced by the 2011 Tohoku–Oki Earthquake. *Science Reports,* 3:1915. **https://doi.org/10.1038/srep01915**

Patton, J.R., Goldfinger, C., Morey, A.E., Ikehara, K., Romsos, C., Stoner, J., and Djadjadihardja, Y., 2015. A 6600 year earthquake history in the region of the 2004 Sumatra-Andaman subduction zone earthquake. *Geosphere,* 11(6):2067–2129. **https://doi.org/10.1130/GES01066.1**

Polonia, A., Bonatti, E., Camerlenghi, A., Lucchi, R.G., Panieri, G., and Gasperini, L., 2013. Mediterranean megaturbidite triggered by the AD 365 Crete earthquake and tsunami. *Scientific Reports,* 3:1285. **https://doi.org/10.1038/srep01285**

Polonia, A., Nelson, C.H., Romano, S., Vaiani, S.C., Colizza, E., Gasparotto, G., and Gasperini, L., 2017. A depositional model for seismo-turbidites in confined basins based on Ionian Sea deposits. *Marine Geology,* 384:177–198. **https://doi.org/10.1016/j.margeo.2016.05.010**

Polonia, A., Vaiani, S.C., and de Lange, G.J., 2016. Did the A.D. 365 Crete earthquake/tsunami trigger synchronous giant turbidity currents in the Mediterranean Sea? *Geology,* 44(3):191–194. **https://doi.org/10.1130/G37486.1**

Pope, E.L., Talling, P.J., and Carter, L., 2017. Which earthquakes trigger damaging submarine mass movements: insights from a global record of submarine cable breaks? *Marine Geology,* 384:131–146. **https://doi.org/10.1016/j.margeo.2016.01.009**

Pouderoux, H., Lamarche, G., and Proust, J.-N., 2012. Building an 18 000-year-long paleo-earthquake record from detailed deep-sea turbidite characterisation in Poverty Bay, New Zealand. *Natural Hazards and Earth System Sciences,* 12(6):2077–2101. **https://doi.org/10.5194/nhess-12-2077-2012**

Pouderoux, H., Proust, J.-N., and Lamarche, G., 2014. Submarine paleoseismology of the northern Hikurangi subduction margin of New Zealand as deduced from Turbidite record since 16 ka. *Quaternary Science Reviews,* 84:116–131. **https://doi.org/10.1016/j.quascirev.2013.11.015**

Ratzov, G., Cattaneo, A., Babonneau, N., Déverchère, J., Yelles, K., Bracene, R., and Courboulex, F., 2015. Holocene turbidites record earthquake super-

cycles at a slow-rate plate boundary. *Geology,* 43(4):331–334. **https://doi.org/10.1130/G36170.1**

Rosenheim, B.E., Day, M.B., Domack, E., Schrum, H., Benthien, A., and Hayes, J.M., 2008. Antarctic sediment chronology by programmed-temperature pyrolysis: methodology and data treatment. *Geochemistry, Geophysics, Geosystems,* 9(4):Q04005. **https://doi.org/10.1029/2007GC001816**

Saino, T., Shang, Sh., Mino, Y., Suzuki, K., Nomura, H., Saitoh, S., Miyake, H., Masuzawa, T., and Harada, K., 1998. Short term variability of particle fluxes and its relation to variability in sea surface temperature and chlorophylla field detected by Ocean Color and Temperature Scanner (OCTS) off Sanriku, northwestern North Pacific in the spring of 1997. *Journal of Oceanography,* 54(5):583–592. **https://doi.org/10.1007/BF02742460**

Sawai, Y., Namegaya, Y., Okamura, Y., Satake, K., and Shishikura, M., 2012. Challenges of anticipating the 2011 Tohoku earthquake and tsunami using coastal geology. *Geophysical Research Letters,* 39(21):L21309. **https://doi.org/10.1029/2012GL053692**

Sawai, Y., Namegaya, Y., Tamura, T., Nakashima, R., and Tanigawa, K., 2015. Shorter intervals between great earthquakes near Sendai: Scour ponds and a sand layer attributable to A.D. 1454 overwash. *Geophysical Research Letters,* 42(12):4795–4800. **https://doi.org/10.1002/2015GL064167**

Sawyer, D.E., and DeVore, J.R., 2015. Elevated shear strength of sediments on active margins: evidence for seismic strengthening. *Geophysical Research Letters,* 42(23):10216–10221. **https://doi.org/10.1002/2015GL066603**

Seeber, L., Mueller, C., Fujiwara, T., Arai, K., Soh, W., Djajadihardja, Y.S., and Cormier, M.-H., 2007. Accretion, mass wasting, and partitioned strain over the 26 Dec 2004 Mw9.2 rupture offshore Aceh, northern Sumatra. *Earth and Planetary Science Letters,* 263(1–2):16–31. **https://doi.org/10.1016/j.epsl.2007.07.057**

Shibazaki, B., Matsuzawa, T., Tsutsumi, A., Ujiie, K., Hasegawa, A., and Ito, Y., 2011. 3D modeling of the cycle of a great Tohoku-Oki earthquake, considering frictional behavior at low to high slip velocities. *Geophysical Research Letters,* 38(21):L21305. **https://doi.org/10.1029/2011GL049308**

Shipboard Scientific Party, 1980. Site 440: Japan Trench midslope terrace, Leg 57. *In* Scientific Party, *Initial Reports of the Deep Sea Drilling Project,* 56/57: Washington, DC (U.S. Government Printing Office), 225–317. **https://doi.org/10.2973/dsdp.proc.5657.1980**

Shirasaki, Y., Ito, K., Kuwazuru, M, and Shimizu K., 2012. Submarine landslides as cause of submarine cable fault. *Marine Survey & Technology,* 24(1):17–20.

Sieh, K., Natawidjaja, D.H., Meltzner, A.J., Shen, C.-C., Cheng, H., Li, K.-S., Suwargadi, B.W., Galetzka, J., Philbosian, B., and Edwards, R.L., 2008. Earthquake supercycles inferred from sea-level changes recorded in the corals of west Sumatra. *Science,* 322(5908):1674–1678. **https://doi.org/10.1126/science.1163589**

St-Onge, G., Chapron, E., Mulsow, S., Salas, M., Viel, M., Debret, M., Foucher, A., Mulder, T., et al., 2012. Comparison of earthquake-triggered turbidites from the Saguenay (Eastern Canada) and Reloncavi (Chilean margin) Fjords: implications for paleoseismicity and sedimentology. *Sedimentary Geology,* 243–244:89–107. **https://doi.org/10.1016/j.sedgeo.2011.11.003**

Strasser, M., Cattaneo, A., Ikehara, K., and McHugh, C., 2015. Submarine paleoseismology: using giant-piston coring within IODP to fill the gap in long-term records of great earthquakes—16–18 July 2015, Zurich (Switzerland). *ECORD Newsletter,* 25:24. **https://www.ecord.org/?ddownload=1108**

Strasser, M., Kölling, M., dos Santos Ferreira, C., Fink, H.G., Fujiwara, T., Henkel, S., Ikehara, K., et al., 2013. A slump in the trench: tracking the impact of the 2011 Tohoku-Oki earthquake. *Geology,* 41(8):935–938. **https://doi.org/10.1130/G34477.1**

Strasser, M., Kopf, A.J., Abegg, F., Asada, M., Bachmann, A.K., Cuno, P., Dos Santos Ferreira, C., et al., 2017. Report and preliminary results of R/V *Sonne* Cruise SO251, extreme events archived in the geological record of Japan's subduction margins (EAGER-Japan), Berichte, MARUM – Zentrum für Marine Umweltwissenschaften, Fachbereich Geowissenschaften, Universität Bremen, 318. **http://publications.marum.de/id/eprint/3677**

Sumner, E.J., Siti, M.I., McNeill, L.C., Talling, P.J., Henstock, T.J., Wynn, R.B., Djajadihardja, Y.S., and Permana, H., 2013. Can turbidites be used to reconstruct a paleoearthquake record for the central Sumatran margin? *Geology,* 41(7):763–766. **https://doi.org/10.1130/G34298.1**

Sun, T., Wang, K., Fujiwara, T., Kodaira, S., He, J., 2017. Large fault slip peaking at trench in the 2011 Tohoku-Oki earthquake. *Nature Communications,* 8:14044. **https://doi.org/10.1038/ncomms14044**

Talling, P.J., 2014. On the triggers, resulting flow types and frequencies of subaqueous sediment density flows in different settings. *Marine Geology,* 352:155–182. **https://doi.org/10.1016/j.margeo.2014.02.006**

ten Brink, U.S., Andrews, B.D., and Miller, N.C., 2016. Seismicity and sedimentation rate effects on submarine slope stability. *Geology,* 44(7):563–566. **https://doi.org/10.1130/G37866.1**

Tsuru, T., Park, J.-O., Miura, S., Kodaira, S., Kido, Y., and Hayashi, T., 2002. Along-arc structural variation of the plate boundary at the Japan Trench margin: Implication of interplate coupling. *Journal of Geophysical Research: Solid Earth,* 107(B12):ESE 11-1–ESE 11-15. **https://doi.org/10.1029/2001JB001664**

Uchida, N., and Matsuzawa, T., 2011. Coupling coefficient, hierarchical structure, and earthquake cycle for the source area of the 2011 off the Pacific coast of Tohoku earthquake inferred from small repeating earthquake data. *Earth, Planets and Space,* 63(7): 675–679. **https://doi.org/10.5047/eps.2011.07.006**

Usami, K., Ikehara, K., Jenkins, R.G., and Ashi, J., 2017. Benthic foraminiferal evidence of deep-sea sediment transport by the 2011 Tohoku-Oki earthquake and tsunami. *Marine Geology,* 384:214–224. **https://doi.org/10.1016/j.margeo.2016.04.001**

Usami, K., Ikehara, K., Kanamatsu, T., and McHugh, C.M., 2018. Supercycle in great earthquake recurrence along the Japan Trench over the last 4000 years. *Geosciences Letters,* 5:11. **https://doi.org/10.1186/s40562-018-0110-2**

von Huene, R., and Lallemand, S., 1990. Tectonic erosion along the Japan and Peru convergent margins. *Geological Society of America Bulletin,* 102(6):704–720. **https://doi.org/10.1130/0016-7606(1990)102<0704:TEATJA>2.3.CO;2**

von Huene, R., Langseth, M., and Nasu, N., 1980. Summary, Japan Trench Transect. *In* Scientific Party, *Initial Reports of the Deep Sea Drilling Project,* 56/57: Washington, DC (U.S. Government Printing Office), 473–488. **https://doi.org/10.2973/dsdp.proc.5657.111.1980**

Ye, L., Lay, T., and Kanamori, H., 2013. Ground shaking and seismic source spectra for large earthquakes around the megathrust fault offshore of northeastern Honshu, Japan. *Bulletin of the Seismological Society of America,* 103(2B):1221–1241. **https://doi.org/10.1785/0120120115**

Yoshikawa, S., Kanamatsu, T., and Kasaya, T., 2016. Small-scale spatial variation in near-surface turbidites around the JFAST site near the Japan Trench. *Geochemistry, Geophysics, Geosystems,* 17(3):1238–1246. **https://doi.org/10.1002/2015GC006114**

Table T1. Location of and information for proposed primary and alternate sites. JTPS = southern Japan Trench, JTPC = central Japan Trench, JTPN = northern Japan Trench, JT = Japan Trench. O = objective. (Continued on next three pages.)

Site	Position (latitude, longitude)	Water depth (m)	Penetration (m)	Site-specific objectives
JTPS-01A (primary)	36.07202, 142.73503	8030	40	1. Recover an expanded (relative to coupled Site JTPS-02A) continuous Holocene stratigraphic succession (potentially reaching the upper Pleistocene) comprising event deposits from the deepest depocenter in the southernmost part of the JT. 2. Analyze the stratigraphic pattern and event deposit characteristics and integrate with Site JTPS-02A to establish robust stratigraphic pattern recognition of proxy evidence of earthquakes (O-1). 3. Compare results with all other sites to explore spatiotemporal distribution of event deposits and the northward extent of sediment transport routed through the Nakaminato Canyon (O-2) to develop a long-term record for giant earthquakes (O-3).
JTPS-02A (primary)	36.10118, 142.75813	8000	40	1. Recover a condensed (relative to coupled Site JTPS-01A), continuous upper Pleistocene–Holocene stratigraphic succession, comprising thin sedimentary event deposits on a trench floor high near the deepest depocenter in the southernmost part of the JT study area. 2. Analyze the stratigraphic pattern and event deposit characteristics and integrate with results from expanded couple Site JTPS-01A to establish robust stratigraphic pattern recognition of proxy evidence of earthquakes (O-1). 3. Compare results with all other sites to explore spatiotemporal distribution of event deposits and the northward extent of sediment transport routed through the Nakaminato Canyon (O-2) to develop a long-term record for giant earthquakes (O-3).
JTPS-03A (alternate)	36.22997, 142.88166	7990	35	1. Recover a condensed (relative to coupled Site JTPS-04A) continuous upper Pleistocene–Holocene stratigraphic succession, comprising event deposits on an elevated trench floor morphology in the southernmost trench basin (alternate site to JTPS-02A in <8 km water depth). 2. Analyze the stratigraphic pattern and event deposit characteristics and integrate with Site JTPS-04A to establish robust stratigraphic pattern recognition of proxy evidence of earthquakes (O-1). 3. Compare results with all other sites to explore spatiotemporal distribution of event deposits and the northward extent of sediment transport routed through the Nakaminato Canyon (O-2) to develop a long-term record for giant earthquakes (O-3).
JTPS-04A (alternate)	36.24424, 142.89031	7990	40	1. Recover an expanded (relative to coupled Site JTPS-03A), continuous Holocene stratigraphic succession (potentially reaching the upper Pleistocene), comprising event deposits from a local depocenter on an elevated trench floor morphology in the southernmost trench basin (alternate site to JTPS-01A in <8 km water depth). 2. Analyze the stratigraphic pattern and event deposit characteristics and integrate with Site JTPS-03A to establish robust stratigraphic pattern recognition of proxy evidence of earthquakes (O-1). 3. Compare results with all other sites to explore spatiotemporal distribution of event deposits and the northward extent of sediment transport routed through the Nakaminato Canyon (O-2) to develop a long-term record for giant earthquakes (O-3).
JTPS-05B (primary)	36.89173, 143.40772	7700	40	1. Recover a continuous upper Pleistocene–Holocene stratigraphic succession (condensed in the upper part and more expanded in the lower part; relative to coupled Site JTPS-06B), comprising event deposits from a small isolated trench basin in the central part of the southern JT. 2. Analyze the stratigraphic pattern and event deposit characteristics and integrate with Site JTPS-06B to establish robust stratigraphic pattern recognition of proxy evidence of earthquakes (O-1). 3. Compare results with all other sites to explore spatiotemporal distribution of event deposits and the northward extent of sediment transport routed through the Nakaminato Canyon (O-2) to develop a long-term record for giant earthquakes (O-3).
JTPS-06B (primary)	36.91171, 143.42432	7710	40	1. Recover a continuous upper Pleistocene–Holocene stratigraphic succession (expanded in the upper part and more condensed in the lower part; relative to coupled Site JTPS-05B), comprising event deposits from a small isolated trench basin in the central part of the southern JT. 2. Analyze the stratigraphic pattern and event deposit characteristics and integrate with Site JTPS-05B to establish robust stratigraphic pattern recognition of proxy evidence of earthquakes (O-1). 3. Compare results with all other sites to explore spatiotemporal distribution of event deposits and the northward extent of sediment transport routed through the Nakaminato Canyon (O-2) to develop a long-term record for giant earthquakes (O-3).
JTPS-07A (primary)	37.41496, 143.73196	7820	40	1. Recover a continuous upper Pleistocene–Holocene stratigraphic succession comprising event deposits from an isolated trench basin in the north-central part of the southern JT (would be expanded section relative to coupled contingency Site JTPS-08A). 2. Analyze the stratigraphic pattern and event deposit characteristics (at best integrated with contingency coring Site JTPS-08A) and compare with integrated results from Sites JTPS-09A and JTPS-10A to establish robust stratigraphic pattern recognition of proxy evidence of earthquakes (O-1). 3. Compare results with all other sites to explore spatiotemporal distribution of event deposits (O-2) to develop a long-term record for giant earthquakes (O-3).
JTPS-08A (alternate)	37.42749, 143.73726	7820	30	1. Recover a continuous upper Pleistocene–Holocene stratigraphic succession comprising event deposits from the isolated trench basin in the north-central part of the southern JT. Contingency site as condensed section relative to coupled Site JTPS-07A. 2. Analyze the stratigraphic pattern and event deposit characteristics and integrate with Site JTPS-07A to establish robust stratigraphic pattern recognition of proxy evidence of earthquakes (O-1). 3. Compare results with all other sites to explore spatiotemporal distribution of event deposits (O-2) to develop a long-term record for giant earthquakes (O-3).
JTPS-09A (primary)	37.68110, 143.86610	7550	40	1. Recover an expanded (relative to coupled Site JTPS-10A) continuous upper Pleistocene–Holocene stratigraphic succession comprising event deposits from an isolated trench basin in the northernmost part of the southern JT. 2. Analyze the stratigraphic pattern and event deposit characteristics and integrate with Site JTPS-10A to establish robust stratigraphic pattern recognition of proxy evidence of earthquakes (O-1). 3. Compare results with all other sites to explore spatiotemporal distribution of event deposits (O-2) to develop a long-term record for giant earthquakes (O-3).

Table T1 (continued). (Continued on next page.)

Site	Position (latitude, longitude)	Water depth (m)	Penetration (m)	Site-specific objectives
JTPS-10A (primary)	37.70031, 143.87689	7540	40	1. Recover a condensed (relative to coupled Site JTPS-09A) continuous upper Pleistocene–Holocene stratigraphic succession comprising event deposits from the isolated trench basin in the northernmost part of the southern JT. 2. Analyze the stratigraphic pattern and event deposit characteristics and integrate with Site JTPS-09A to establish robust stratigraphic pattern recognition of proxy evidence of earthquakes (O-1). 3. Compare results with all other sites to explore spatiotemporal distribution of event deposits (O-2) to develop a long-term record for giant earthquakes (O-3).
JTPC-01A (primary)	38.00853, 144.00566	7570	30	1. Recover a condensed (relative to coupled Site JTPC-02A) continuous Holocene stratigraphic succession (potentially reaching the upper Pleistocene) comprising event deposits from the isolated trench basin in the structurally complex area affected by 2011 coseismic rupture propagation to the trench. 2. Recover and analyze the top of an older trench-fill deformation event. 3. Analyze the stratigraphic pattern and event deposit characteristics and integrate with Site JTPC-02A to assess local variability and establish robust stratigraphic pattern recognition of proxy evidence of earthquakes (O-1). 4. Compare results with all other sites to explore spatiotemporal distribution of earthquake event deposits (O-2) to develop a long-term record for giant earthquakes (O-3).
JTPC-02A (primary)	38.02804, 144.00227	7570	35	1. Recover an expanded (relative to coupled Site JTPC-01A) continuous Holocene stratigraphic succession (potentially reaching the upper Pleistocene) comprising event deposits from the isolated trench basin in the structurally complex area affected by 2011 coseismic rupture propagation to the trench. 2. Recover and analyze the top of an older trench-fill deformation event. 3. Analyze the stratigraphic pattern and event deposit characteristics and integrate with Site JTPC-01A to assess local variability and establish robust stratigraphic pattern recognition of proxy evidence of earthquakes (O-1). 4. Compare results with all other sites to explore spatiotemporal distribution of event deposits (O-2) to develop a long-term record for giant earthquakes (O-3).
JTPC-03B (primary)	38.29761, 144.05920	7460	40	1. Recover a continuous upper Pleistocene–Holocene stratigraphic succession comprising event deposits from the isolated trench basin within the relatively elevated trench floor segment in the central JT. 2. Analyze the stratigraphic pattern and event deposit characteristics and compare with integrated results from couple Sites JTPC-01A and JTPC-02A in the south and Site JTPC-05B in the north to establish robust stratigraphic pattern recognition of proxy evidence of earthquakes (O-1). 3. Compare results with all other sites to explore spatiotemporal distribution of event deposits (O-2) to develop a long-term record for giant earthquakes (O-3).
JTPC-04A (alternate)	38.57586, 144.12499	7560	40	1. Recover a continuous upper Pleistocene–Holocene stratigraphic succession comprising event deposits from an isolated graben-fill basin in the structurally complex central part of the central JT, where the neighboring trench basin only comprises disturbed sections. Contingency site as condensed section relative to coupled Site (s. l.) JTPC-05A. 2. Analyze the stratigraphic pattern and event deposit characteristics and integrate with Site JTPC-05A to establish robust stratigraphic pattern recognition of proxy evidence of earthquakes (O-1). 3. Compare results with all other sites to explore spatiotemporal distribution of event deposits (O-2) to develop a long-term record for giant earthquakes (O-3).
JTPC-05A (primary)	38.75801, 144.12942	7620	40	1. Recover continuous upper Pleistocene–Holocene stratigraphic succession comprising event deposits from a trench basin in the central JT (expanded section of coupled contingency graben basin Sites (s.l.) JTPC-04A and JTPC-07A). 2. Analyze stratigraphic pattern and event deposit characteristics (at best integrated with contingency Sites JTPC-04A and JTPC-07A) and compare with results from couple Sites JTPC-08A and JTPC-09A in the north and Site JTPC-03A in the south to establish robust stratigraphic pattern recognition of proxy evidence of earthquakes (O-1). 3. Compare results with all other sites to explore spatiotemporal distribution of event deposits (O-2) to develop a long-term record for giant earthquakes (O-3).
JTPC-06B (alternate)	38.86920, 144.15224	7630	35	1. Recover a continuous upper Pleistocene–Holocene stratigraphic succession comprising event deposits from the isolated trench basin in the northern–central part of the central JT. Alternate sites to JTPC-05B and JTPC-09A, and contingency coring site (coupled [s.l.] with the relatively condensed Site JTPC-07A). 2. Analyze the stratigraphic pattern and event deposit characteristics and integrate with Site JTPC-07A to establish robust stratigraphic pattern recognition of proxy evidence of earthquakes (O-1). 3. Compare results with all other sites to explore spatiotemporal distribution of event deposits (O-2) to develop a long-term record for giant earthquakes (O-3).
JTPC-07A (alternate)	38.91249, 144.21916	7400	40	1. Recover a continuous upper Pleistocene–Holocene stratigraphic succession comprising event deposits from an isolated graben-fill basin in the northern–central part of the central JT. Alternate sites to JTPC-04A and JTPC-08A, and contingency coring site (coupled [s.l.] with the relatively expanded sections at Sites JTPC-06B/JTPC-10A). 2. Analyze the stratigraphic pattern and event deposit characteristics and integrate with Sites JTPC-06B/JTPC-10A to establish robust stratigraphic pattern recognition of proxy evidence of earthquakes (O-1). 3. Compare results with all other sites to explore spatiotemporal distribution of event deposits (O-2) to develop a long-term record for giant earthquakes (O-3).

Table T1 (continued). (Continued on next page.)

Site	Position (latitude, longitude)	Water depth (m)	Penetration (m)	Site-specific objectives
JTPC-08A (primary)	39.03126, 144.24752	7340	40	1. Recover a condensed (relative to coupled Site s.l. JTPC-09A) continuous upper Pleistocene–Holocene stratigraphic succession comprising event deposits from an isolated graben-fill basin in the structurally complex northern part of the central JT, where the neighboring trench basin is at the same water depth but only comprises disturbed sections. 2. Analyze the stratigraphic pattern and event deposit characteristics and integrate with Site JTPC-09A to establish robust stratigraphic pattern recognition of proxy evidence of earthquakes (O-1). 3. Compare results with all other sites to explore spatiotemporal distribution of event deposits (O-2) to develop a long-term record for giant earthquakes (O-3).
JTPC-09A (primary)	39.08195, 144.21682	7440	35	1. Recover an expanded (relative to coupled Site s.l. JTPC-08A) continuous upper Pleistocene–Holocene stratigraphic succession comprising event deposits from an isolated narrow trench basin in the structurally complex northern part of the central JT. 2. Analyze the stratigraphic pattern and event deposit characteristics and integrate with Site JTPC-08A to establish robust stratigraphic pattern recognition of proxy evidence of earthquakes (O-1). 3. Compare results with all other sites to explore spatiotemporal distribution of event deposits (O-2) to develop a long-term record for giant earthquakes (O-3).
JTPC-10A (alternate)	38.90768, 144.15905	7640	40	1. Recover a continuous upper Pleistocene–Holocene stratigraphic succession comprising event deposits from the isolated trench basin in the northern–central part of the central JT. Alternate sites to JTPC-05A and JTPC-09A, and contingency coring site (coupled [s.l.] with the relatively condensed Site JTPC-07A). 2. Analyze the stratigraphic pattern and event deposit characteristics and integrate with Site JTPC-07A to establish robust stratigraphic pattern recognition of proxy evidence of earthquakes (O-1). 3. Compare results with all other sites to explore spatiotemporal distribution of event deposits (O-2) to develop a long-term record for giant earthquakes (O-3).
JTPN-01A (alternate)	39.24858, 144.20297	7460	30	1. Recover a continuous upper Pleistocene–Holocene stratigraphic succession (potentially reaching the middle Pleistocene) comprising event deposits from the trench basin south of the large >1 km high escarpment at 39.4°N (alternate site to JTPN-02A). 2. Recover and analyze the top of mass transport deposits potentially linked to the megalandslide. 3. Analyze the stratigraphic pattern and event deposit characteristics and compare with Sites JTPC-08A and JTPC-09A to assess local variability and establish robust stratigraphic pattern recognition of proxy evidence of earthquakes (O-1). 4. Compare results with all other sites to explore spatiotemporal distribution of event deposits (O-2) to develop a long-term record for giant earthquakes (O-3).
JTPN-02A (primary)	39.44436, 144.21630	7520	30	1. Recover continuous upper Pleistocene–Holocene stratigraphic succession (potentially reaching the middle Pleistocene) comprising event deposits from the trench basin north of the large >1 km high escarpment at 39.4°N. 2. Recover and analyze the top of mass transport deposits potentially linked to the megalandslide. 3. Analyze the stratigraphic pattern and event deposit characteristics (at best integrated with contingency coring Site JTPN-03A) and compare with Sites JTPN-04A and JTPN-05A/JTPC-08A and JTPN-09A to assess local variability and establish robust stratigraphic pattern recognition of proxy evidence of earthquakes (O-1). 4. Compare results with all other sites to explore spatiotemporal distribution of event deposits (O-2) to develop a long-term record for giant earthquakes (O-3).
JTPN-03A (alternate)	39.51979, 144.32902	7250	40	1. Recover a continuous upper Pleistocene–Holocene stratigraphic succession (potentially reaching the middle Pleistocene) comprising event deposits from an isolated graben-fill basin near the large >1 km high escarpment and petit-spot volcano field. Contingency site as condensed section relative to coupled Site (s.l.) JTPN-02A. 2. Analyze the stratigraphic pattern and event deposit characteristics and integrate with Site JTPN-02A to establish robust stratigraphic pattern recognition of proxy evidence of earthquakes (O-1). 3. Compare results with all other sites to explore spatiotemporal distribution of event deposits (O-2) to develop a long-term record for giant earthquakes (O-3).
JTPN-04A (alternate)	39.76647, 144.26910	7470	40	1. Recover continuous upper Pleistocene–Holocene stratigraphic succession (potentially reaching the middle Pleistocene) comprising event deposits from the isolated trench basin in the central part of the northern JT. Alternate site to JTPN-07A and contingency site as condensed section relative to coupled Site JTPN-05A. 2. Analyze the stratigraphic pattern and event deposit characteristics and integrate with Site JTPN-05A to establish robust stratigraphic pattern recognition of proxy evidence of earthquakes (O-1). 3. Compare results with all other sites to explore spatiotemporal distribution of event deposits and the southward extent of sediment transport routed through the Ogawara Canyon (O-2) to develop a long-term record for giant earthquakes (O-3).
JTPN-05A (primary)	39.78013, 144.27636	7480	40	1. Recover continuous upper Pleistocene–Holocene (potentially reaching the middle Pleistocene) stratigraphic succession comprising event deposits from a trench basin in the central area of northern JT (would be expanded section relative to coupled contingency Site JTPN-04A). 2. Analyze the stratigraphic pattern and event deposit characteristics (at best integrated with Site JTPN-04A) and compare with Sites JTPN-02A and JTPN-07A to establish robust stratigraphic pattern recognition of proxy evidence of earthquakes (O-1). 3. Compare results with all other sites to explore spatiotemporal distribution of event deposits and the southward extent of sediment transport routed through the Ogawara Canyon (O-2) to develop a long-term record for giant earthquakes (O-3).

Table T1 (continued).

Site	Position (latitude, longitude)	Water depth (m)	Penetration (m)	Site-specific objectives
JTPN-06A (alternate)	40.05940, 144.31855	7570	40	1. Recover a continuous upper Pleistocene–Holocene stratigraphic succession (potentially reaching the middle Pleistocene) comprising event deposits from a trench basin in the central area of the northern JT. Alternate site to JTPN-05A and contingency site as condensed section relative to coupled Site JTPN-07A. 2. Analyze the stratigraphic pattern and event deposit characteristics and integrate with Site JTPN-07A to establish robust stratigraphic pattern recognition of proxy evidence of earthquakes (O-1). 3. Compare results with all other sites to explore spatiotemporal distribution of event deposits and the southward extent of sediment transport routed through the Ogawara Canyon (O-2) to develop a long-term record for giant earthquakes (O-3).
JTPN-07A (primary)	40.09392, 144.32612	7560	40	1. Recover continuous upper Pleistocene–Holocene (potentially reaching the middle Pleistocene) stratigraphic succession comprising event deposits from the isolated trench basin in the central part of the northern JT (would be expanded section relative to coupled contingency Site JTPN-04A). 2. Analyze the stratigraphic pattern and event deposit characteristics (at best integrated with Site JTPN-06A) and compare with Site JTPN-05A to establish robust stratigraphic pattern recognition of proxy evidence of earthquakes (O-1). 3. Compare results with all other sites to explore spatiotemporal distribution of event deposits and the southward extent of sediment transport routed through the Ogawara Canyon (O-2) to develop a long-term record for giant earthquakes (O-3).
JTPN-08A (alternate)	40.32440, 144.40110	7600	40	1. Recover an expanded (relative to coupled Site JTPN-11A) continuous upper Pleistocene–Holocene stratigraphic succession (potentially reaching the middle Pleistocene) comprising event deposits from the isolated trench basin in the northernmost JT. Alternate site to JTPN-09A. 2. Analyze the stratigraphic pattern and event deposit characteristics and integrate with results from couple Site JTPN-11A to establish robust stratigraphic pattern recognition of proxy evidence of earthquakes (O-1). 3. Compare results with all other sites to explore spatiotemporal distribution of event deposits and the southward extent of sediment transport routed through the Ogawara Canyon (O-2) to develop a long term record for giant earthquakes (O-3).
JTPN-09A (primary)	40.39568, 144.42047	7620	40	1. Recover an expanded (relative to coupled Site JTPN-10A), continuous upper Pleistocene–Holocene stratigraphic succession (potentially reaching the middle Pleistocene) comprising event deposits from the deepest depocenter in the northernmost part of the JT. 2. Analyze the stratigraphic pattern and event deposit characteristics and integrate with results from couple Site JTPN-10A to establish robust stratigraphic pattern recognition of proxy evidence of earthquakes (O-1). 3. Compare results with all other sites to explore spatiotemporal distribution of event deposits and the southward extent of sediment transport routed through the Ogawara Canyon (O-2) to develop a long-term record for giant earthquakes (O-3).
JTPN-10A (primary)	40.43742, 144.43687	7600	30	1. Recover a condensed (relative to coupled Site JTPN-09A), continuous upper Pleistocene–Holocene stratigraphic succession (potentially reaching the middle Pleistocene) comprising event deposits on a trench floor high near the deepest depocenter in the northernmost part of the JT. 2. Analyze the stratigraphic pattern and event deposit characteristics and integrate with results from coupled Site JTPN-10A to establish robust stratigraphic pattern recognition of proxy evidence of earthquakes (O-1). 3. Compare results with all other sites to explore spatiotemporal distribution of event deposits and the southward extent of sediment transport routed through the Ogawara Canyon (O-2) to develop a long-term record for giant earthquakes (O-3).
JTPN-11A (alternate)	40.25341, 144.39081	7550	30	1. Recover a condensed (relative to coupled Site JTPN-08A) continuous upper Pleistocene–Holocene stratigraphic succession (potentially reaching the middle Pleistocene) comprising event deposits from an isolated trench basin in the northernmost JT. Alternate site to JTPN-10A. 2. Analyze the stratigraphic pattern and event deposit characteristics and integrate with Site JTPN-08A to establish robust stratigraphic pattern recognition of proxy evidence of earthquakes (O-1). 3. Compare results with all other sites to explore spatiotemporal distribution of event deposits and the southward extent of sediment transport routed through the Ogawara Canyon (O-2) to develop a long-term record for giant earthquakes (O-3).

Table T2. Geophysical and hydroacoustic site survey data used to implement this project. Center for Marine Environmental Sciences (MARUM)/Bundesamt für Seeschifffahrt und Hydrographie (BSH) data sets are publicly available at the time of publication. JAMSTEC = Japan Agency for Marine-Earth Science and Technology, MCS = multichannel seismic reflection poststack time-migrated data, SBP = subbottom profiler data.

Source	Data type	Trench distribution with reference to respective proposed sites
JAMSTEC	MCS, deep penetrating, digital data (SEGY), profile images (PDF), navigation data (ASCII)	JTPS-07A, 09A, JTPC-01A, 02A, 04A, 05A, 06B, 08A, 10A, JTPN-01A, 02A, 03A, 04A, 06A, 07A, 08A
MARUM/BSH	SBP (Parasound), digital data (SEGY), profile images (PDF), navigation data (ASCII)	JTPS-01A, 02A, 03A, 04A, 05B, 06B, 07A, 08A, 09A, 10A, JTPC-02A, 03B, 04A, 05A, 06B, 07A, 09A, 10A, JTPN-01A, 02A, 03A, 04A, 05A, 06A, 07A, 08A, 09A, 10A, 11A
JAMSTEC	SBP (Topas), digital data (SEGY), profile images (PDF), navigation data (ASCII)	JTPS-02A, 05B, 06B, 08A, JTPC-01A, 05A, 06B, 08A, 09A, JTPN-02A, 03A, 06A, 07A, 08A, 11A
JAMSTEC	SBP (Bathy2010), digital data (SEGY), profile images (PDF), navigation data (ASCII)	JTPN-10A
JAMSTEC	SBP (EdgeTech), digital data (SEGY), profile images (PDF), navigation data (ASCII)	JTPS-08A
MARUM/BSH	Multibeam, digital data (GMT netCDF, 32-bit float, COARDS), bathymetry map (PDF, TIFF)	Throughout

Table T3. Science party and operator (ESO) personnel, offshore Expedition 386 (on R/V *Kaimei*). JAMSTEC = Japan Agency for Marine-Earth Science and Technology, MarE3 = Marine-Earth Exploration and Engineering, MWJ = Marine Works Japan, NME = Nippon Marine Enterprises.

ESO (10)	JAMSTEC/MarE3 (21)	Offshore scientists (8)
1 Expedition Project Manager (EPM)	1 MarE3 Liaison/EPM	2 Co-Chief Scientists
1 EPM/Outreach (second leg)	1 MarE3 Observer	2 Geochemists
2 Curators	10 NME Technicians	1 Physical Properties Specialist
1 Geochemist	9 MWJ Technicians	1 Microbiologist
1 Petrophysics Staff Scientist		1 Marine Geophysicist/Hydroacoustic Interpreter (stratigraphic correlation)
1 Petrophysicist (first leg)		1 Core-Log-Seismic Integrator (stratigraphic correlation)
1 Data Manager		
2 Drilling Coordinators		

Table T4. Science party and operator (ESO) personnel at the onshore science party (OSP), Expedition 386 (on D/V Chikyu in port). JAMSTEC = Japan Agency for Marine-Earth Science and Technology.

ESO (NN)	JAMSTEC (NN)	Scientists OSP – initial indication
1 Expedition Project Manager (EPM)	1 Liaison	2 Co-Chief Scientists
1 Trainee EPM		4 Geochemists
2 Curators		2 Tephra Specialists
2 Core curation/splitting		7 Physical Properties Specialists
1 Geochemist		2 Micropaleontologists
1 Petrophysics Staff Scientist		2 Structural Geologists
2 Petrophysicists		9 Sedimentologists
2–4 Data		1 Microbiologist
1 Publications Specialist		2 Paleomagnetists
		2 Stratigraphic Correlators

Figure F1. Japan Trench subduction margin physiography and the epicenter and coseismic slip distribution of the 2011 Mw 9.0 Tohoku-Oki earthquake (EQ) (40 and 20 m slip contour lines from compilation in Chester et al. [2013]; 2 m contour line from Sun et al. [2017]). Also shown are previous IODP/ODP/DSDP drilling sites in the region and sites where surface cores and/or conventional (as long as 10 m) gravity and piston cores were retrieved after the 2011 earthquake. Solid red symbols = core locations with water depth >100 m where recent publications (Arai et al., 2013; Ikehara et al., 2014, 2016, 2018; Kioka et al., 2019, submitted; McHugh et al., 2016; Noguchi et al., 2012; Nomaki et al., 2016; Oguri et al., 2013; Strasser et al., 2013; Usami et al., 2017, 2018; Yoshikawa et al., 2016) or preliminary results from the most recent *Sonne* Cruise SO-251 (Strasser et al., 2017) document various distinct earthquake-related event deposits or stratigraphic gaps (Molenaar et al., 2019) linked to the 2011 earthquake and tsunami; open red symbols = locations where core data reveal no indication for recent sediment deposition (or erosion) related to the 2011 earthquake and tsunami as documented by Fink et al. (2014), Ikehara et al. (2016), Yoshikawa et al. (2016), and Kioka et al. (2019); black symbols = location of cores for which no detailed information is available; cross symbols = sediment-trapped ocean-bottom seismometers (OBSs) or buried/displaced ocean-bottom pressure (OBP) recorders associated with the 2011 earthquake (Arai et al., 2013; Miura et al., 2014).

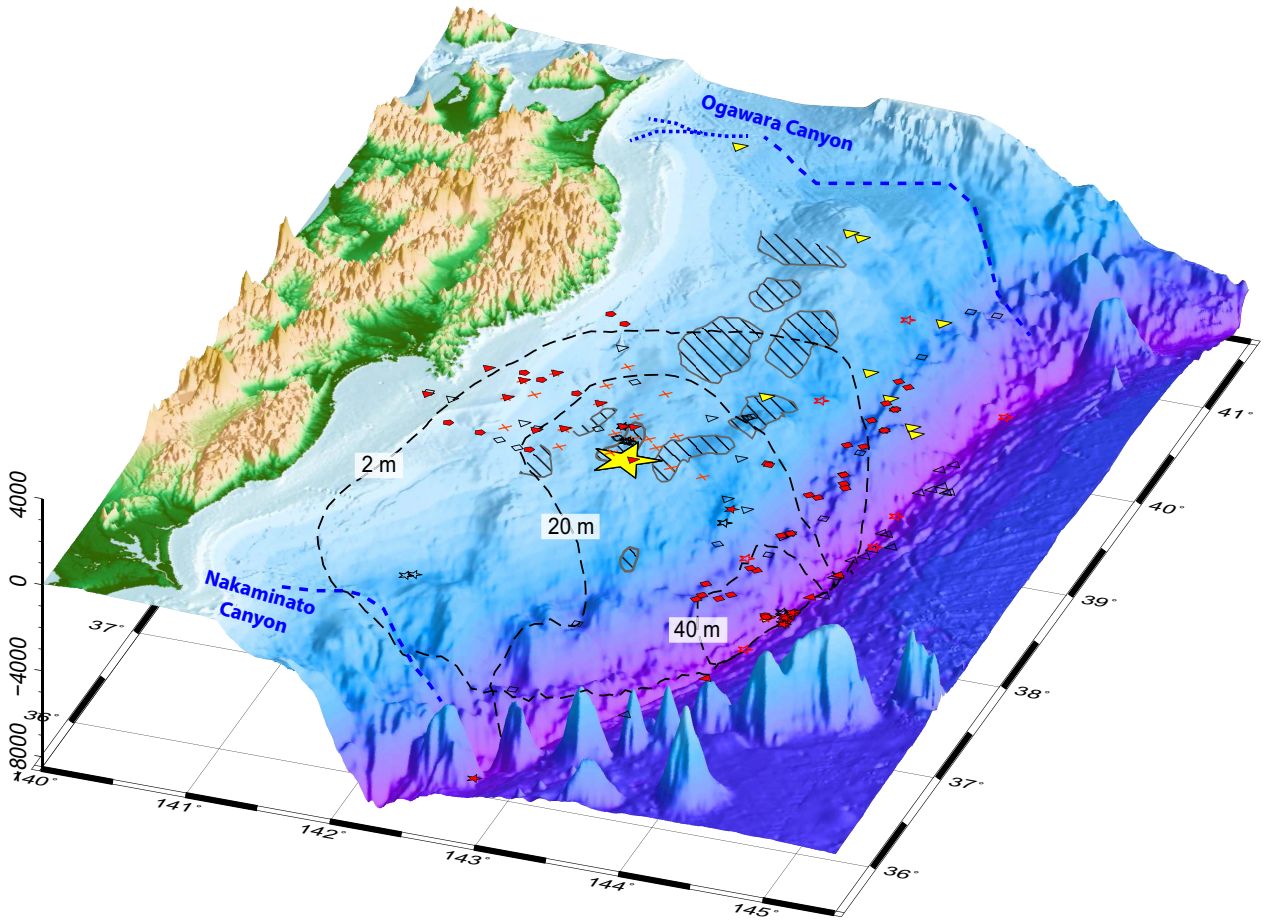

Legend

- ☆ Japan Meteorological Agency Epicenter of The 2011 Tohoku-oki EQ
- Coseismic slip due to the 2011 EQ compiled in Chester et al. (2013) and Sun et al. (2017)
- Isolated basin identified by Arai et al. (2014)
- Submarine canyon
- × OBSs & OBPs

Cores previously obtained

- ▽ IODP/ODP/DSDP
- ★ ☆ ☆ *R/V Sonne*: SO219A & SO251A
- ▼ ▽ ▽ *R/V Tansei-Maru*: KT-11-17 & KT-12-9
- ● ○ ○ *R/V Mirai*: MR12-E01 & MR12-E02
- ◆ ◇ ◇ *R/V Natsushima*: NT12-02 & NT13-19
- ■ □ □ *R/V Yokosuka*: YK11-E06 & YK14-E01
- ▲ △ △ *R/V Shinsei-Maru*: KS-14-16, KS-15-3, KS-15-16
- ● ○ *R/V Kairei*: KR13-08

Figure F2. Stratigraphic correlation between cores from isolated trench-fill basins in the central part of the Japan Trench (between 37°40′N and 38°10′N; along-trench axis distance = ~50 km). The records preserve evidence for three major sediment remobilization events (referred to as thick turbidite [TT] units), each consisting of 30–240 cm thick, stacked fine-grained turbidites. Also shown is correlation of TT units to coastal tsunami deposits, reported run-up heights >5 m from historical documents (Sawai et al., 2012), and inferred occurrence of three earthquakes with comparable sedimentary imprint as the 2011 Tohoku earthquake (Ikehara et al., 2016).

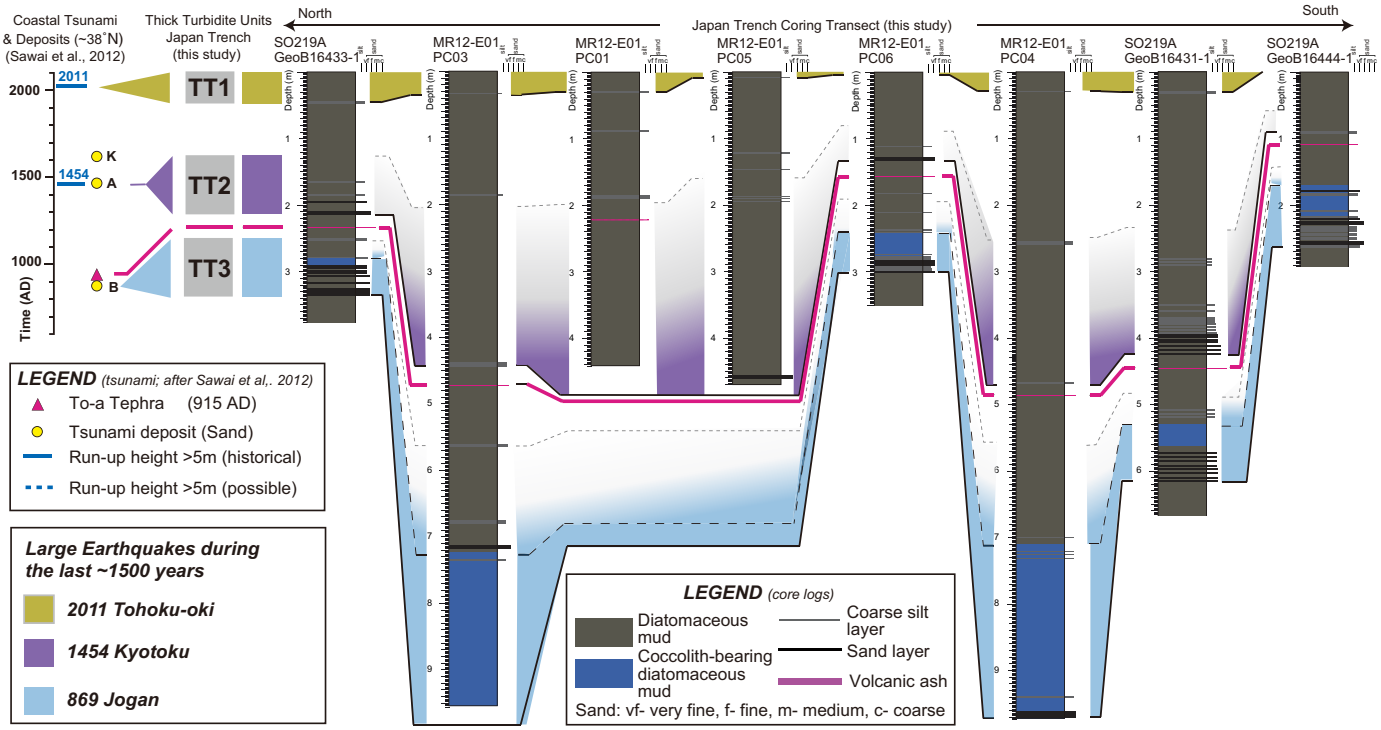

Figure F3. Compiled results from OM radiocarbon analyses on samples from GeoB16431-1 and colored TT units linked to historic volcanic eruption and earthquakes (Bao et al., 2018). A. Lithology core log with volcanic tephra (pink) (see Figure F2 for legend). B. High-resolution bulk OC ^{14}C age profile measured using the new online $\delta^{13}C$ and ^{14}C gas measurements by coupled elemental analyzer–isotope ratio mass spectrometry–accelerator mass spectrometry (EA-IRMS-AMS) at ETH Zürich (McIntyre et al., 2016), which allows for high-throughput bulk sediment OC ^{14}C determination. BP = before present. C. OC flux calculated using TOC measured using EA-IRMS-AMS, sedimentation rates calculated by ratio of sediment depth spanning time intervals constraints by historic events, and density measured by gamma ray attenuation. D. Chronology and radiocarbon characteristics of ramped pyrolysis/oxidation ("Ramped PyrOX"; RPO) thermal fractions of OM for five selected samples. Measurement error is smaller than the symbol. The method following Rosenheim et al. (2008) analyzes CO_2 gas samples collected from ramped temperature pyrolysis/oxidation integrated over five temperature intervals (T1–T5) by AMS radiocarbon measurements. Results document (1) very high OC fluxes (two orders of magnitude higher than background) of pre-aged OC input to the hadal environment of the Japan Trench that are directly linked to the earthquake-triggered sediment remobilization process; (2) bulk OM radiocarbon ages have consistent offsets of ~2000 y, likely related to constant transport of pre-aged OM to the trench; and (3) consistency in ^{14}C differences of thermal fractions ages ("parallel" lines in D) and their correspondence (in terms of absolute time between known volcanic and correlated tectonic events), which might reflect radioactive decay in the sediment after deposition. The latter result holds promise for placing chronological constraints on Japan Trench sediment cores (accurate floating chronology), which can be anchored to dated tephra layers.

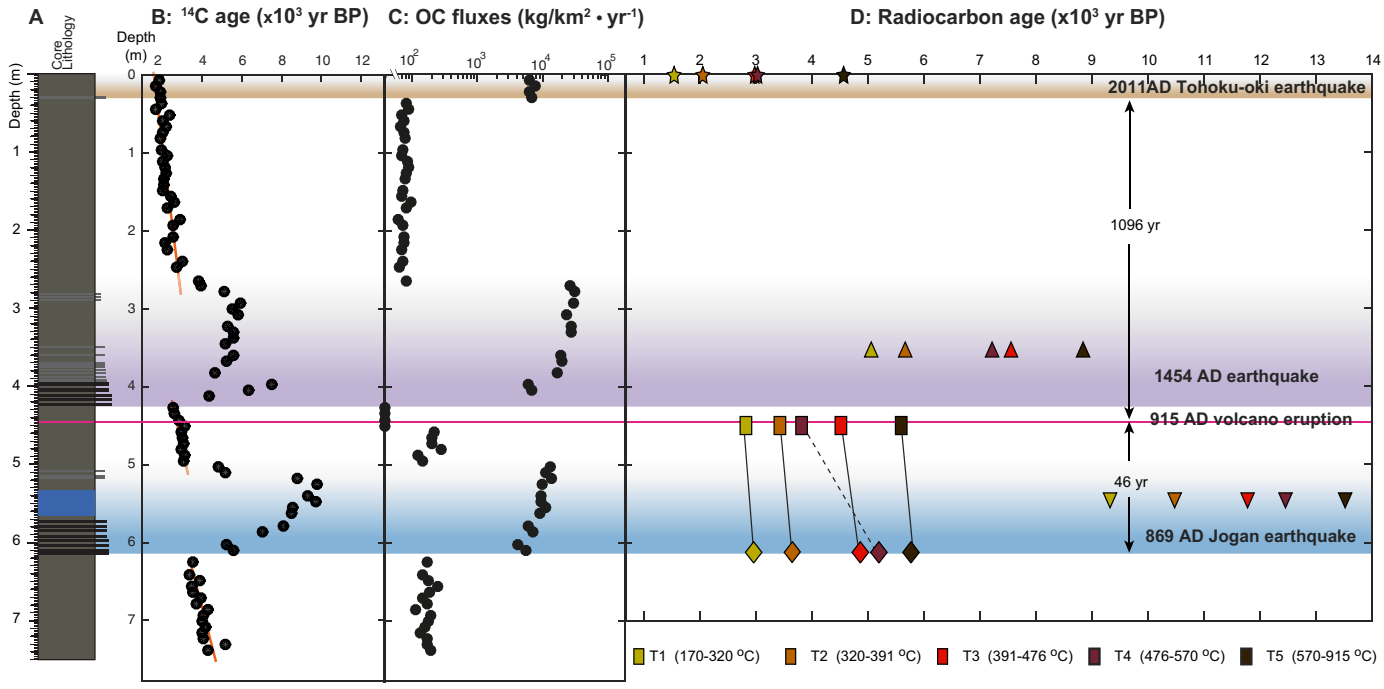

Figure F4. Top left: High-resolution bathymetric map (acquired in October 2016 during Cruise SO251-1 with the state-of-the-art EM 122 Kongsberg multibeam echo sounder system installed on *Sonne*) with the 5 m contours and track lines of high-resolution subbottom profiles. Top right: SSW–NNE noise-attenuated Parasound Line GeoB21806-part2 along the Japan Trench. SP = shotpoint. Bottom left: WNW–ESE noise-attenuated Parasound Line SLF120318225 crossing the Japan Trench. Colored units represent low-amplitude to homogeneous seismic facies in an otherwise layered reflection pattern (colored as in bottom right panel). Dotted lines are continuous high-amplitude reflections often traceable throughout multiple basins. Bottom right: Core-seismic correlation of Core KS-15-03 PC08 of Ikehara et al. (2018) and Kioka et al. (submitted). The fine sandy tephra at 2.1 m subsurface is identified as the Towada-a (To-a) tephra and clearly corresponds to a strong reflection on the Parasound data. Homogeneous units in the core interpreted to be sedimentary event deposits (i.e., yellow, purple, and blue layers) correspond to low-amplitude acoustic units with a basin-fill geometry (see top right panel). Green is for similar low-amplitude units below the cored interval that form targets for IODP piston coring. This HRS data was acquired using the Atlas Parasound P70 echo sounder on *Sonne*. Interference of two signals with high frequencies (18 and 22 kHz) produces a secondary low frequency of ~4 kHz that is used for subbottom profiling. Generally, acquisition parameters were as follows: low-pass filter at 6 kHz, pulse length 1 ms, sampling rate 12.2 kHz.

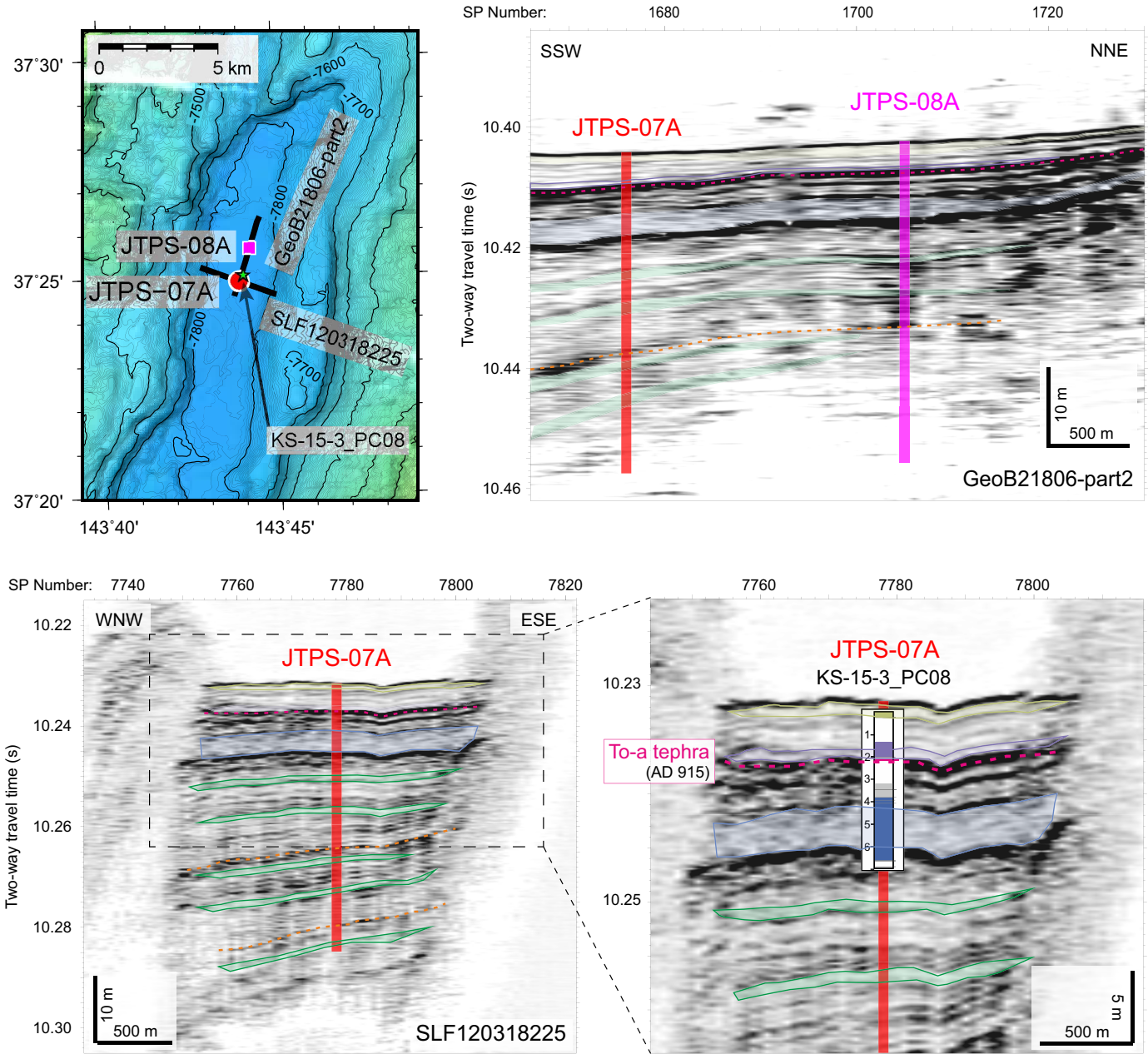

Figure F5. Left: High-resolution bathymetric map (Kioka et al., 2019) with ship track of *Sonne* and *Shinsei-Maru* cruises during which high-resolution subbottom data by Atlas Parasound P70 echo sounder and Kongsberg Topas Chirp subbottom profiler have been acquired. Also shown are proposed site locations and available cores from conventional coring during recent research cruises conducted since 2011. The colored bathymetry combines two different data sets: (1) data acquired in October 2016 with the state-of-the-art EM 122 Kongsberg multibeam echo sounder system installed on *Sonne* and (2) 150 m grid acquired by JAMSTEC. Shaded relief in the background = water depth. Right: Along-trench Parasound seismic profiles representing the northern, central, and southern part of the Japan Trench. Additionally, one west–east profile illustrates the approach of coring a graben basin instead of the trench fill because the later shows a too complex/disturbed seismic stratigraphy. The Parasound profiles shown are composites of selected parts of SEGY files. The high-resolution subbottom profiles from the small isolated trench basins along the entire Japan Trench axis image acoustic reflection patterns with transparent units consistent with basin-fill successions interbedded by episodic deposition of fine-grained turbidites (Kioka et al., 2019, submitted). TWT = two-way traveltime.

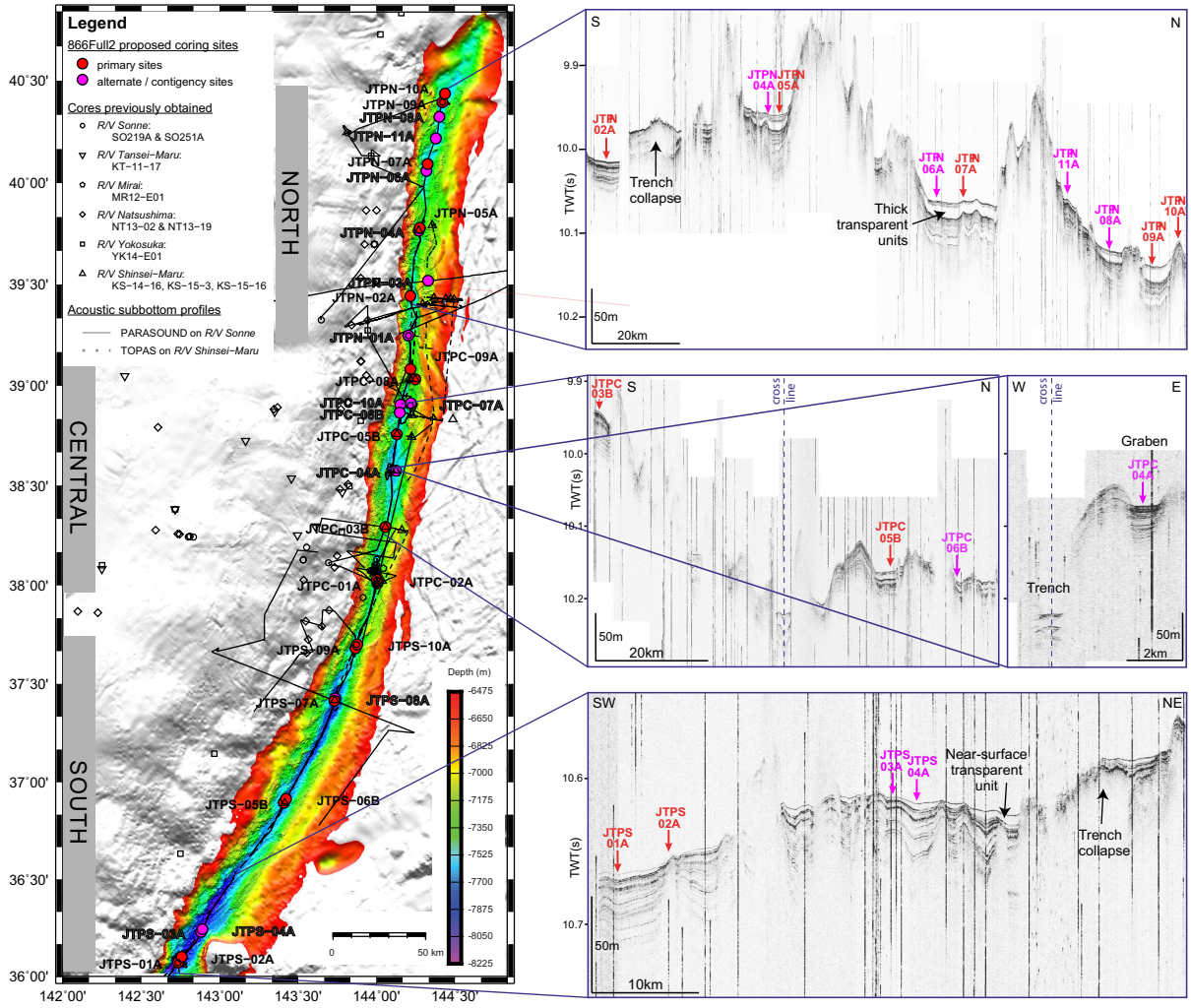

Figure F6. A. Seismic profiles acquired by JAMSTEC since 1997 and Expedition 386 primary and alternate proposed site locations. Profiles from before the earthquake (EQ) were acquired using the following parameters: 12,000 inch^3 nontuned air gun array and 3,000–4,500 m long 120–168 channel streamer cable. Parameters for profiles acquired after the earthquake: 7,800 tuned air gun array and 6,000 m long 444 channel (MCS) and 320–380 inch^3 cluster gun array with 37.5 m shot interval and 1,200 m long 192 channel with 6.25 m channel interval streamer cable (HRMCS). Previous IODP/ODP/DSDP drilling sites and submarine cables are also shown. All coring sites are placed >8 km away from submarine cables to eliminate operational risk. White dashed outlined rectangles indicate working areas of most recent Japanese cruises (YK17-22, KS17-13, and MR17-06 [data not yet integrated into this compilation]). B. Isopach map of trench-fill sediment thickness mapped in HRMCS profiles (orange lines in A) and proposed sites for 30–40 m long piston coring, most of which were located in basins where trench-fill sediment thickness is more than 50 m (blue–purple colors). Exceptions to this are Sites JTPN-02A and JTPN-04A, which both show well-defined, deeply imaged targets in high-resolution subbottom data (see Figures AF22, AF24). C–E. Examples of HRMCS reflection profiles (see line locations in A and B) showing character of horizontally stratified, undisturbed trench- and graben-fill basins and proposed sites. CDP = common depth point. F, G. Examples of noise-attenuated high-resolution subbottom profiles acquired by Atlas Parasound P70 multiparametric system equipped on *Sonne*: (F) west–east Parasound and (G) south–north Parasound lines across Site JTPS-10A (zoomed to trench location of E). The two cross-lines exemplarily illustrate that trench-fill basins typically are asymmetric basins (in west–east direction), formed by normal faults in the downward-bending subducting oceanic crust (see E), are of limited north–south extent and show ponding geometries in the depocenter and more condensed sections toward the basin margins. Sites JTPS-09A and JTPS-10A thus represent typical examples of our coring composite-stratigraphy concept with a two-site couple that allows for coring both an expanded (Site JTPS-09A) and a condensed stratigraphic section (Site JTPS-10A).

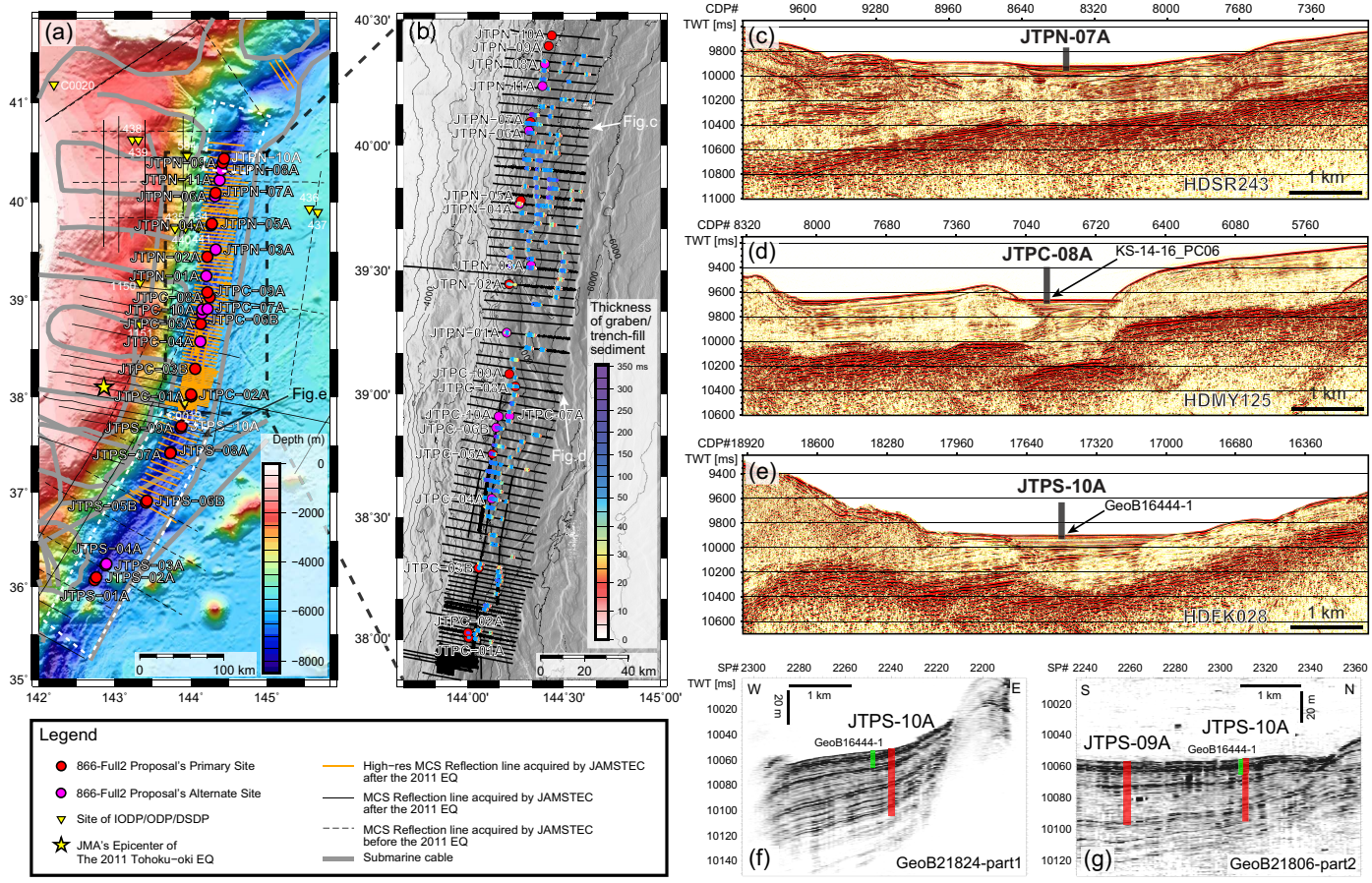

Site summaries

Figure AF1. Primary proposed Site JTPS-01A.

Proposal 866−Full2

Site JTPS−01A (Primary)

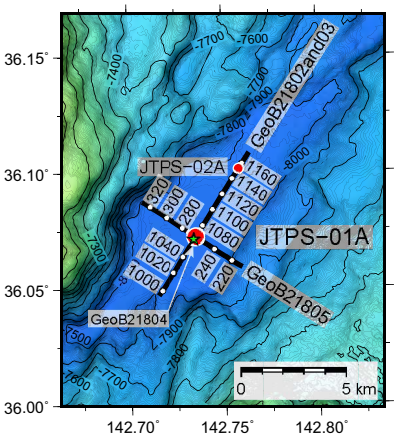

Profiles annotated using shot point (SP) numbers

Site JTPS−01A
SP 1066 on GeoB21802and03
SP 263 on GeoB21805

Site Summary Form 6

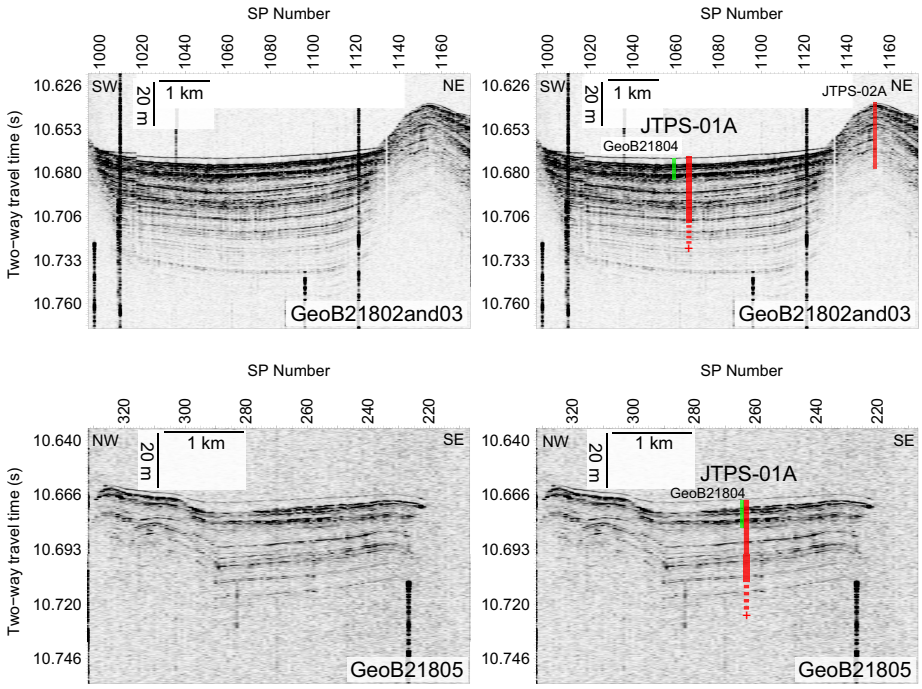

SSDB locations of these graphics and supporting data
Location map: JTPS-01A_Location.pdf
Figures of seismic data:
JTPS−01A_GeoB21802and03.pdf & JTPS−01A_GeoB21805.pdf
SEG−Y data:
JTPS−01A_GeoB21802and03.sgy & JTPS−01A_GeoB21805.sgy
Figures of reference core data: GeoB21804.pdf

Interpretation

Undisturbed trench-basin-fill succession of dominantly diatomaceous mud interbedded with dm- to m-thick muddy turbidites and thin tephra layers.

This is the expanded section relative to site JTPS-02A

Figure AF2. Primary proposed Site JTPS-02A.

Proposal 866−Full2

Site JTPS−02A (Primary)

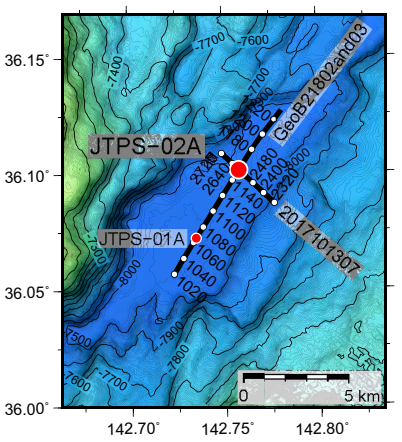

Profiles annotated
using Shot point (SP) numbers

Site JTPS−02A
SP 1153 on GeoB21802and03
SP 2589 on 2017101307

Site Summary Form 6

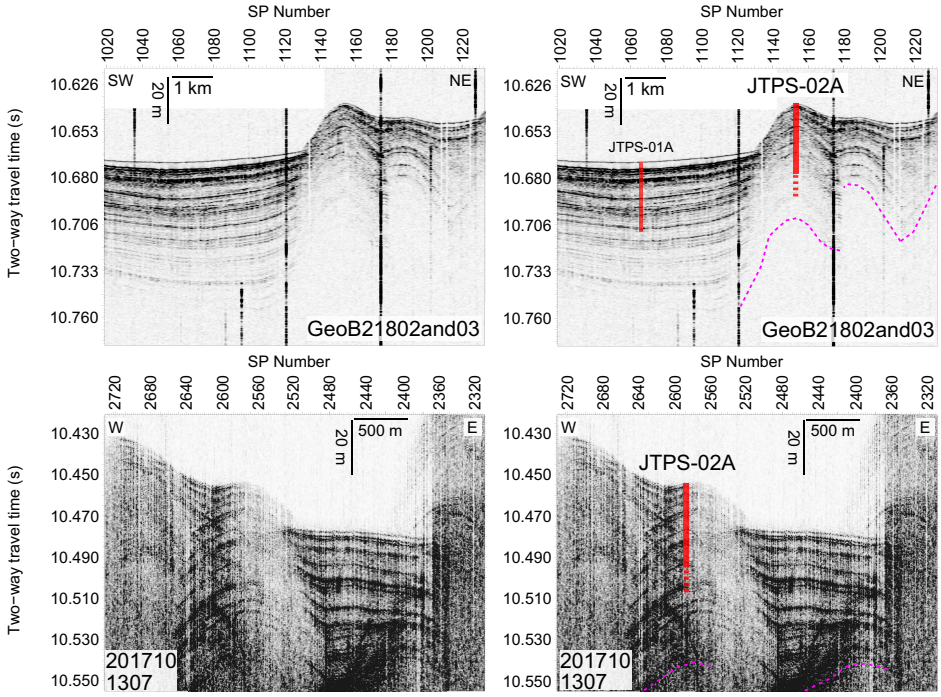

SSDB locations of these graphics and supporting data

Location map: JTPS-02A_Location.pdf

Figures of seismic data:
JTPS−02A_GeoB21802and03.pdf & JTPS−02A_2017101307.pdf

SEG−Y data:
JTPS−02A_GeoB21802and03.sgy & JTPS−02A_2017101307.sgy

Interpretation

Undisturbed trench-basin-fill succession of dominantly diatomaceous mud interbedded with cm- to dm-thick muddy turbidites and thin tephra layers deposited on a trench-floor high at the foot of the landward-slope of the trench. This is the condensed section relative to site JTPS-01A. Magenta: limit of acoustic penetration and possible top of deformed trench-fill deposits (e.g. by local slumping)

Figure AF3. Alternate proposed Site JTPS-03A.

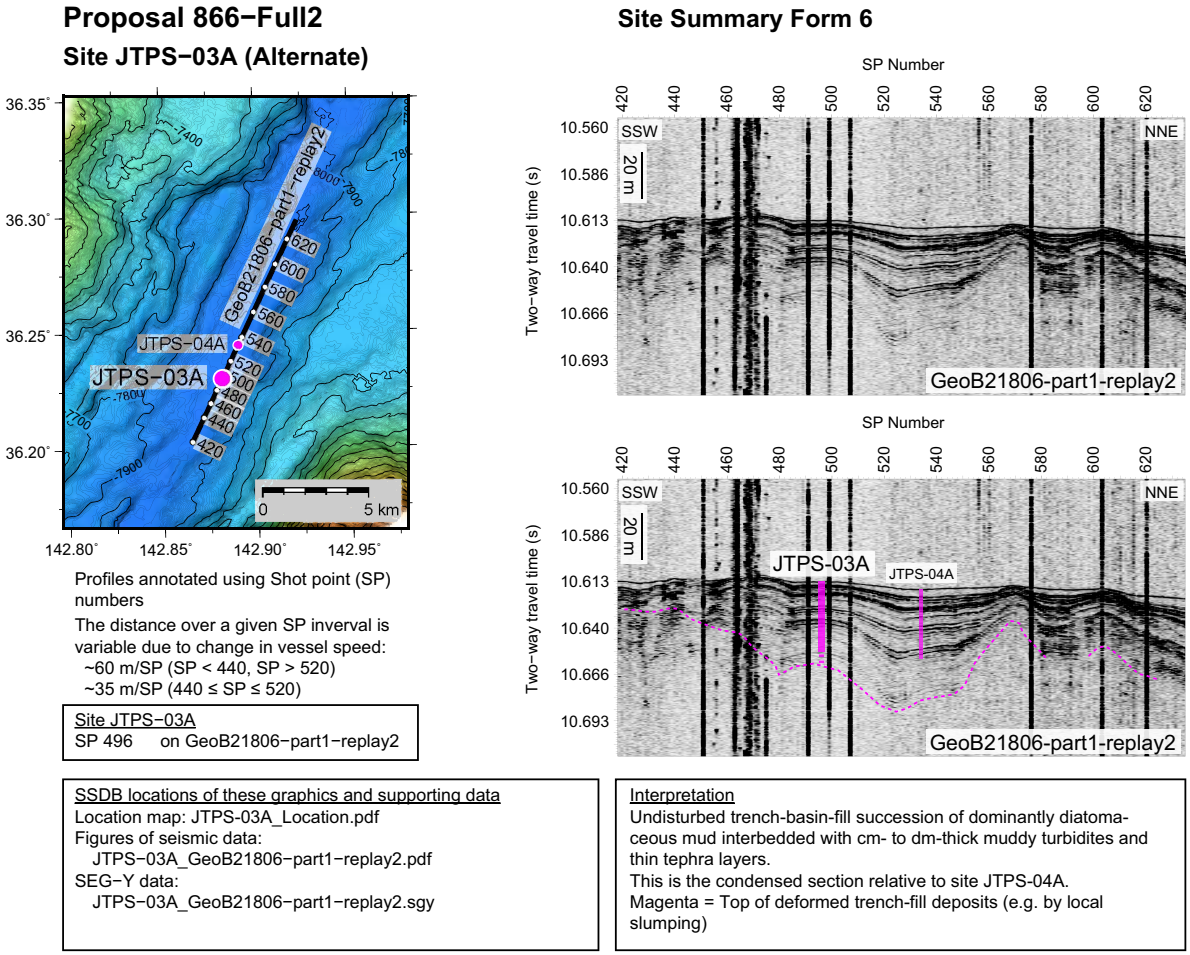

SSDB locations of these graphics and supporting data
Location map: JTPS-03A_Location.pdf
Figures of seismic data:
JTPS−03A_GeoB21806−part1−replay2.pdf
SEG−Y data:
JTPS−03A_GeoB21806−part1−replay2.sgy

Interpretation
Undisturbed trench-basin-fill succession of dominantly diatomaceous mud interbedded with cm- to dm-thick muddy turbidites and thin tephra layers.
This is the condensed section relative to site JTPS-04A.
Magenta = Top of deformed trench-fill deposits (e.g. by local slumping)

Figure AF4. Alternate proposed Site JTPS-04A.

Proposal 866−Full2

Site JTPS−04A (Alternate)

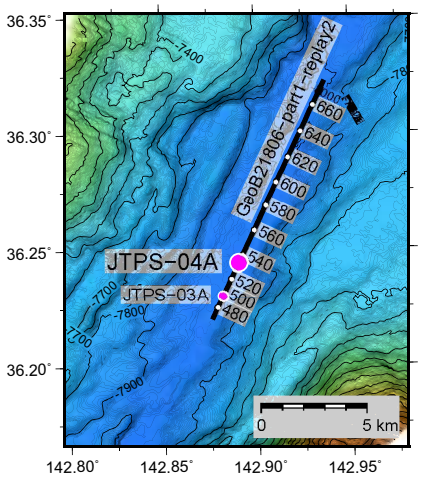

Profiles annotated using Shot point (SP) numbers

The distance over a given SP inverval is variable due to change in vessel speed:
~35 m/SP (SP ≤ 520)
~60 m/SP (SP > 520)

Site JTPS−04A
SP 534 on GeoB21806−part1−replay2

Site Summary Form 6

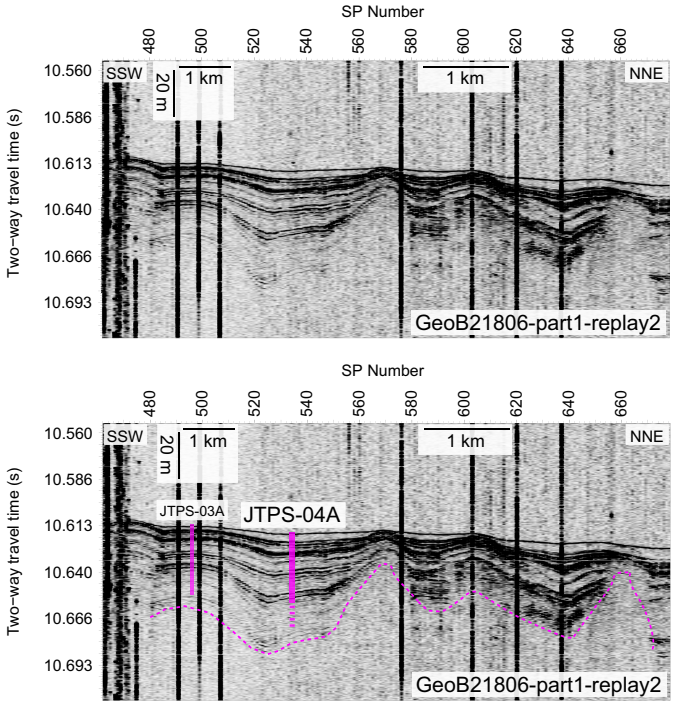

SSDB locations of these graphics and supporting data
Location map: JTPS-04A_Location.pdf
Figures of seismic data:
JTPS−04A_GeoB21806−part1−replay2.pdf
SEG−Y data:
JTPS−04A_GeoB21806−part1−replay2.sgy

Interpretation
Undisturbed trench-basin-fill succession of dominantly diatomaceous mud interbedded with dm- to m-thick muddy turbidites and thin tephra layers.
This is the expanded section relative to site JTPS-03A.
Magenta = Top of deformed trench-fill deposits (e.g. by local slumping)

Figure AF5. Primary proposed Site JTPS-05B.

Proposal 866−Full2

Site JTPS−05B (Primary)

Site Summary Form 6

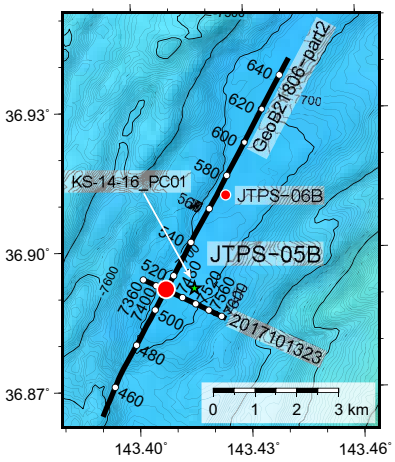

Profiles annotated
using Shot point (SP) numbers

Site JTPS−05B
SP 512 on GeoB21806−part2
SP 7430 on 2017101323

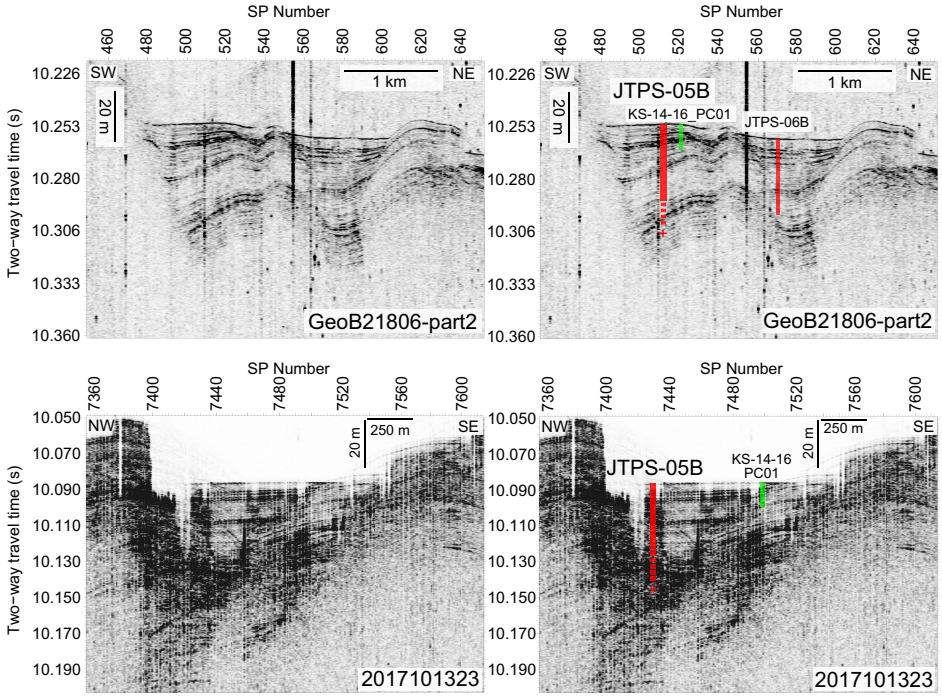

SSDB locations of these graphics and supporting data

Location map: JTPS-05B_Location.pdf

Figures of seismic data:
JTPS−05B_GeoB21806−part2.pdf, JTPS−05B_2017101323.pdf, JTPS-05B_2017101321.pdf, JTPS-05B_2017101400_01.pdf

SEG−Y data:
JTPS−05B_GeoB21806−part2.sgy, JTPS−05B_2017101323.sgy, JTPS-05B_2017101321.sgy, JTPS-05B_2017101400_01.sgy

Figures of reference core data: KS-14-16_PC01.pdf

Interpretation

Undisturbed trench-basin-fill succession of dominantly diatomaceous mud interbedded with cm- to m-thick muddy turbidites and thin tephra layers. This is the composite section relative to site JTPS-06B, (i.e. a condensed section in the upper part and a more expanded section in the lower part)

Figure AF6. Primary proposed Site JTPS-06B.

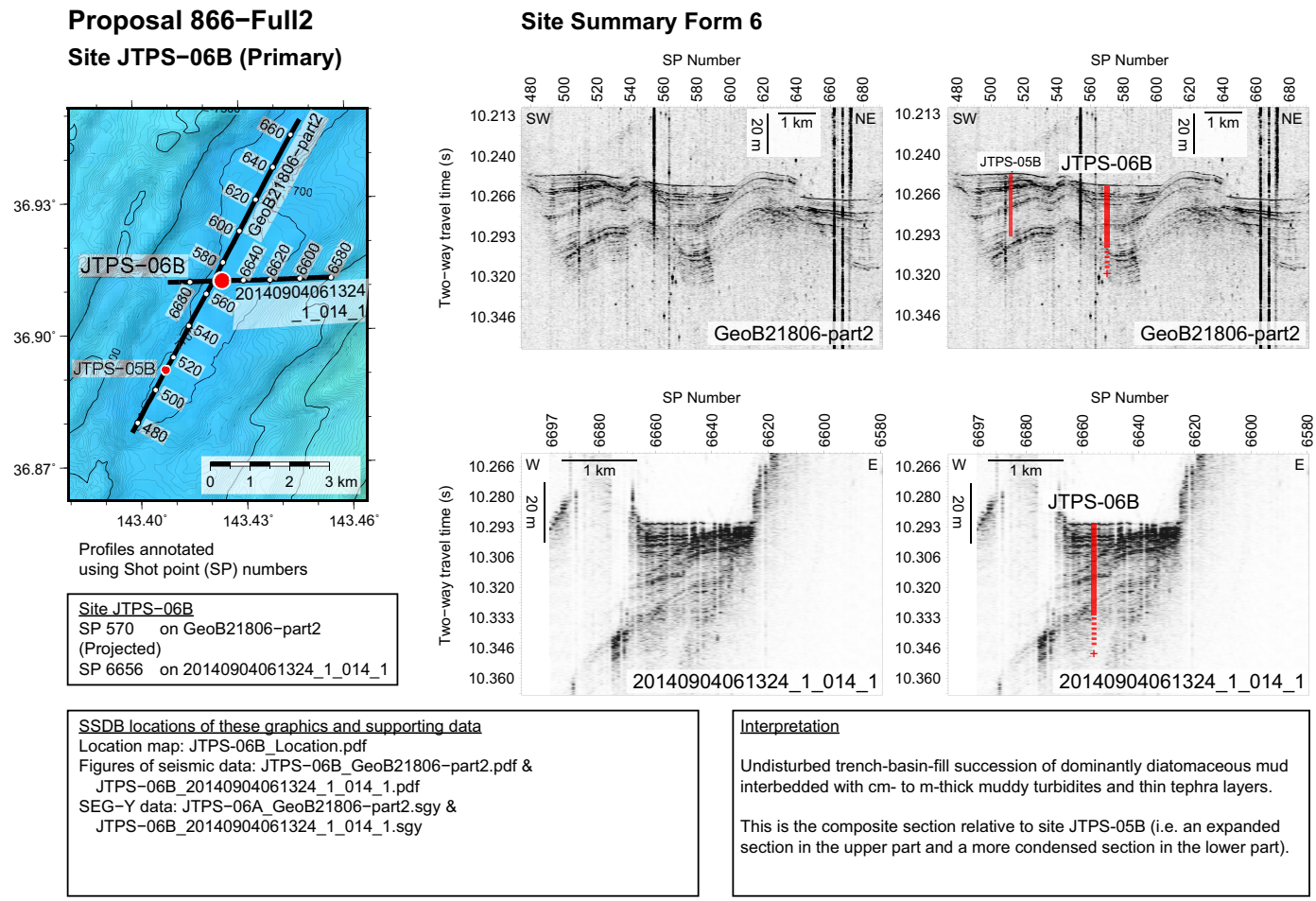

SSDB locations of these graphics and supporting data
Location map: JTPS-06B_Location.pdf
Figures of seismic data: JTPS−06B_GeoB21806−part2.pdf & JTPS−06B_20140904061324_1_014_1.pdf
SEG−Y data: JTPS−06A_GeoB21806−part2.sgy & JTPS−06B_20140904061324_1_014_1.sgy

Interpretation

Undisturbed trench-basin-fill succession of dominantly diatomaceous mud interbedded with cm- to m-thick muddy turbidites and thin tephra layers.

This is the composite section relative to site JTPS-05B (i.e. an expanded section in the upper part and a more condensed section in the lower part).

Figure AF7. Primary proposed Site JTPS-07A.

Proposal 866−Full2

Site JTPS−07A (Primary)

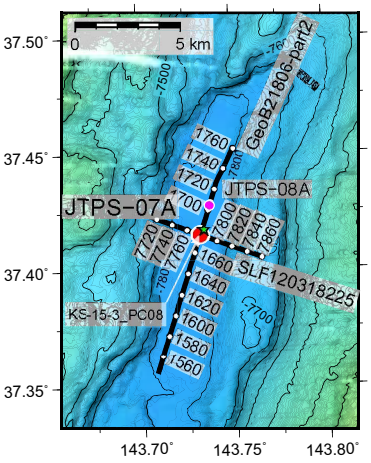

Profiles annotated
using Shot point (SP) numbers

Site JTPS−07A
SP 1676 on GeoB21806−part2
SP 7778 on SLF120318225

Site Summary Form 6

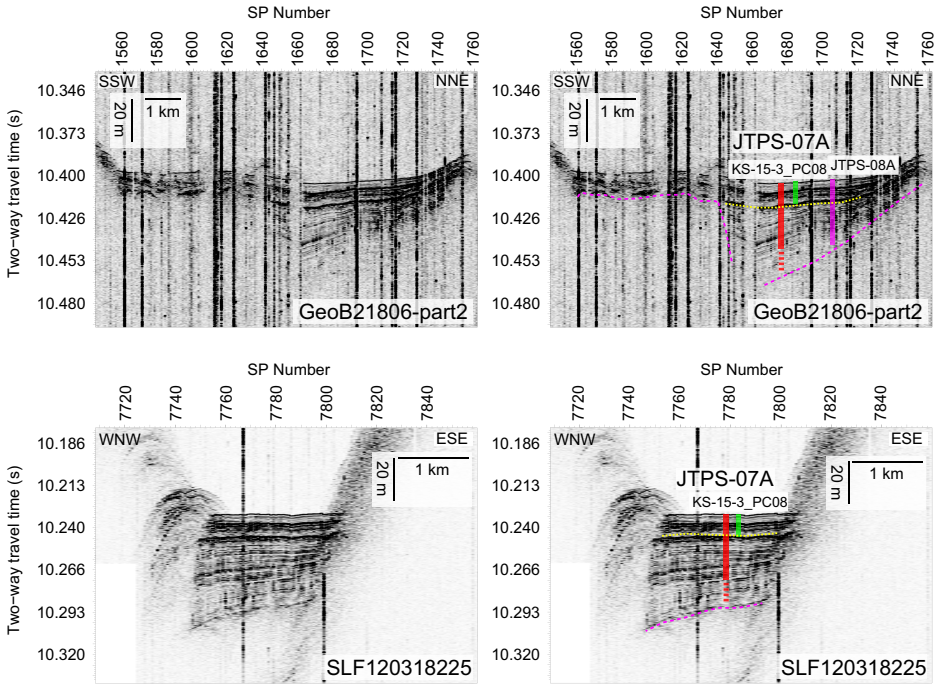

SSDB locations of these graphics and supporting data
Location map: JTPS-07A_Location.pdf
Figures of seismic data:
JTPS−07A_GeoB21806−part2.pdf, JTPS−07A_SLF120318225.pdf
& JTPS-07A_HDFK060_mig.pdf
SEG−Y data:
JTPS−07A_GeoB21806−part2.sgy, JTPS−07A_SLF120318225.sgy
& JTPS-07A_HDFK060_mig.pdf
Figures of reference core data: KS-15-3_PC08.pdf

Interpretation: Undisturbed trench-basin-fill succession of dominantly diatomaceous mud interbedded with cm- to m-thick, muddy turbidites and thin tephra layers. This is the expanded section relative to site JTPS-08A.

Magenta = Top of deformed trench-fill deposits (e.g. by slumping or compression during co-seismic slip to trench)
Yellow = Base of relatively-thick muddy turbidite filling-in local trench-floor depression (potentially time-correlative event-stratigraphic horizon to deformation in the southern part of the profile).

Figure AF8. Alternate proposed Site JTPS-08A.

Proposal 866−Full2

Site JTPS−08A (Alternate)

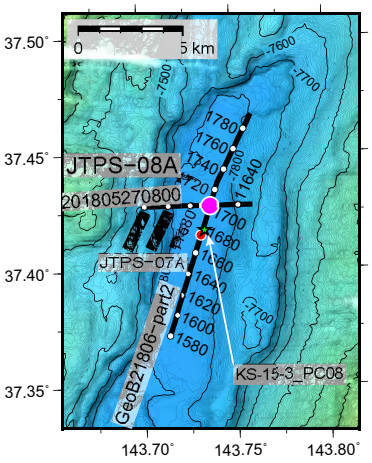

Profiles annotated
using Shot point (SP) numbers

Site JTPS−08A
SP 1705 on GeoB21806−part2
SP 11664 on 201805270800

Site Summary Form 6

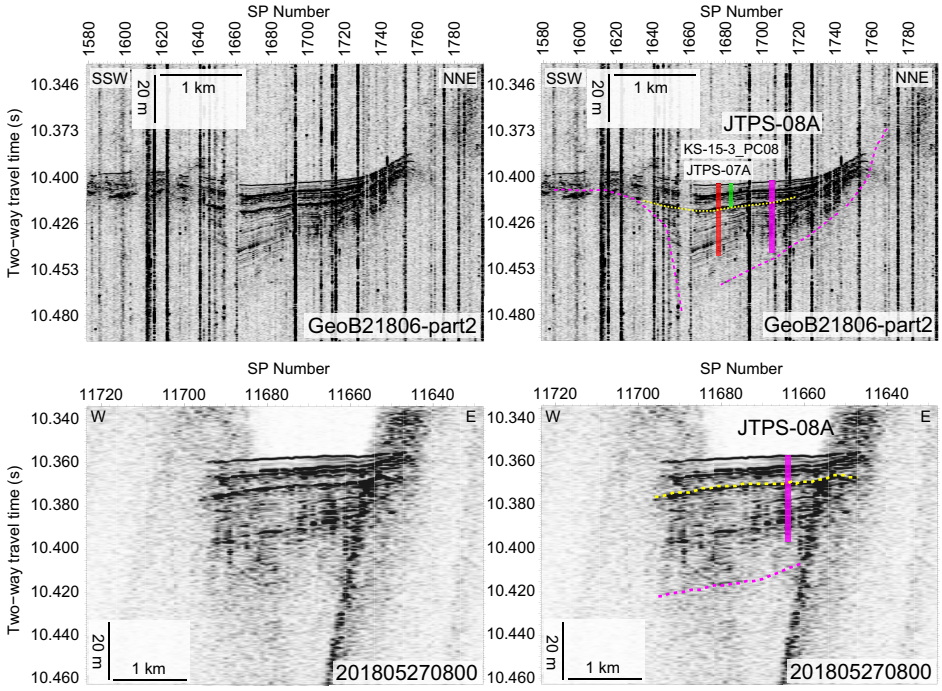

SSDB locations of these graphics and supporting data

Location map: JTPS-08A_Location.pdf

Figures of seismic data:
JTPS−08A_GeoB21806−part2.pdf & JTPS−08A_201805270800.pdf

SEG−Y data:
JTPS−08A_GeoB21806−part2.sgy & JTPS−08A_201805270800.sgy

Figures of reference core data: KS-15-3_PC08.pdf

Interpretation

Undisturbed trench-basin-fill succession of dominantly diatomaceous mud interbedded with cm- to dm-thick muddy turbidites and thin tephra layers. Condensed section relative to JTPS-07A.
Magenta = Top of deformed trench-fill deposits (e.g. by slumping or compression during co-seismic slip to trench)
Yellow = Base of relatively-thick muddy turbidite filling-in local trench-floor depression (potentially time-correlative event-stratigraphic horizon to deformation in the southern part of the profile).

Figure AF9. Primary proposed Site JTPS-09A.

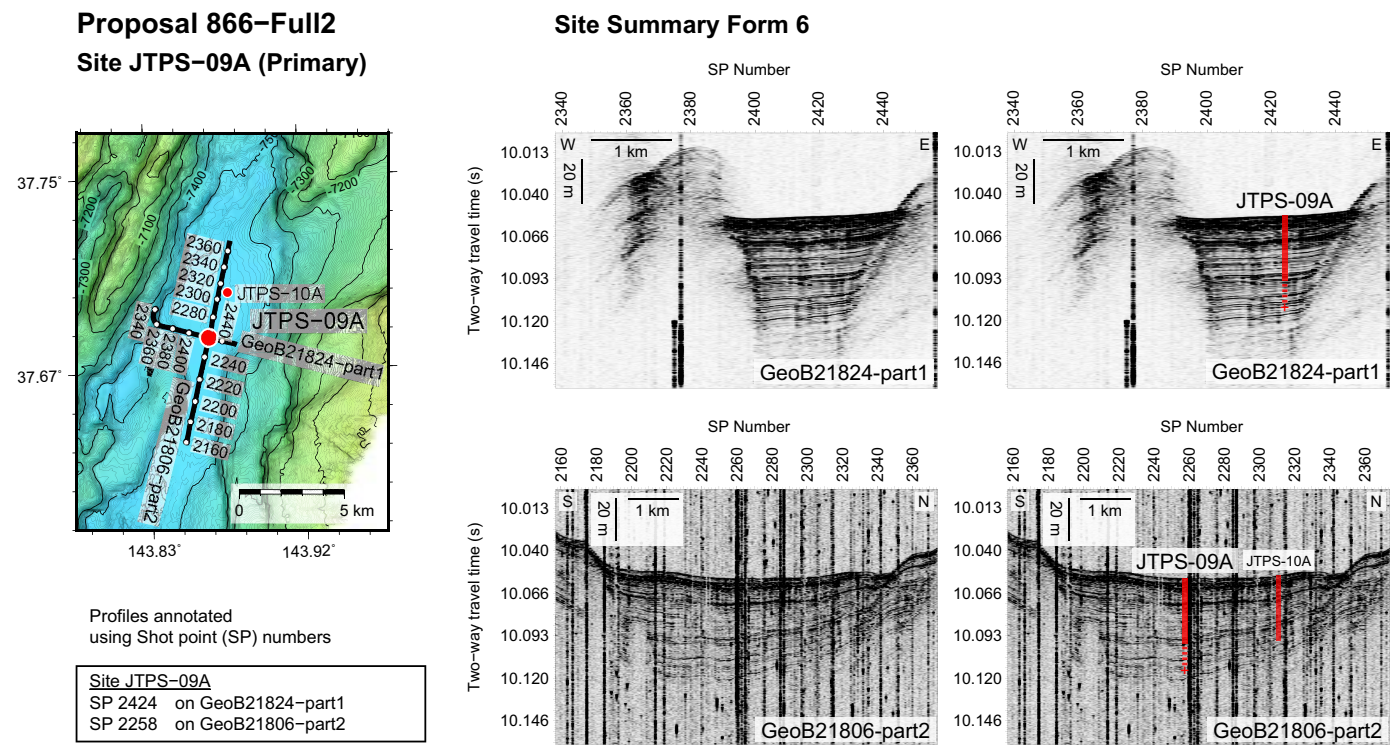

SSDB locations of these graphics and supporting data
Location map: JTPS-09A_Location.pdf
Figures of seismic data:
JTPS−09A_GeoB21824−part1.pdf, JTPS−09A_GeoB21806−part2.pdf
& JTPS-09A_HDFK028_mig.pdf
SEG−Y data:
JTPS−09A_GeoB21824−part1.sgy, JTPS−09A_GeoB21806−part2.sgy
& JTPS-09A_HDFK028_mig.sgy

Interpretation

Undisturbed trench-basin-fill succession of dominantly diatomaceous mud interbedded with dm- to m-thick muddy turbidites and thin tephra layers.

This is the expanded section relative to site JTPS-10A.

Figure AF10. Primary proposed Site JTPS-10A.

Proposal 866−Full2

Site JTPS−10A (Primary)

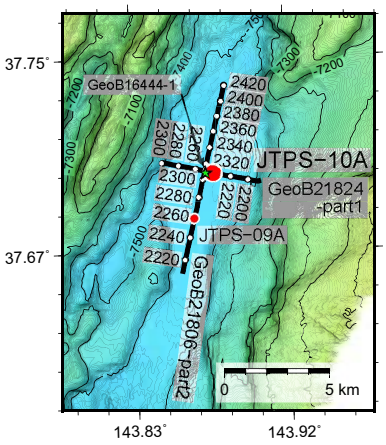

Profiles annotated
using Shot point (SP) numbers

Site JTPS−10A
SP 2240 on GeoB21824−part1
SP 2311 on GeoB21806−part2
(projected)

Site Summary Form 6

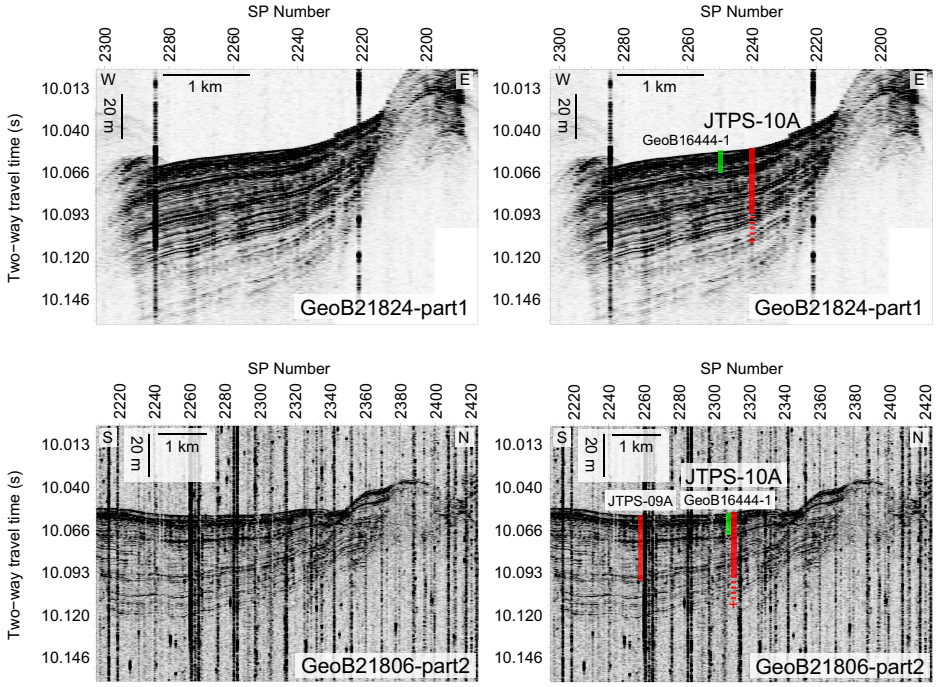

SSDB locations of these graphics and supporting data
Location map: JTPS-10A_Location.pdf
Figures of seismic data:
JTPS−10A_GeoB21824−part1.pdf & JTPS−10A_GeoB21806−part2.pdf
SEG−Y data:
JTPS−10A_GeoB21824−part1.sgy & JTPS−10A_GeoB21806−part2.sgy
Figures of reference core data: GeoB16444-1.pdf

Interpretation

Undisturbed trench-basin-fill succession of dominantly diatomaceous mud interbedded with cm- to dm-thick muddy turbidites and thin tephra layers.

This is the condensed section relative to site JTPS-09A.

Figure AF11. Primary proposed Site JTPC-01A.

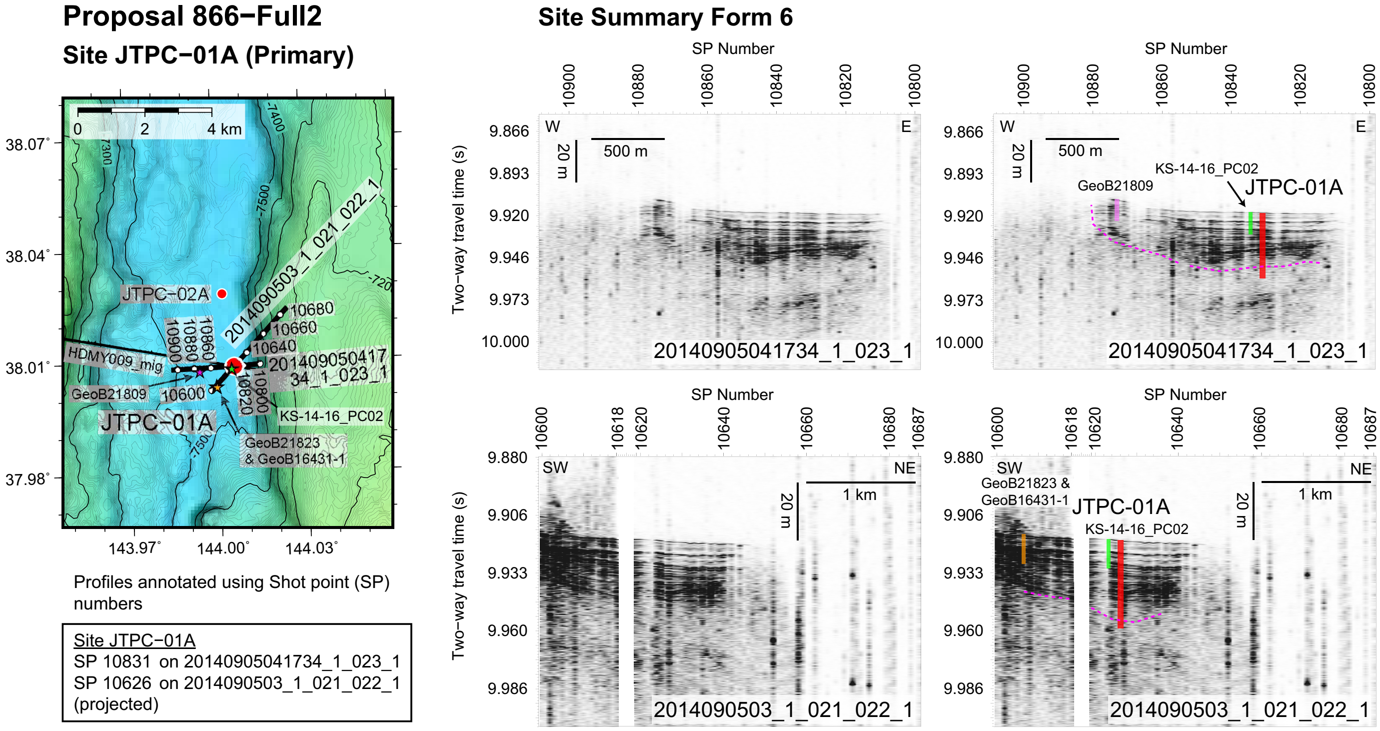

SSDB locations of these graphics and supporting data

Location map: JTPC-01A_Location.pdf
Figures of seismic data: JTPC−01A_20140905041734_1_023_1.pdf, JTPC−01A_2014090503_1_021_022_1.pdf, JTPC−01A_HDMY009_mig.pdf
SEG−Y data: JTPC−01A_20140905041734_1_023_1.sgy, JTPC−01A_2014090503_1_021_022_1.sgy, JTPC−01A_HDMY009_mig.sgy
Figures of reference core data: KS-14-16_PC02.pdf, GeoB21809.pdf, GeoB21823.pdf, GeoB16431-1.pdf

Interpretation

Undisturbed trench-basin-fill succession of dominantly diatomaceous mud interbedded with cm-to-dm-thick, muddy turbidites and thin tephra layers, overlying deformed trench-fill deposits

Magenta = Top of deformed trench-fill deposits (e.g. by slumping or compression during co-seismic slip to trench)

Figure AF12. Primary proposed Site JTPC-02A.

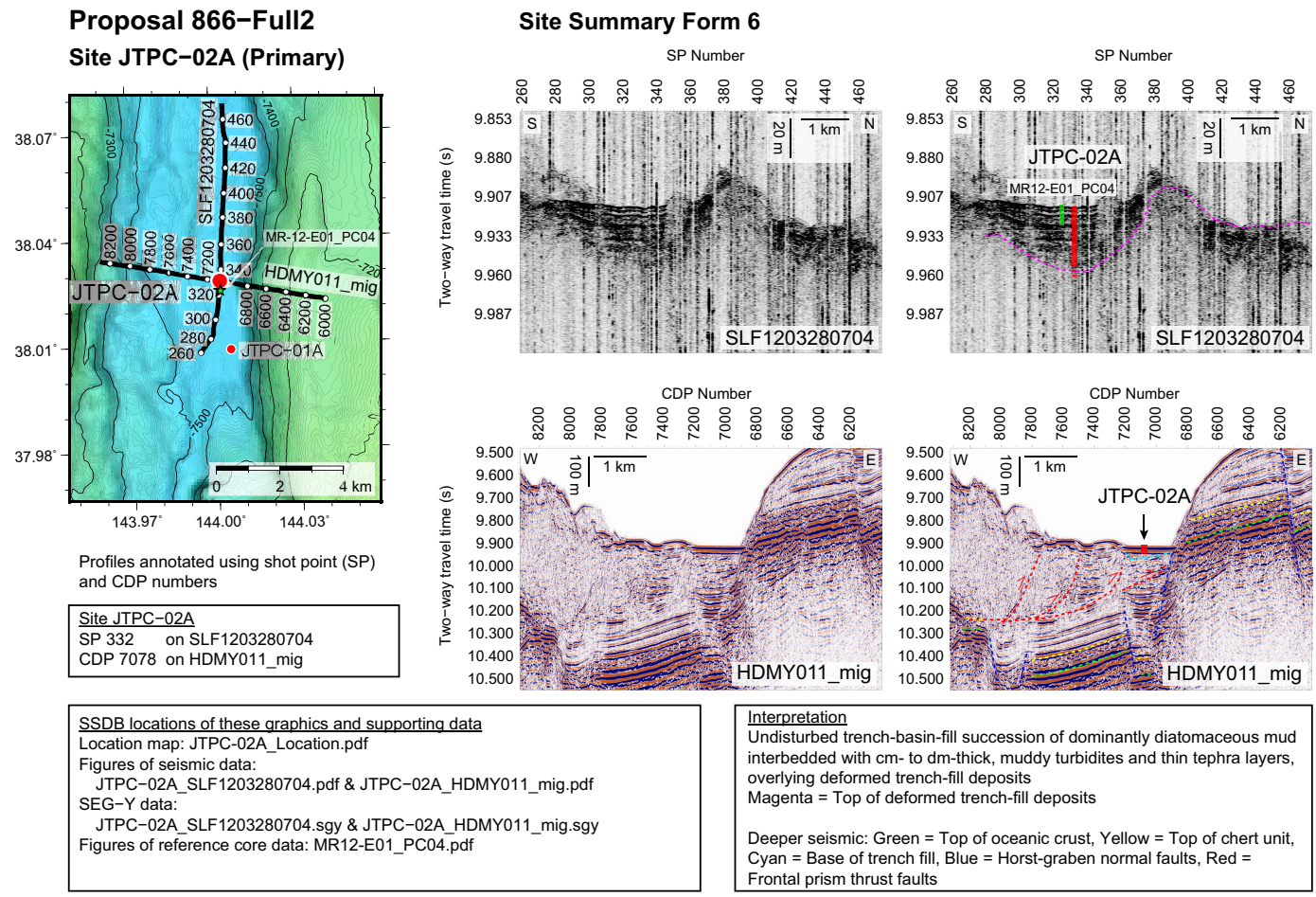

Figure AF13. Primary proposed Site JTPC-03B.

Proposal 866−Full2

Site JTPC−03B (Primary)

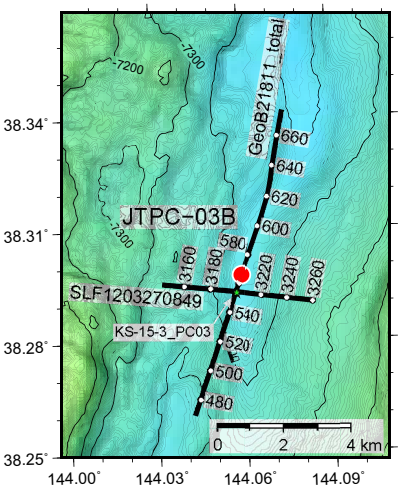

Profiles annotated using Shot point (SP) numbers

Site JTPC−03B
SP 566 on GeoB21811_total
SP 3203 on SLF1203270849 (Projected)

Site Summary Form 6

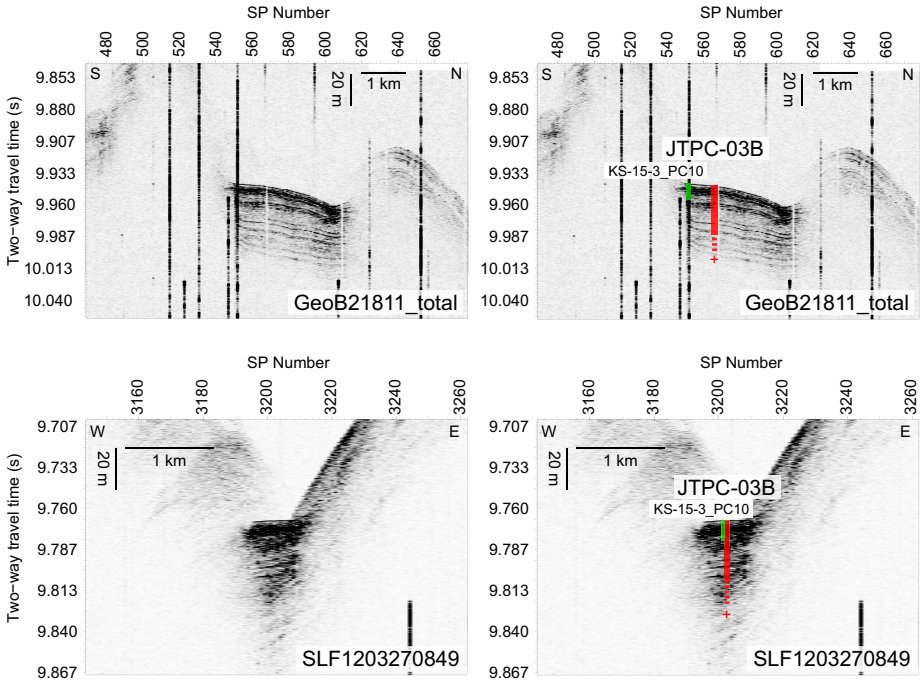

SSDB locations of these graphics and supporting data
Location map: JTPC-03B_Location.pdf
Figures of seismic data:
JTPC−03B_GeoB21811_total.pdf & JTPC−03B_SLF1203270849.pdf
SEG−Y data:
JTPC−03B_GeoB21811_total.sgy & JTPC−03B_SLF1203270849.sgy
Figures of reference core data: KS-15-3_PC10.pdf

Interpretation

Narrow trench-basin with undisturbed trench-fill succession of dominantly diatomaceous mud interbedded with cm- to dm-thick, muddy turbidites and thin tephra layers.

Figure AF14. Alternate proposed Site JTPC-04A.

Proposal 866−Full2

Site JTPC−04A (Alternate)

Site Summary Form 6

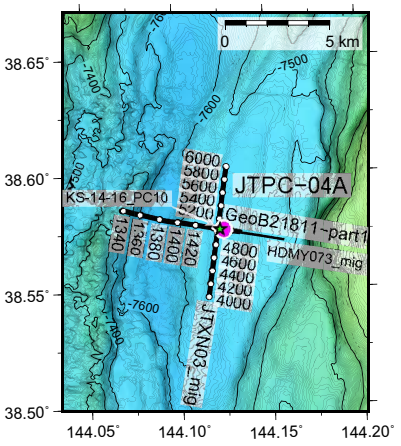

Profiles annotated using shot point (SP) and CDP numbers

Site JTPC−04A
SP 1451 on GeoB21811−part1
CDP 5034 on JTXN03_mig

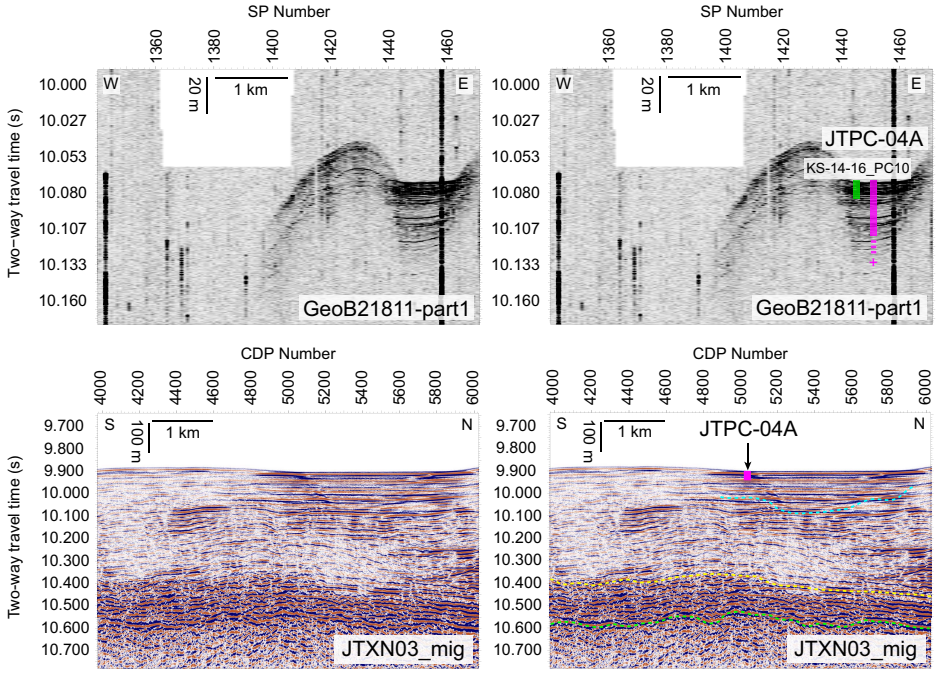

SSDB locations of these graphics and supporting data
Location map: JTPC-04A_Location.pdf
Figures of seismic data: JTPC−04A_GeoB21811−part1.pdf, JTPC−04A_JTXN03_mig.pdf, JTPC−04A_HDMY073_mig.pdf
SEG−Y data: JTPC−04A_GeoB21811−part1.sgy, JTPC−04A_JTXN03_mig.sgy, JTPC−04A_HDMY073_mig.sgy
Figures of reference core data: KS-14-16_PC10.pdf

Interpretation

Undisturbed graben-basin-fill succession of dominantly diatomaceous mud interbedded with cm- to dm-thick, muddy turbidites, and thin tephra layers.

Green = Top of oceanic crust, Yellow = Top of chert unit, Cyan = Base of graben fill

Figure AF15. Primary proposed Site JTPC-05A.

Proposal 866−Full2

Site JTPC−05A (Primary)

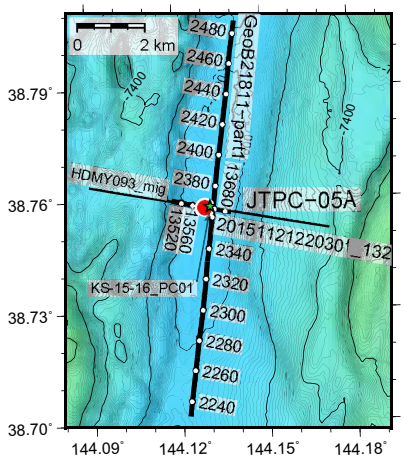

Profiles annotated using Shot point (SP) numbers

Site JTPC−05A
SP 13605 on 20151121220301_132
SP 2365 on GeoB21811−part1 (projected)

Site Summary Form 6

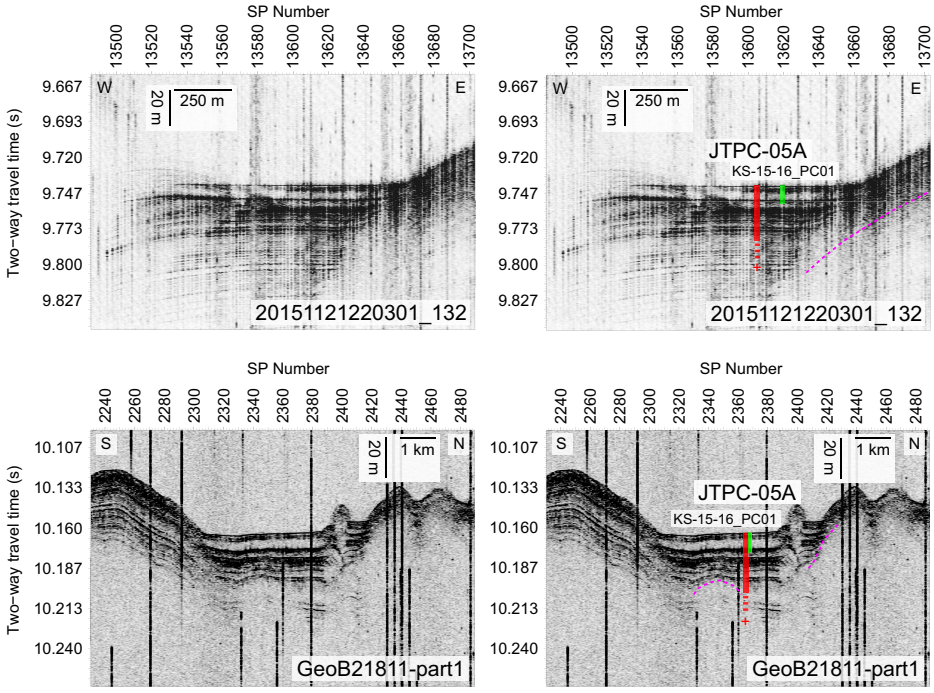

SSDB locations of these graphics and supporting data
Location map: JTPC-05A_Location.pdf
Figures of seismic data: JTPC−05A_20151121220301_132.pdf, JTPC−05A_GeoB21811−part1.pdf, JTPC−05A_HDMY093_mig.pdf
SEG−Y data: JTPC−05A_20151121220301_132.sgy, JTPC−05A_GeoB21811−part1.sgy, JTPC−05A_HDMY093_mig.sgy
Figures of reference core data: KS-15-16_PC01.pdf
Figure for positioning accuracy of deep-water coring: JTPC-05A_Positioning.pdf

Interpretation

Undisturbed trench-basin-fill succession of dominantly diatomaceous mud interbedded with cm- to dm-thick muddy turbidites, thin tephra layers, and few m-thick homogenites.

Magenta = Top of deformed trench-fill deposits (e.g. by slumping or compression during co-seismic slip to trench)

Figure AF16. Alternate proposed Site JTPC-06B.

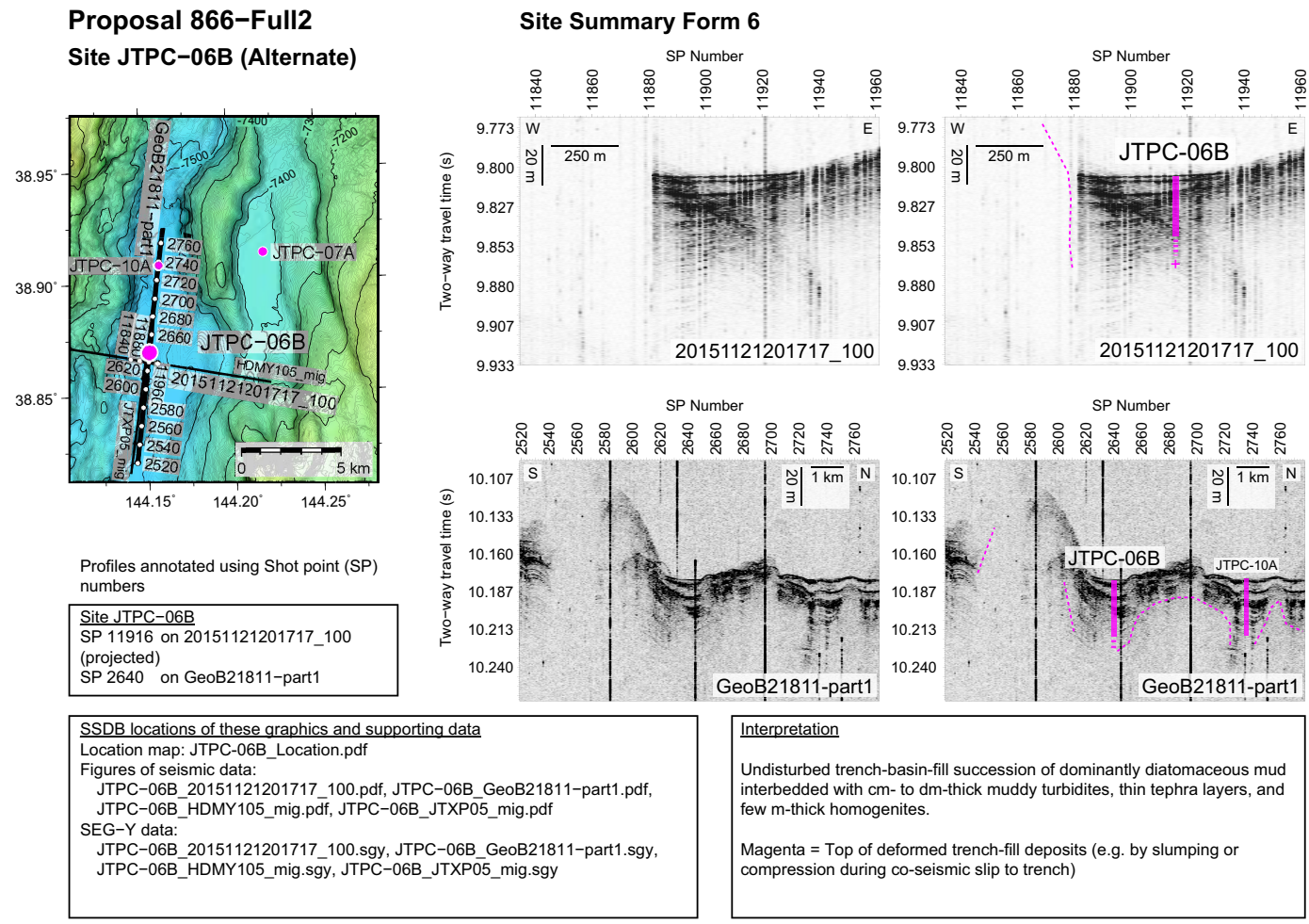

Figure AF17. Alternate proposed Site JTPC-07A.

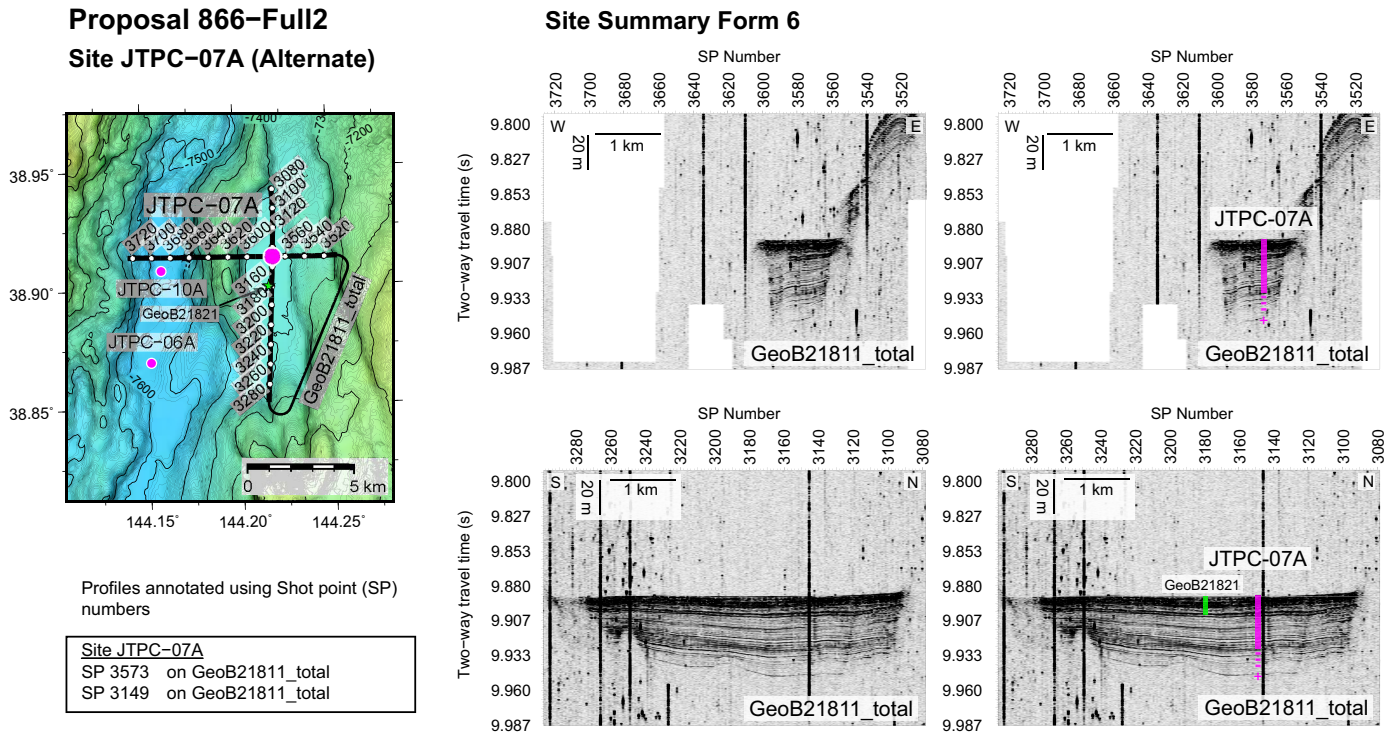

Figure AF18. Primary proposed Site JTPC-08A.

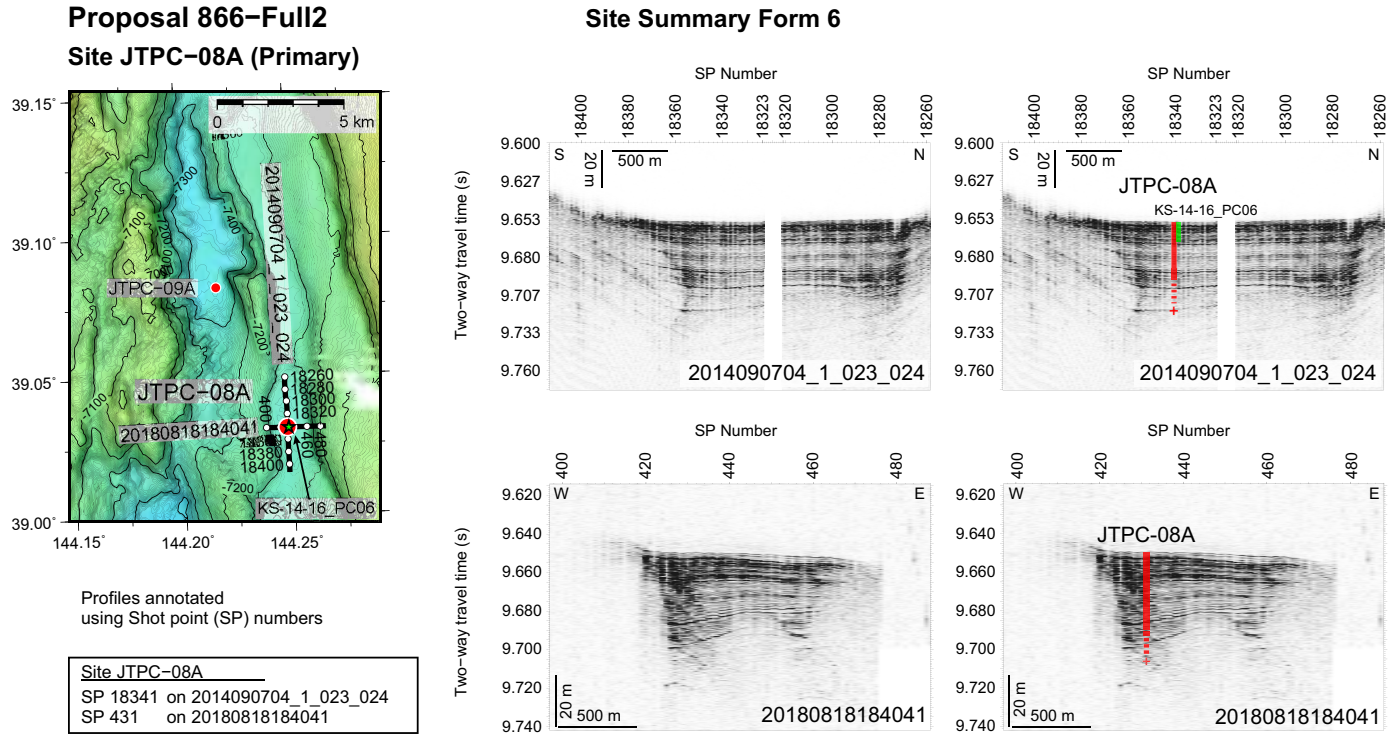

SSDB locations of these graphics and supporting data

Location map: JTPC-08A_Location.pdf

Figures of seismic data:
JTPC−08A_2014090704_1_023_024.pdf, JTPC−08A_20180818184041.pdf, JTPC−08A_HDMY125_mig.pdf

SEG−Y data:
JTPC−08A_2014090704_1_023_024.sgy, JTPC−08A_20180818184041.sgy, JTPC−08A_HDMY125_mig.sgy

Figures of reference core data: KS-14-16_PC06.pdf

Interpretation

Undisturbed graben-basin-fill succession of dominantly diatomaceous mud interbedded with cm-thick, muddy turbidites thin tephra layers

Figure AF19. Primary proposed Site JTPC-09A.

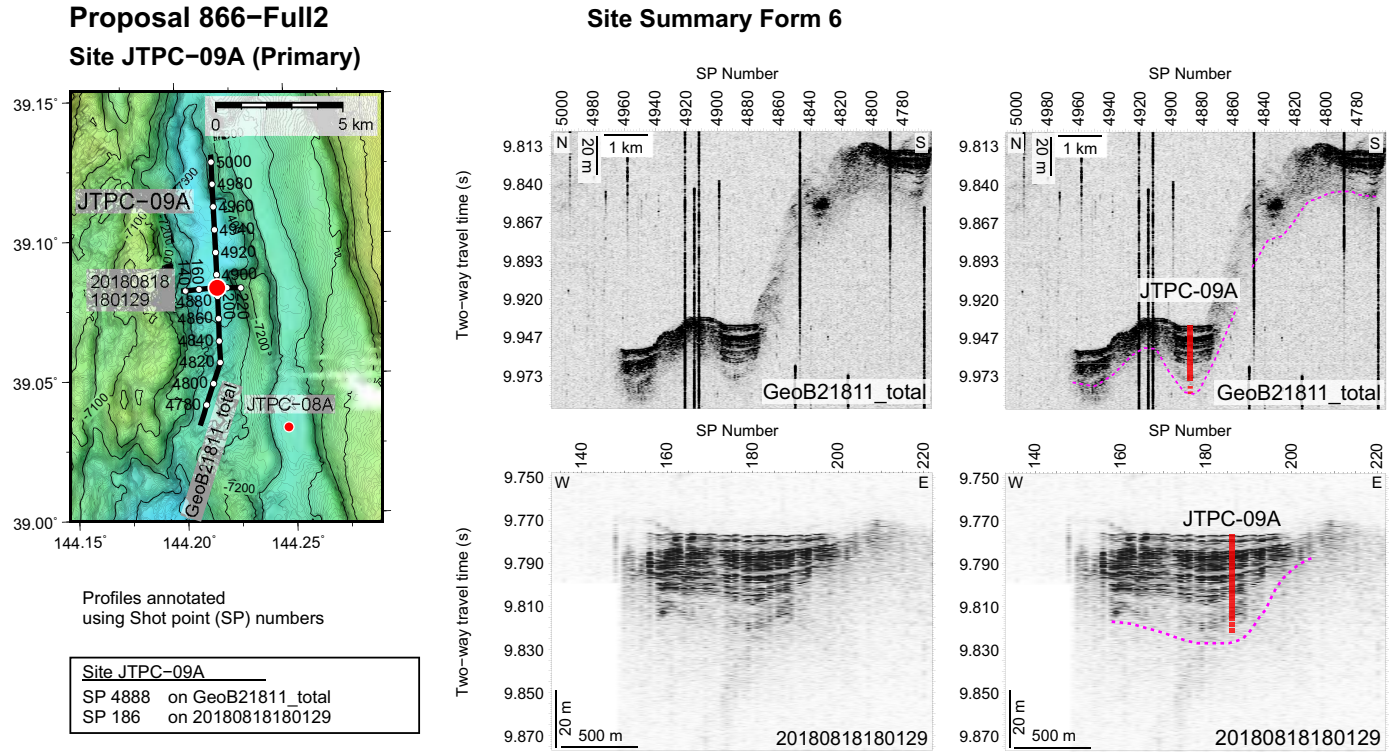

Figure AF20. Alternate proposed Site JTPC-10A.

Proposal 866−Full2

Site JTPC−10A (Alternate)

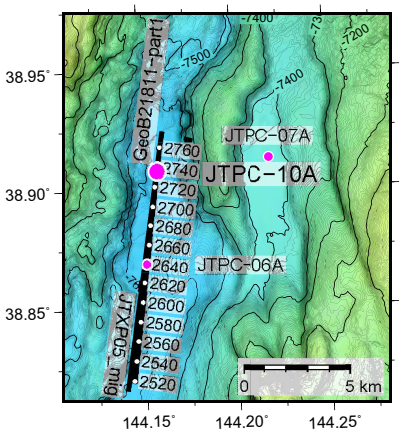

Profiles annotated using Shot point (SP) numbers

Site JTPC−10A
SP 2736 on GeoB21811−part1

Site Summary Form 6

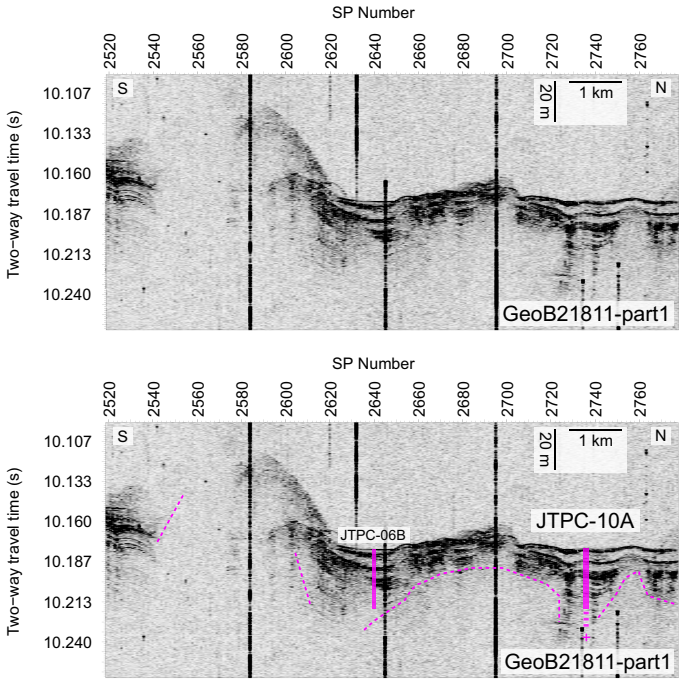

SSDB locations of these graphics and supporting data
Location map: JTPC-10A_Location.pdf
Figures of seismic data:
JTPC−10A_GeoB21811−part1.pdf, JTPC−10A_JTXP05_mig.pdf
SEG−Y data:
JTPC−10A_GeoB21811−part1.sgy, JTPC−10A_JTXP05_mig.sgy

Interpretation

Undisturbed trench-basin-fill succession of dominantly diatomaceous mud interbedded with cm- to dm-thick muddy turbidites, thin tephra layers, and few m-thick homogenites.

Magenta = Top of deformed trench-fill deposits (e.g. by slumping or compression during co-seismic slip to trench)

Figure AF21. Alternate proposed Site JTPN-01A.

Proposal 866−Full2

Site JTPN−01A (Alternate)

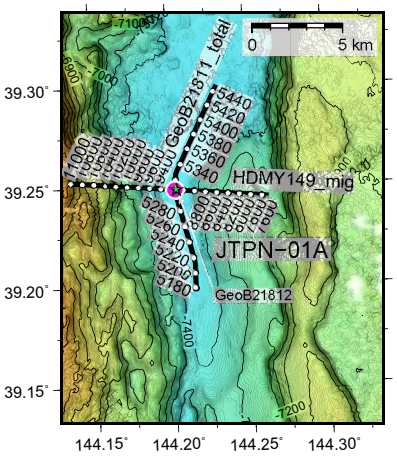

Profiles annotated using shot point (SP) and CDP numbers

Site JTPN−01A
SP 5308 on GeoB21811_total
CDP 9149 on HDMY149_mig

Site Summary Form 6

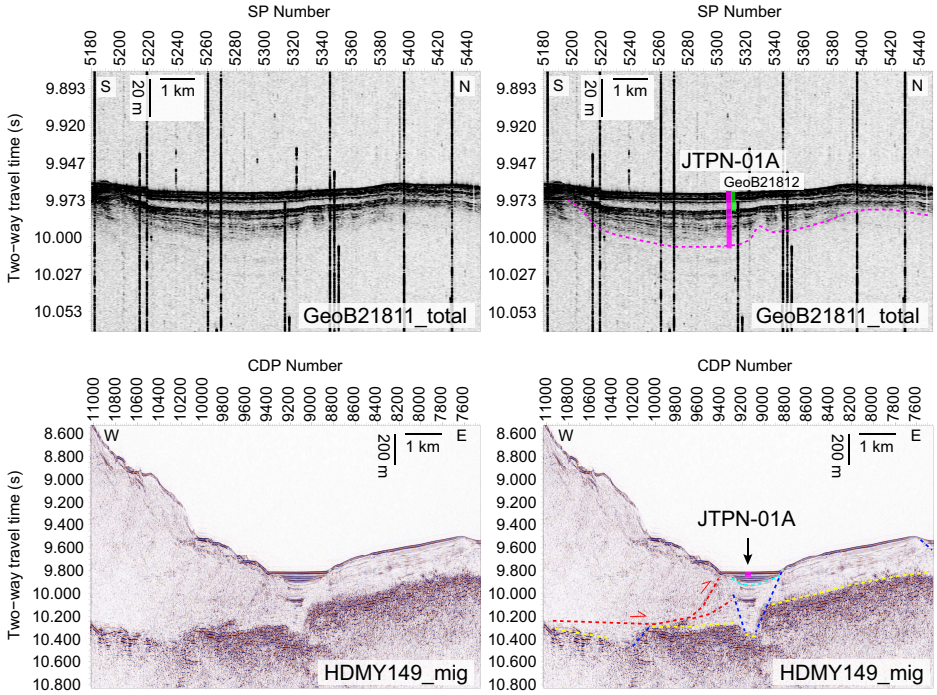

SSDB locations of these graphics and supporting data
Location map: JTPN-01A_Location.pdf
Figures of seismic data: JTPN−01A_GeoB21811_total.pdf, JTPN−01A_HDMY149_mig.pdf, JTPN−01A_20151123010940_246.pdf
SEG−Y data: JTPN−01A_GeoB21811_total.sgy, JTPN−01A_HDMY149_mig.sgy, JTPN−01A_20151123010940_246.sgy
Figures of reference core data: GeoB21812.pdf

Interpretation Undisturbed trench-basin-fill succession of dominantly diatomaceous mud interbedded with cm- to dm-thick muddy turbidites, thin tephra layers, and few m-thick homogenites, overlying deformed trench-basin or mass-transport deposits (MTD).

Magenta = Top of deformed trench-fill / MTDs
Deeper seismic: Yellow = Top of chert unit or oceanic crust, Cyan = Base of trench fill, Blue = Horst-graben normal faults, Red = Frontal prism thrust faults

Figure AF22. Primary proposed Site JTPN-02A.

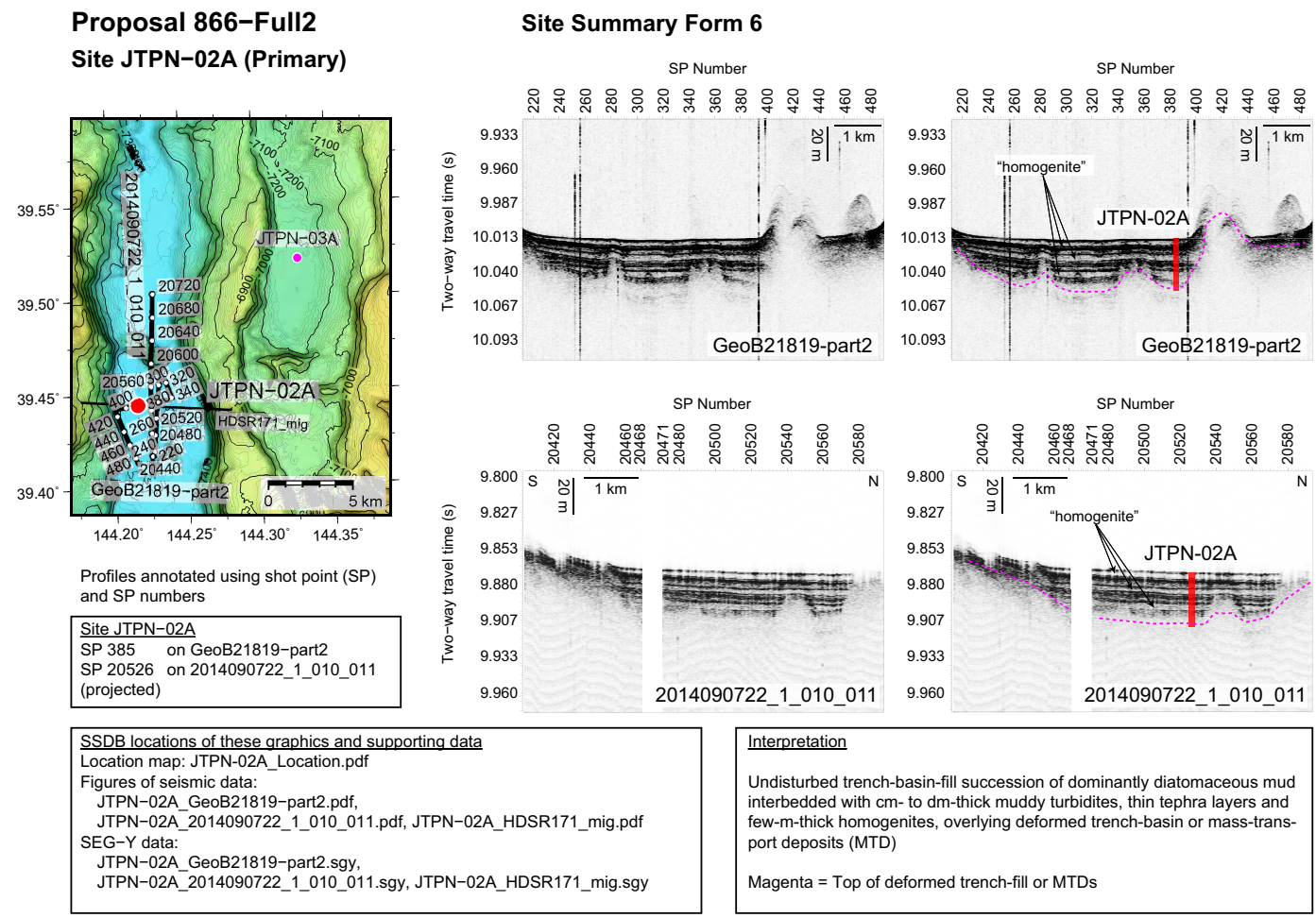

Figure AF23. Alternate proposed Site JTPN-03A.

Proposal 866−Full2

Site JTPN−03A (Alternate)

Site Summary Form 6

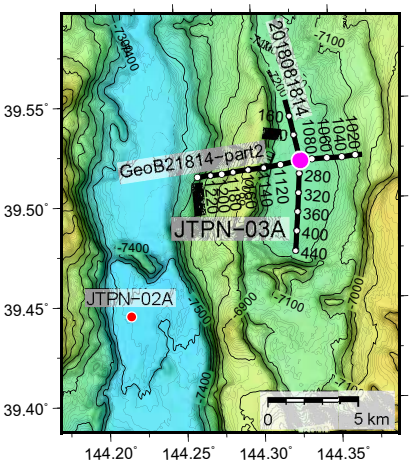

Profiles annotated
using Shot point (SP) numbers

Site JTPN−03A
SP 1095 on GeoB21814−part2
SP 388 on 2018081814

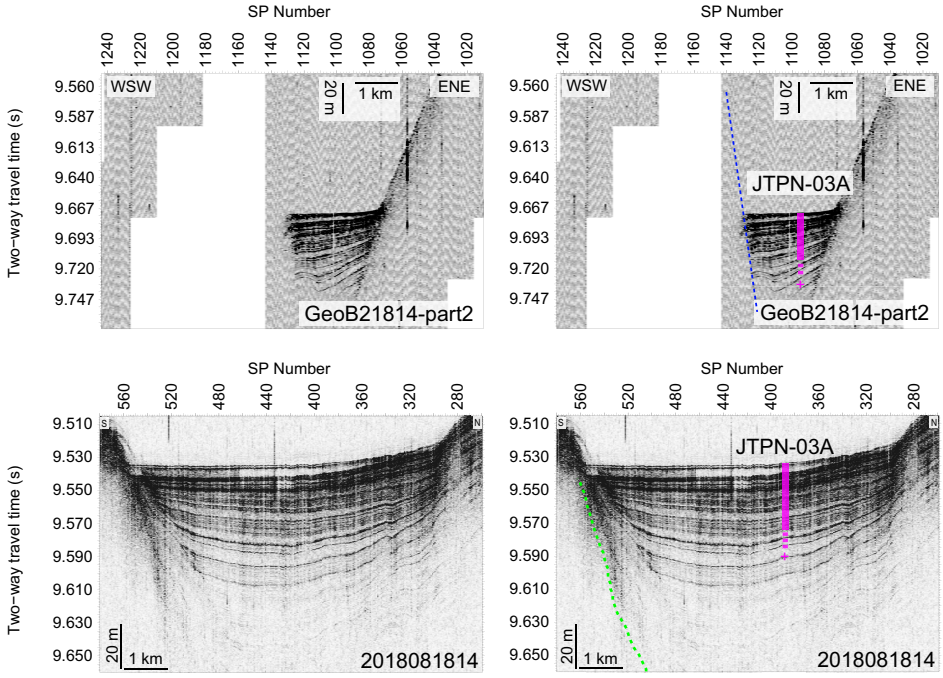

SSDB locations of these graphics and supporting data

Location map: JTPN-03A_Location.pdf

Figures of seismic data:
JTPN−03A_GeoB21814−part2.pdf, JTPN−03A_2018081814.pdf, JTPN−03A_HDSR179_mig.pdf

SEG−Y data:
JTPN−03A_GeoB21814−part2.sgy, JTPN−03A_2018081814.sgy, JTPN−03A_HDSR179_mig.sgy

Interpretation

Undisturbed graben-basin-fill succession of dominantly diatomaceous mud interbedded with cm- to dm-thick muddy turbidites and thin tephra layers.
Green = Acoustic basement (probably linked to Petit-spot volcanism?)
Blue = Horst-graben normal faults

Figure AF24. Alternate proposed Site JTPN-04A.

Proposal 866−Full2

Site JTPN−04A (Alternate)

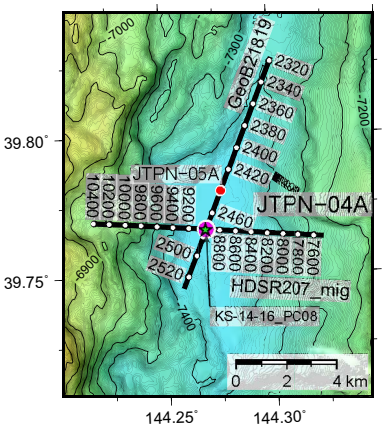

Profiles annotated using shot point (SP) and CDP numbers

Site JTPN−04A
SP 2475 on GeoB21819
CDP 8972 on HDSR207_mig

Site Summary Form 6

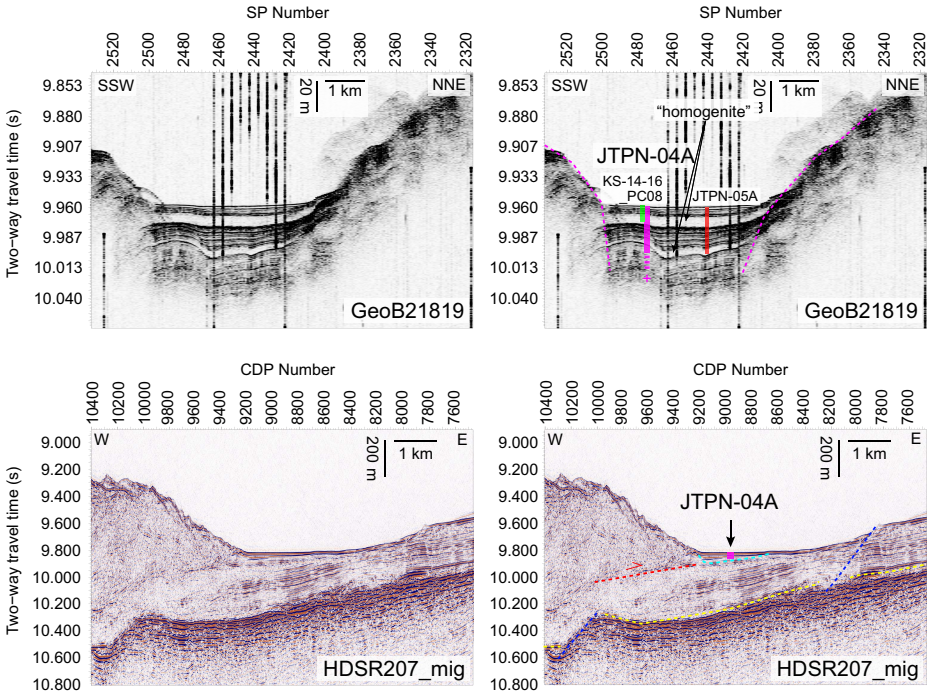

SSDB locations of these graphics and supporting data
Location map: JTPN-04A_Location.pdf
Figures of seismic data:
JTPN−04A_GeoB21819.pdf & JTPN−04A_HDSR207_mig.pdf
SEG−Y data:
JTPN−04A_GeoB21819.sgy & JTPN−04A_HDSR207_mig.sgy
Figures of reference core data: KS-14-16_PC08.pdf

Interpretation
Undisturbed trench-basin-fill succession of dominantly diatomaceous mud interbedded with cm- to dm-thick muddy turbidites, thin tephra layers and several-m-thick homogenites. This is the condensed section relative to JTPN-05A. Magenta = Top of deformed trench-fill deposits (e.g. by local slumping). Deeper seismic: Yellow = Top of chert unit or oceanic crust, Cyan = Base of trench fill, Blue = Horst-graben normal faults, Red = Frontal prism thrust faults.

Figure AF25. Primary proposed Site JTPN-05A.

Proposal 866−Full2

Site JTPN−05A (Primary)

Site Summary Form 6

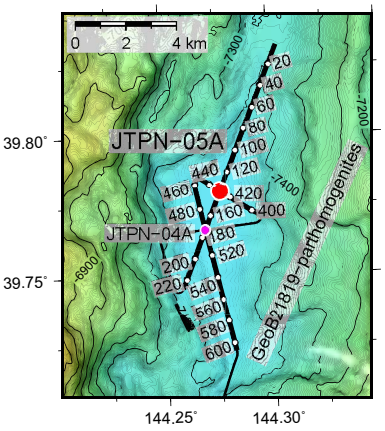

Profiles annotated using Shot point (SP) numbers

Site JTPN−05A
SP 138 on GeoB21819−parthomogenites
SP 429 on GeoB21819−parthomogenites

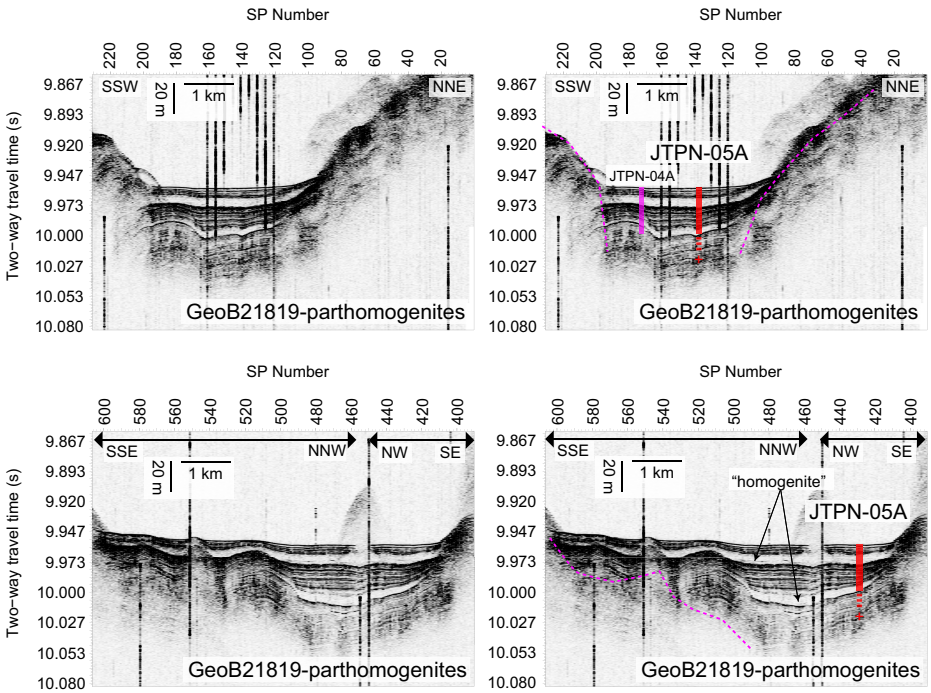

SSDB locations of these graphics and supporting data
Location map: JTPN-05A_Location.pdf
Figures of seismic data:
JTPN−05A_01_GeoB21819−parthomogenites.pdf,
JTPN−05A_02_GeoB21819−parthomogenites.pdf
SEG−Y data:
JTPN−05A_GeoB21819−parthomogenites.sgy

Interpretation

Undisturbed trench-basin-fill succession of dominantly diatomaceous mud interbedded with cm- to dm-thick muddy turbidites, thin tephra layers and several-m-thick homogenites. This is the expanded section relative to JTPN-04A.

Magenta = Top of deformed trench-fill sediments (e.g. by local slumping)

Figure AF26. Alternate proposed Site JTPN-06A.

Proposal 866−Full2

Site JTPN−06A (Alternate)

Site Summary Form 6

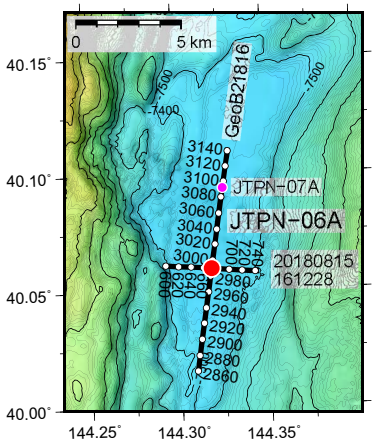

Profiles annotated
using Shot point (SP) numbers

Site JTPN−06A
SP 2990 on GeoB21816
SP 673 on 20180815161228

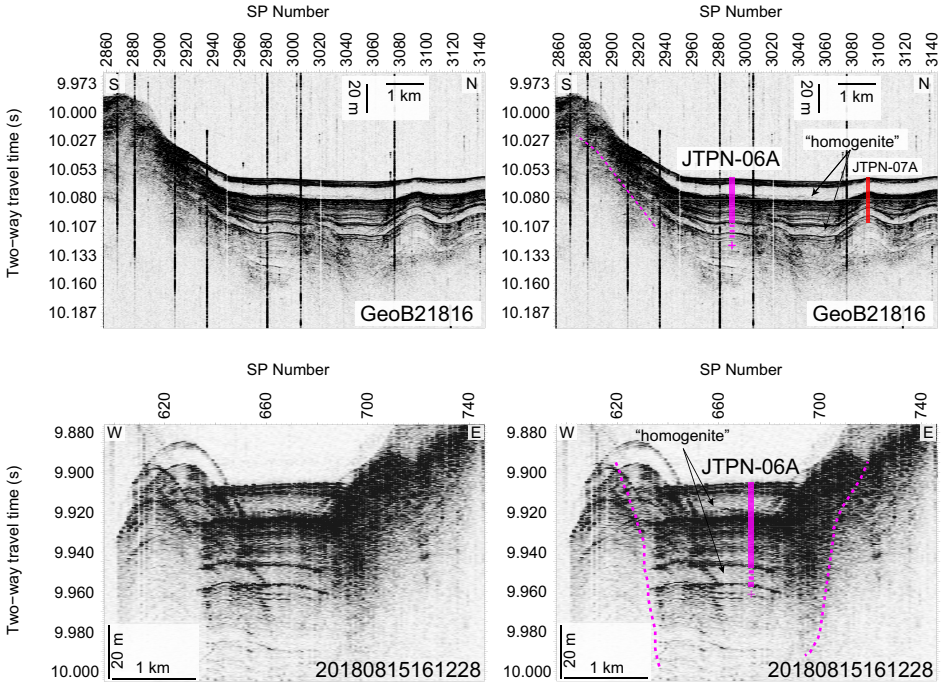

SSDB locations of these graphics and supporting data

Location map: JTPN-06A_Location.pdf

Figures of seismic data:
JTPN−06A_GeoB21816.pdf, JTPN−06A_20180815161228.pdf, JTPN−06A_HDSR239_mig.pdf

SEG−Y data:
JTPN−06A_GeoB21816.sgy, JTPN−06A_20180815161228.sgy, JTPN−06A_HDSR239_mig.sgy

Interpretation

Undisturbed trench-basin-fill succession of dominantly diatomaceous mud interbedded with cm- to dm-thick muddy turbidites, thin tephra layers and several-m-thick homogenites. This is the expanded section relative to JTPN-07A.
Magenta = Top of deformed trench-fill sediments (e.g. by local slumping)

Figure AF27. Primary proposed Site JTPN-07A.

Proposal 866−Full2

Site JTPN−07A (Primary)

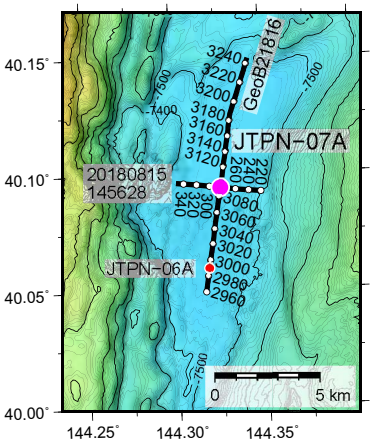

Profiles annotated
using Shot point (SP) numbers

Site JTPN−07A
SP 3092 on GeoB21816
SP 283 on 20180815145628

Site Summary Form 6

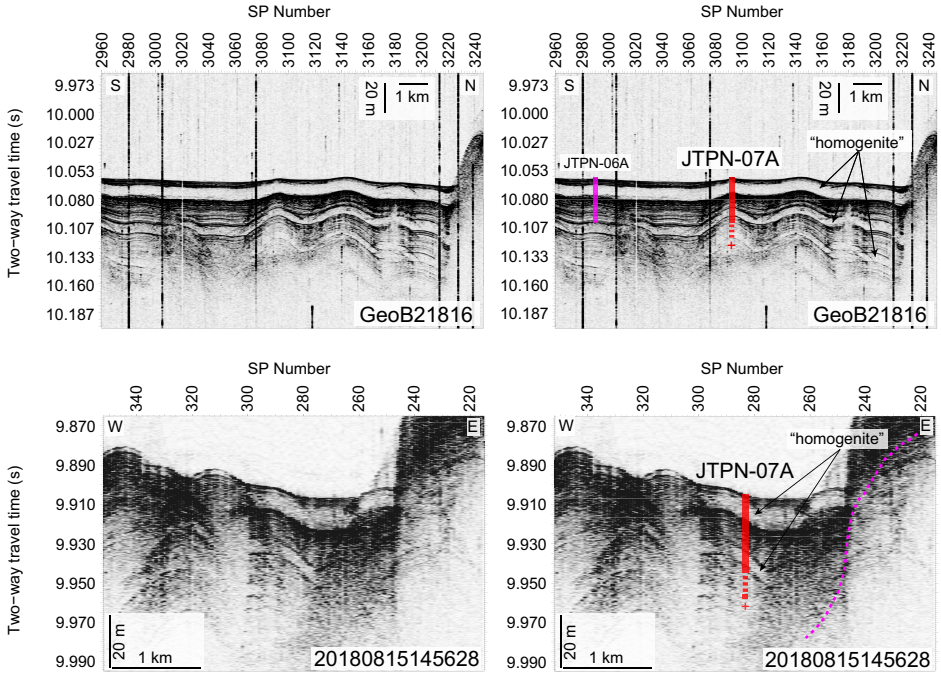

SSDB locations of these graphics and supporting data

Location map: JTPN-07A_Location.pdf

Figures of seismic data:
JTPN−07A_GeoB21816.pdf, JTPN−07A_20180815145628.pdf, JTPN−07A_HDSR243_mig.pdf

SEG−Y data:
JTPN−07A_GeoB21816.sgy, JTPN−07A_20180815145628.sgy, JTPN−07A_HDSR243_mig.sgy

Interpretation

Undisturbed trench-basin-fill succession of dominantly diatomaceous mud interbedded with cm- to dm-thick muddy turbidites, thin tephra layers and several m-thick homogenites. This is the condensed section relative to JTPN-06A.
Magenta = Top of deformed trench-fill sediments (e.g. by local slumping)

Figure AF28. Alternate proposed Site JTPN-08A.

Proposal 866−Full2

Site JTPN−08A (Alternate)

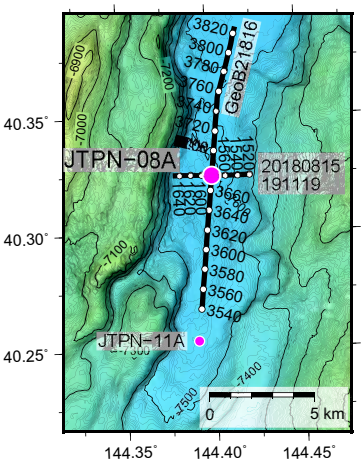

Profiles annotated
using Shot point (SP) numbers

Site JTPN−08A
SP 3675 on GeoB21816
SP 1583 on 20180815191119

Site Summary Form 6

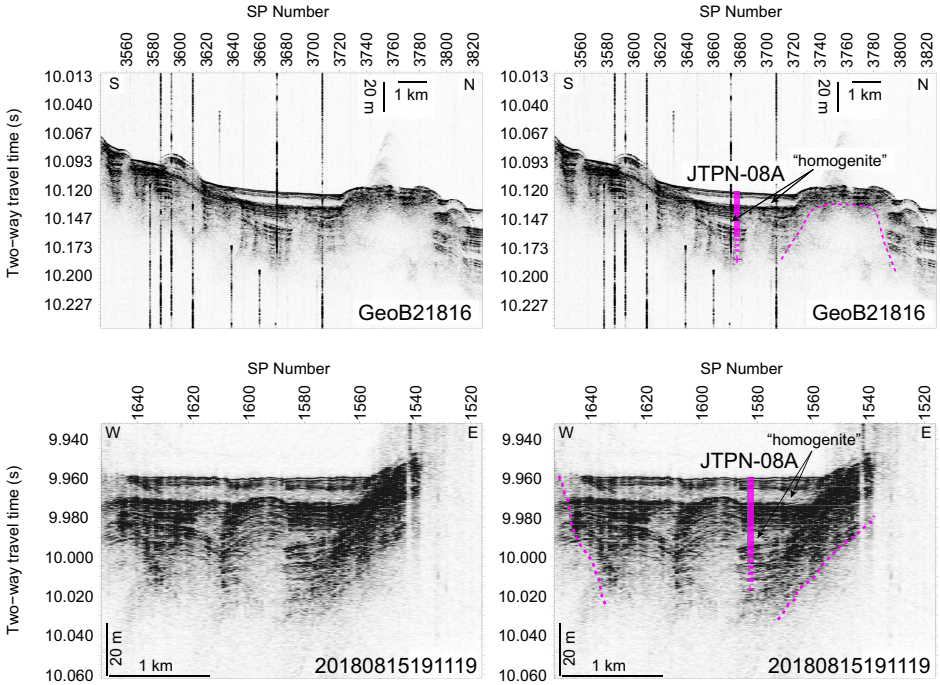

SSDB locations of these graphics and supporting data

Location map: JTPN-08A_Location.pdf

Figures of seismic data:
JTPN−08A_GeoB21816.pdf, JTPN−08A_20180815191119.pdf,
JTPN−08A_HDSR271_mig.pdf

SEG−Y data:
JTPN−08A_GeoB21816.sgy, JTPN−08A_20180815191119.sgy,
JTPN−08A_HDSR271_mig.sgy

Interpretation

Undisturbed trench-basin-fill succession of dominantly diatomaceous mud interbedded with cm- to dm-thick muddy turbidites, thin tephra layers and several m-thick homogenites.
Magenta = Top of deformed trench-fill deposits (e.g. by local slumping)

Figure AF29. Primary proposed Site JTPN-09A.

Proposal 866−Full2

Site JTPN−09A (Primary)

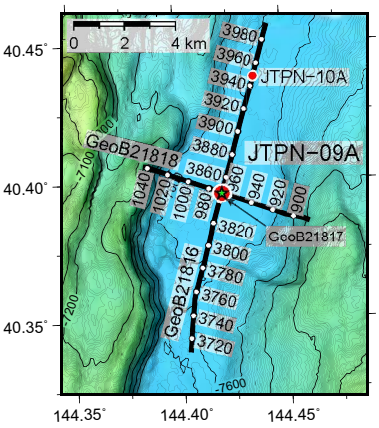

Profiles annotated using shot point (SP) numbers

Site JTPN−09A
SP 3846 on GeoB21816
SP 968 on GeoB21818

Site Summary Form 6

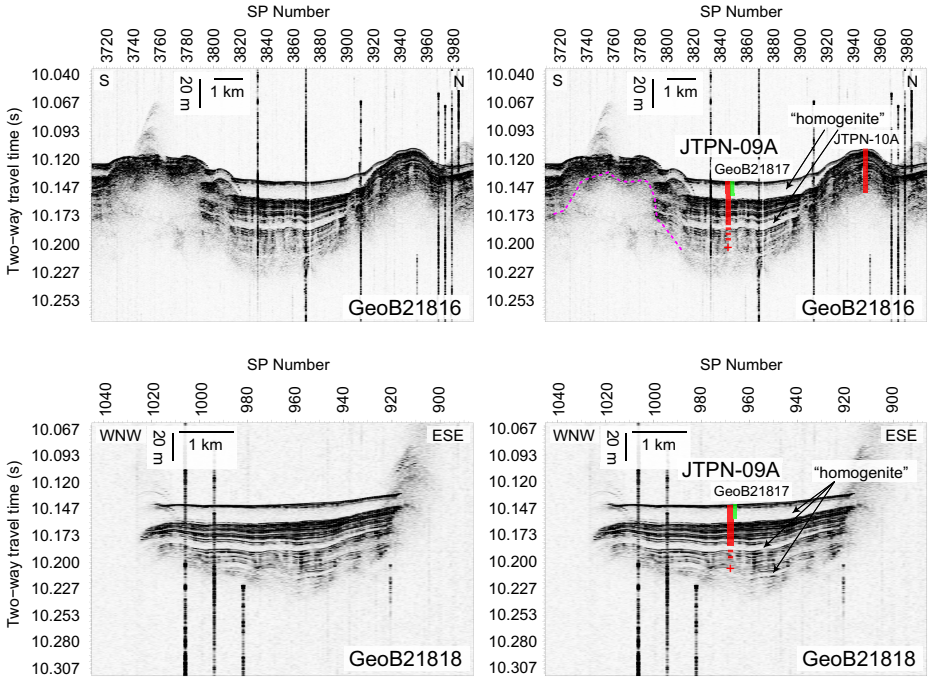

SSDB locations of these graphics and supporting data
Location map: JTPN-09A_Location.pdf
Figures of seismic data:
JTPN−09A_GeoB21816.pdf & JTPN−09A_GeoB21818.pdf
SEG−Y data:
JTPN−09A_GeoB21816.sgy & JTPN−09A_GeoB21818.sgy
Figures of reference core data: GeoB21817.pdf

Interpretation

Undisturbed trench-basin-fill succession of dominantly diatomaceous mud interbedded with cm- to dm-thick muddy turbidites, thin tephra layers and several-m-thick homogenites. This is the expanded section relative to JTPN-10A.

Magenta = Top of deformed trench deposits (e.g. by local slumping)

Figure AF30. Primary proposed Site JTPN-10A.

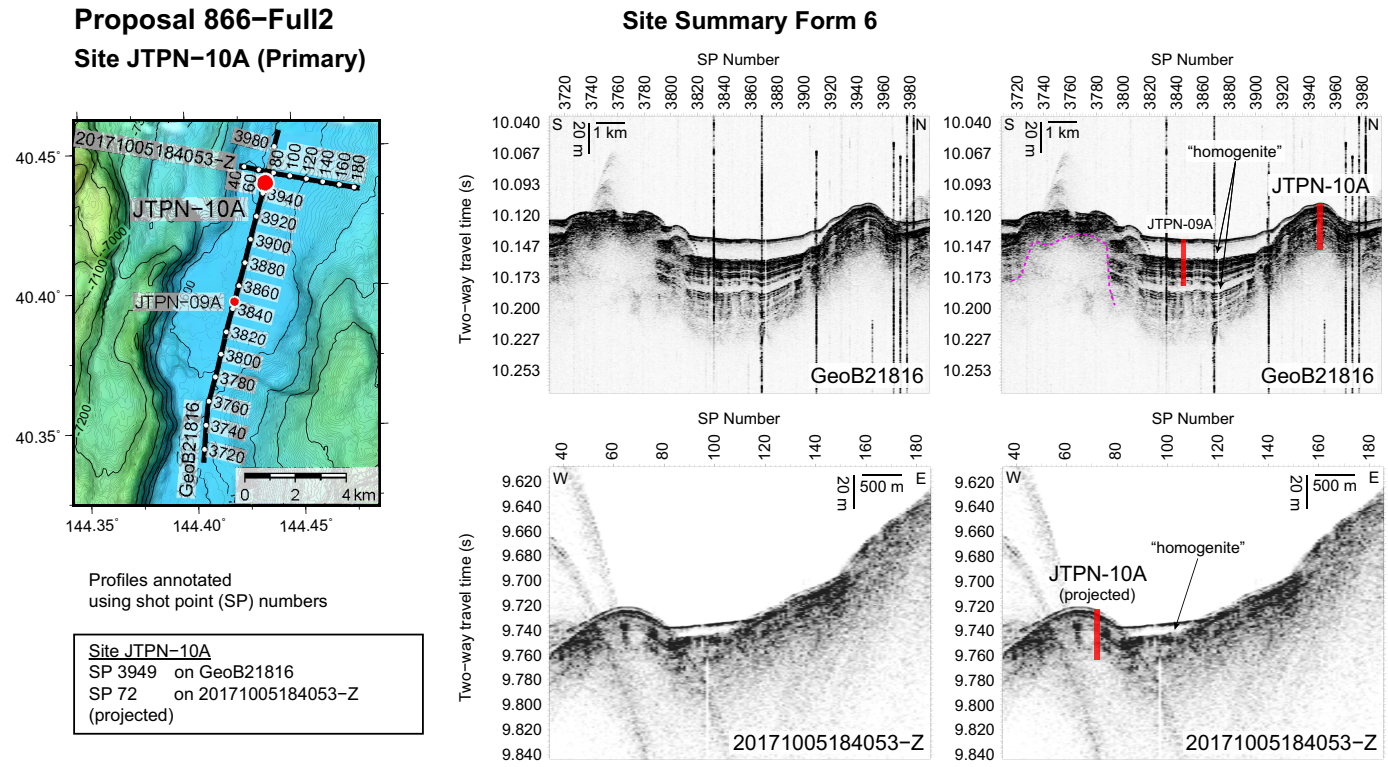

Figure AF31. Alternate proposed Site JTPN-11A.

Proposal 866−Full2

Site JTPN−11A (Alternate)

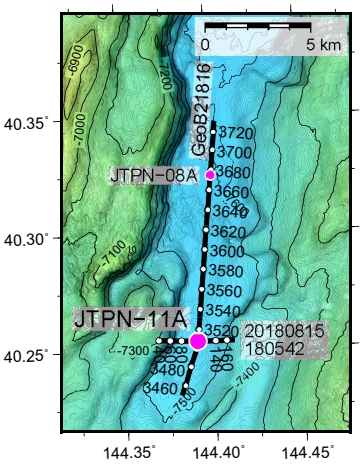

Profiles annotated
using Shot point (SP) numbers

Site JTPN−11A
SP 3507 on GeoB21816
SP 1241 on 20180815180542

Site Summary Form 6

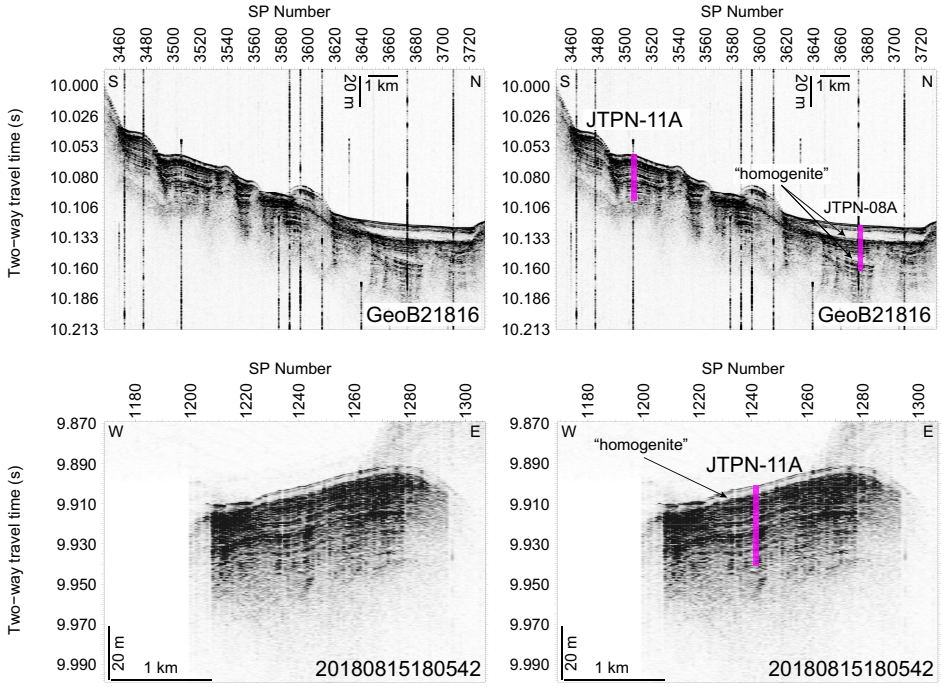

SSDB locations of these graphics and supporting data

Location map: JTPN-11A_Location.pdf

Figures of seismic data:
JTPN−11A_GeoB21816.pdf & JTPN−11A_20180815180542.pdf

SEG−Y data:
JTPN−11A_GeoB21816.sgy & JTPN−11A_20180815180542.sgy

Interpretation

Undisturbed trench-basin-fill succession of dominantly diatomaceous mud interbedded with cm- to dm-thick muddy turbidites and thin tephra layers. This is the condensed section relative to site JTPN-08A comprising thick homogenites.